Adrenal pathology: Elements of biologic models and practical applications

SALVADOR J. DIAZ-CANO

ORCID 0000-0003-1245-2859

BAHRAIN, APRIL 2017

Adrenal Cortical Lesions –

Sequence Hyperplasia-Adenoma-Carcinoma

- **Malignancy criteria**
- **Contributions of gene expression**
- **Cellular heterogeneity**
- **Cell segregation and vascular supply**
- **Morphology and function**

Malignancy Criteria

- Hough sytem
- Weiss system
- Van Slooten system
- SDDS

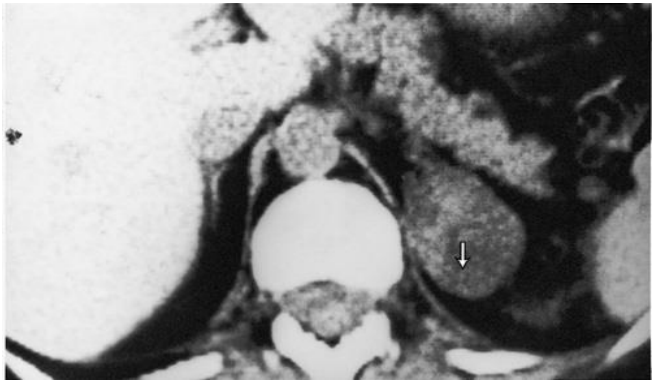

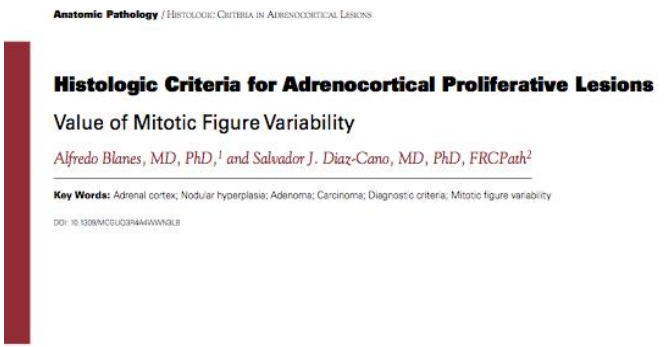

Histologic Criteria for Adrenocortical Proliferative Lesions

Value of Mitotic Figure Variability

Alfredo Blanes, MD, PhD,[1] and Salvador J. Diaz-Cano, MD, PhD, FRCPath[2]

Key Words: Adrenal cortex; Nodular hyperplasia; Adenoma; Carcinoma; Diagnostic criteria; Mitotic figure variability

DOI: 10.1309/MCGUG3R4AWWNGLB

Adrenocortical Neoplasm

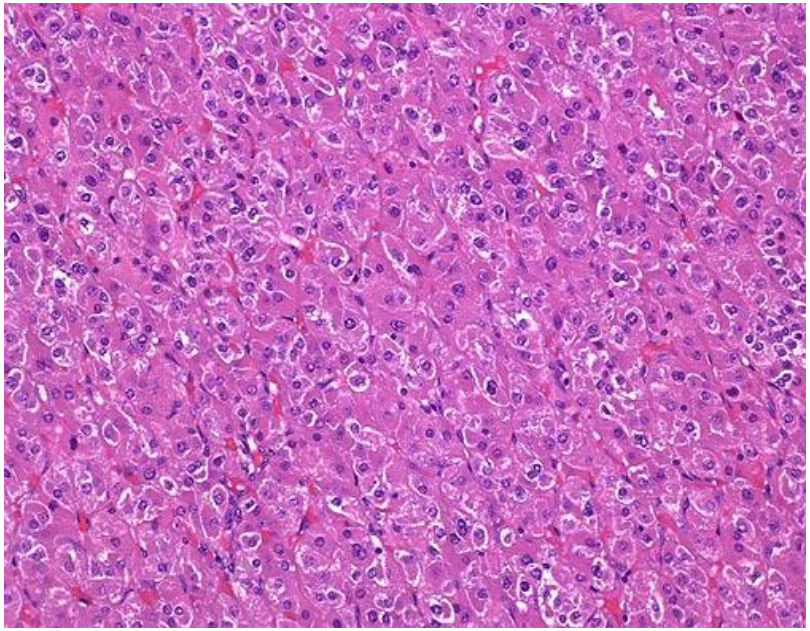

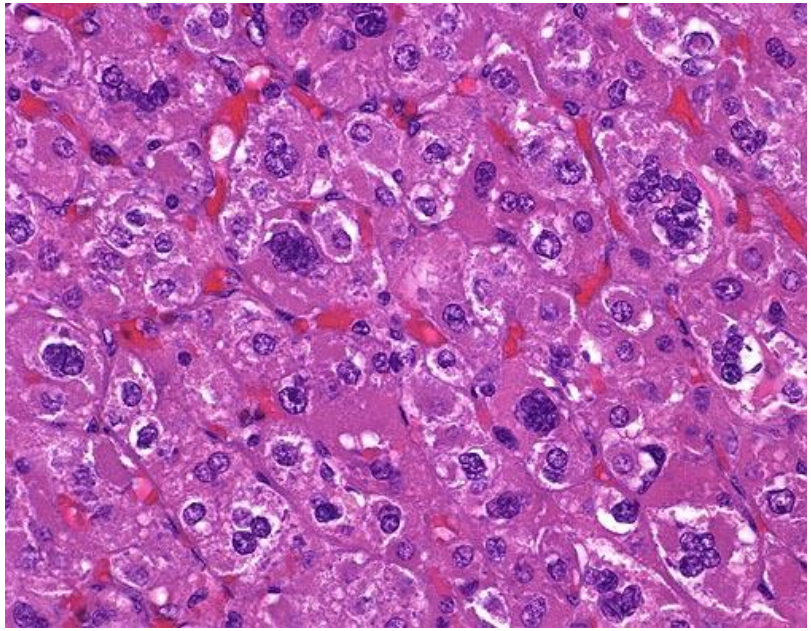

Adrenocortical Neoplasm

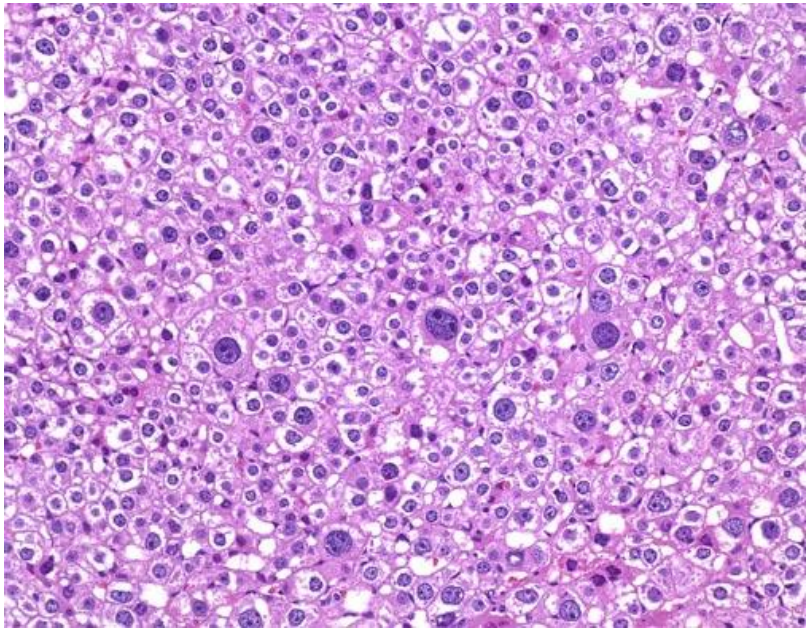

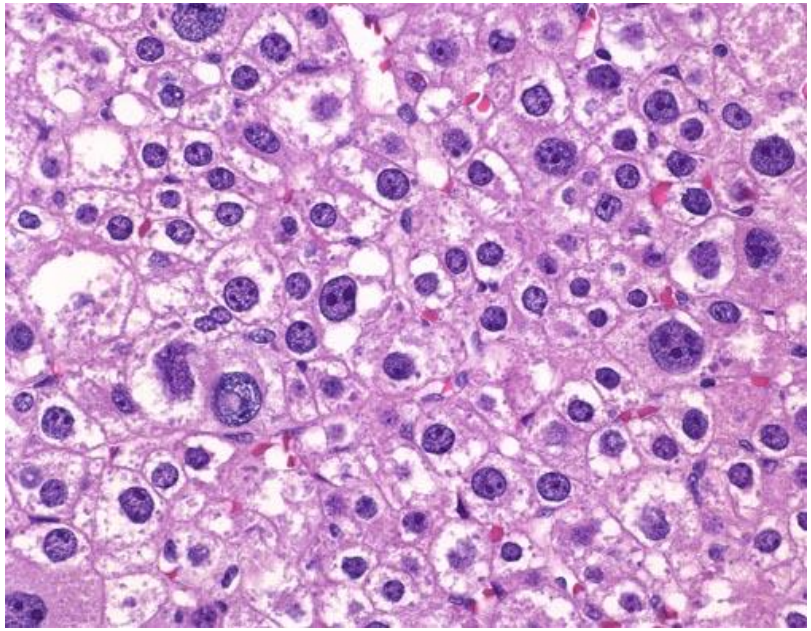

Adrenocortical Carcinoma

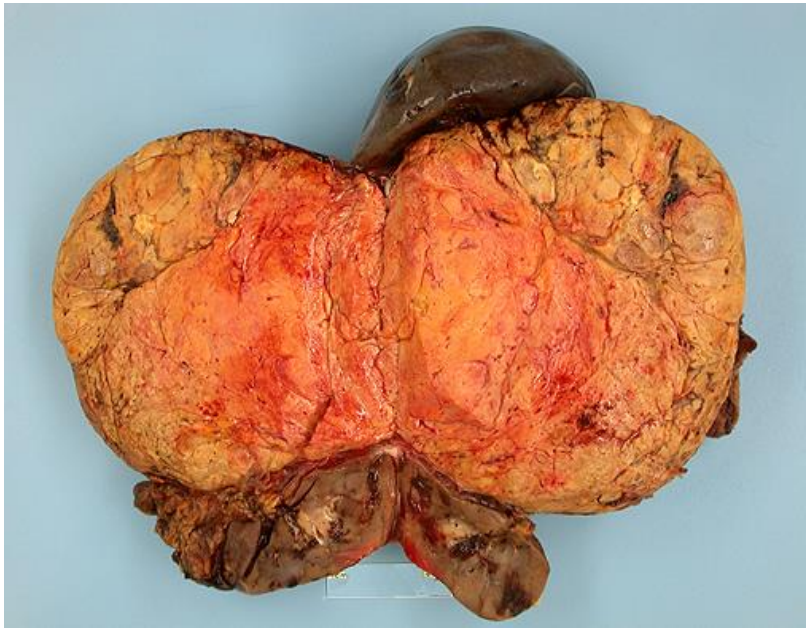

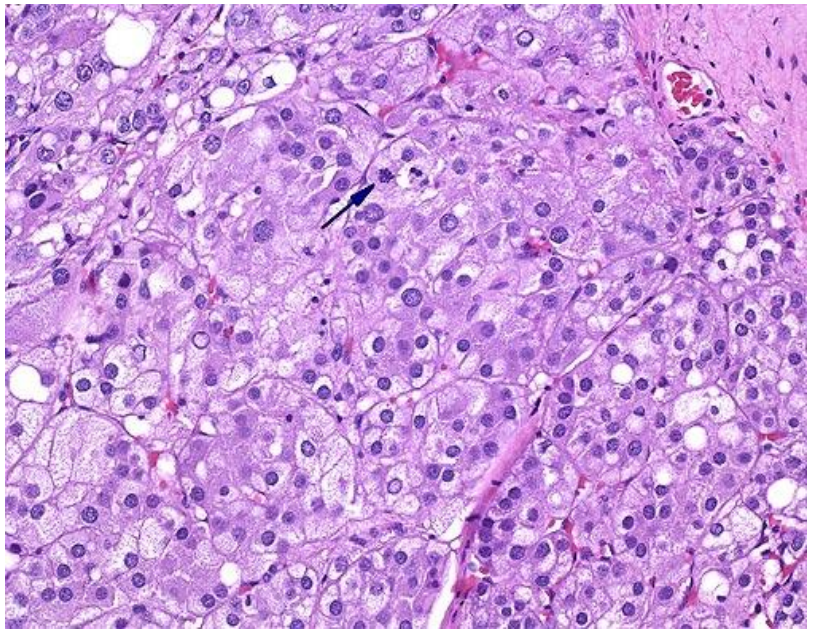

Adrenocortical Carcinoma

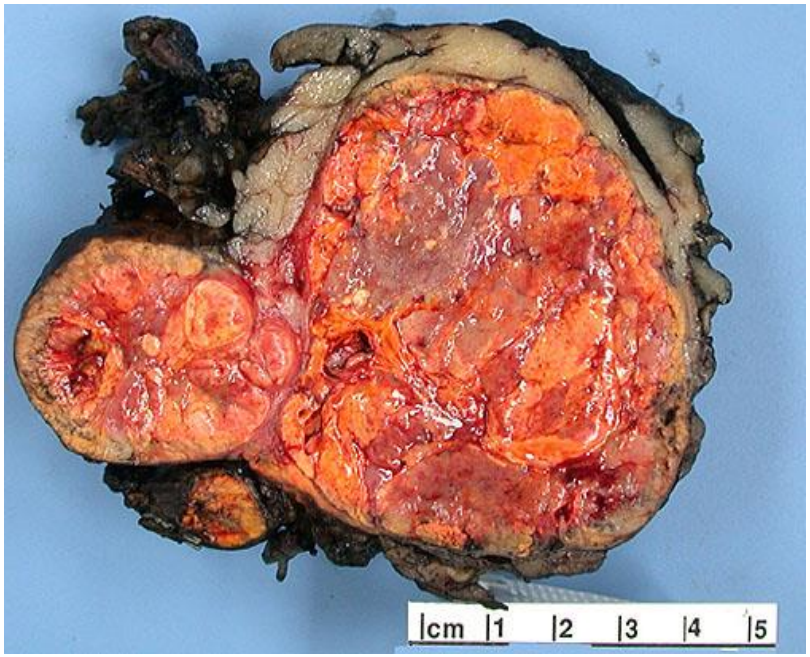

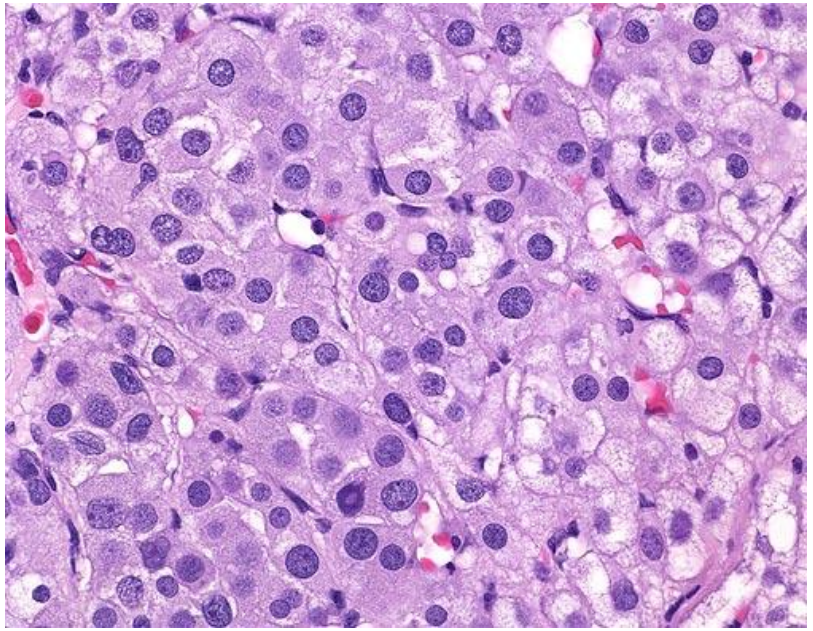

Criteria for the diagnosis of adrenal cortical carcinoma

	HHS	WS	VSS
Capsular invasion	+	+	+
Venous invasion	+	+	+
Sinusoidal invasion	+		
Broad fibrous bands	+		
Diffuse architecture	+	+	
Necrosis	+	+	+
Clear cells (<25%)		+	
Pleomorphism/high grade +	+	+	
Mitoses	+	+	+
Atypical mitoses		+	
Abnormal nucleoli			+

Criteria for the diagnosis of adrenal cortical carcinoma

	HS	WS	VSS
Weight of tumor (>100 g)	+		
Clinical features			
Urinary 17-Ketogenic steroids	+		
Response to ACTH	+		
Weight loss	+		

Full serum steroid panel discriminates ACC from other adrenal lesions

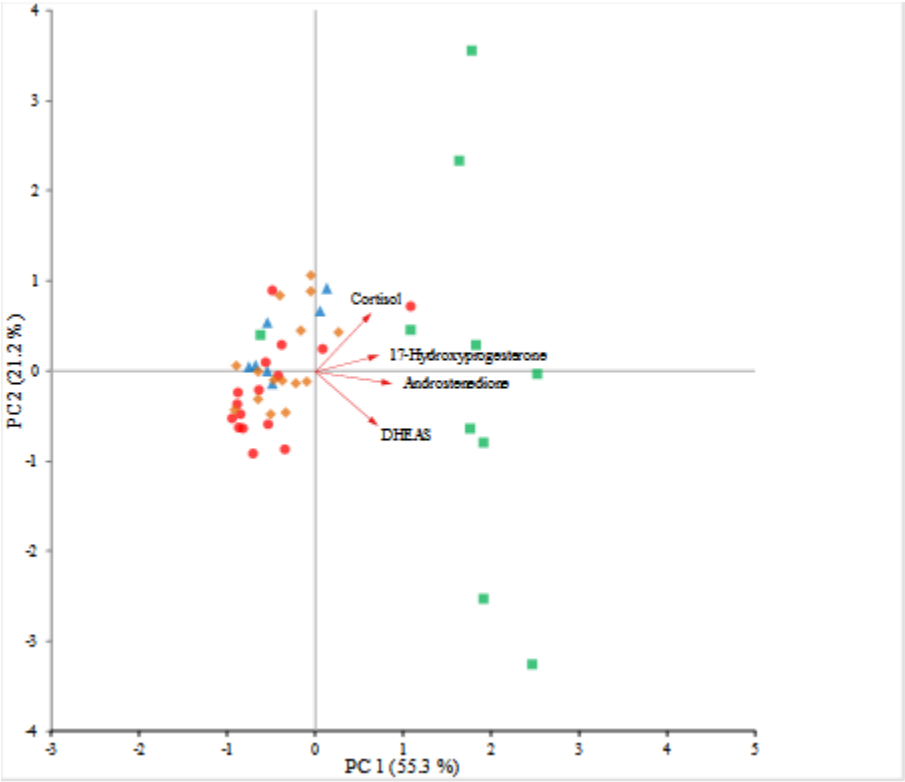

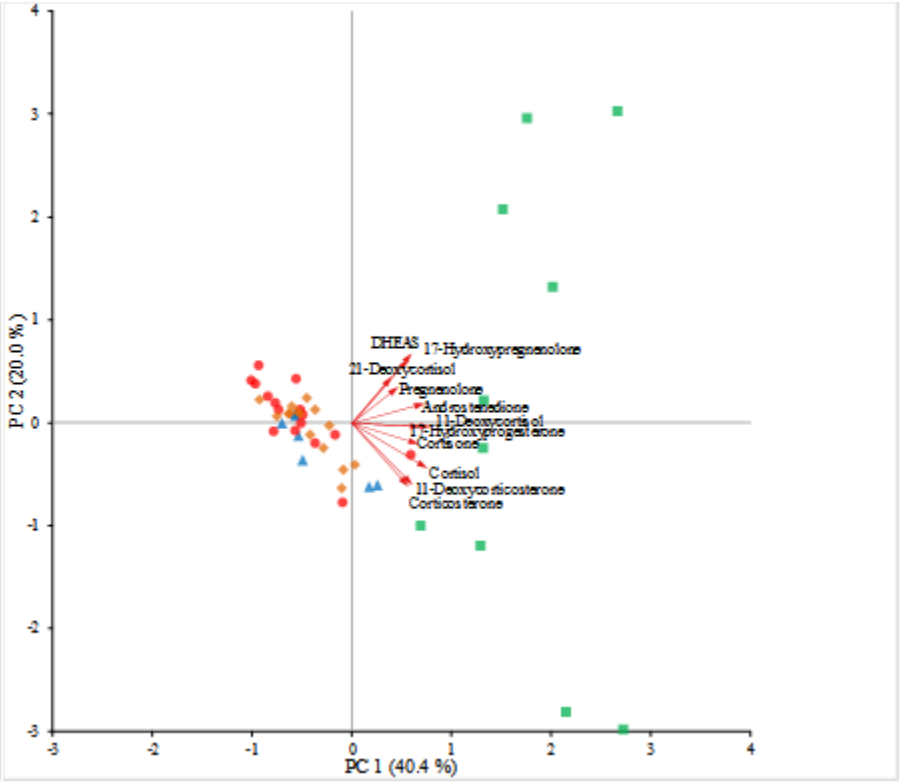

Hough Histologic Score

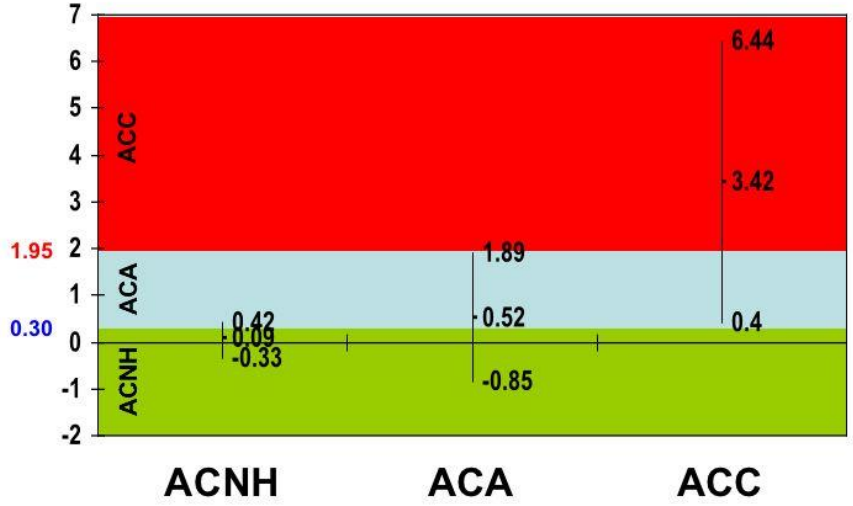

Weiss System

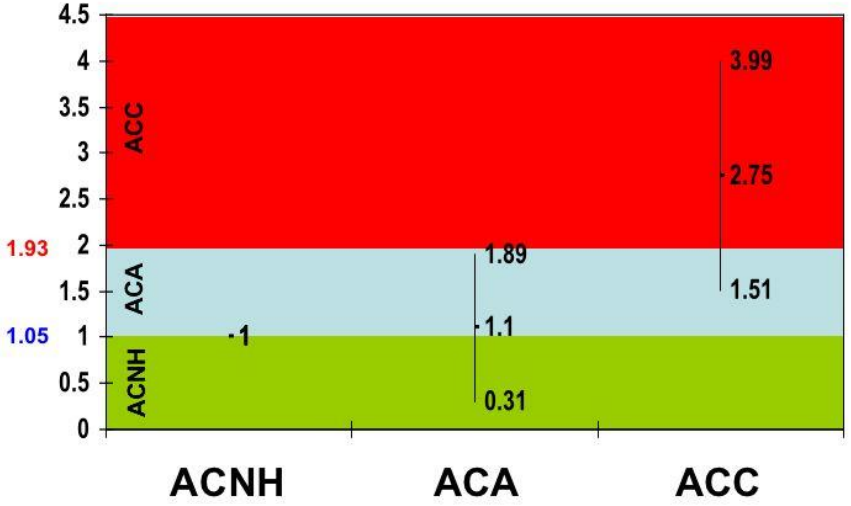

Van Slooten System

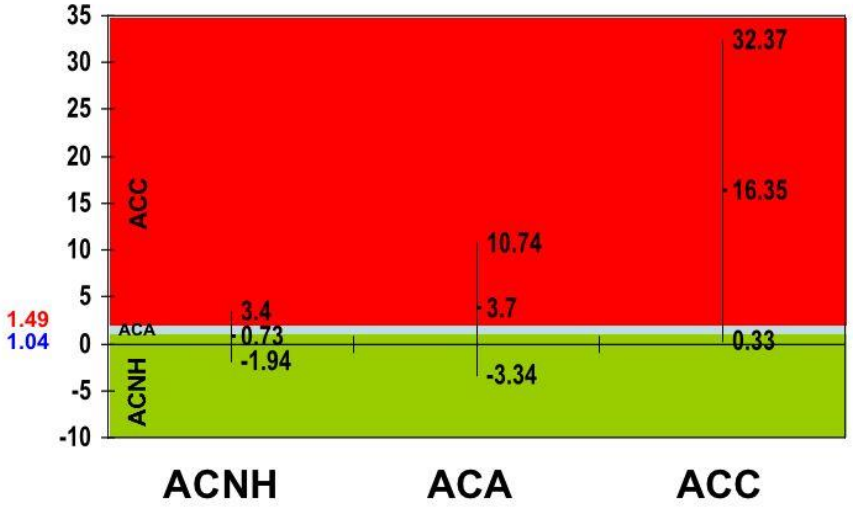

Blanes, Diaz-Cano. **Am J Clin Pathol** 2007;127:398-408

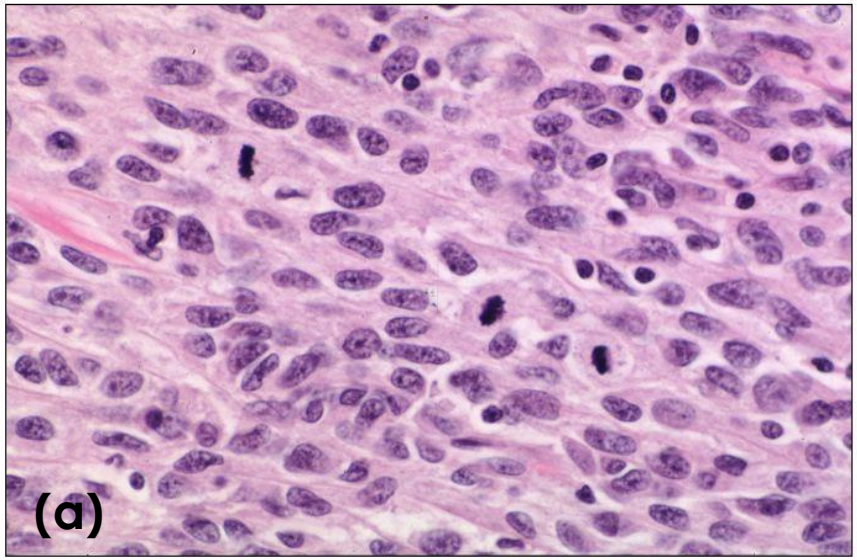

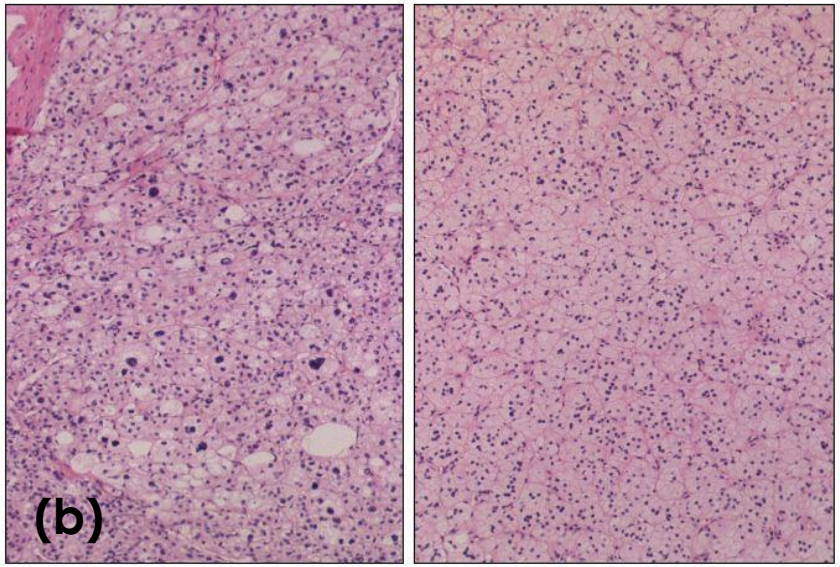

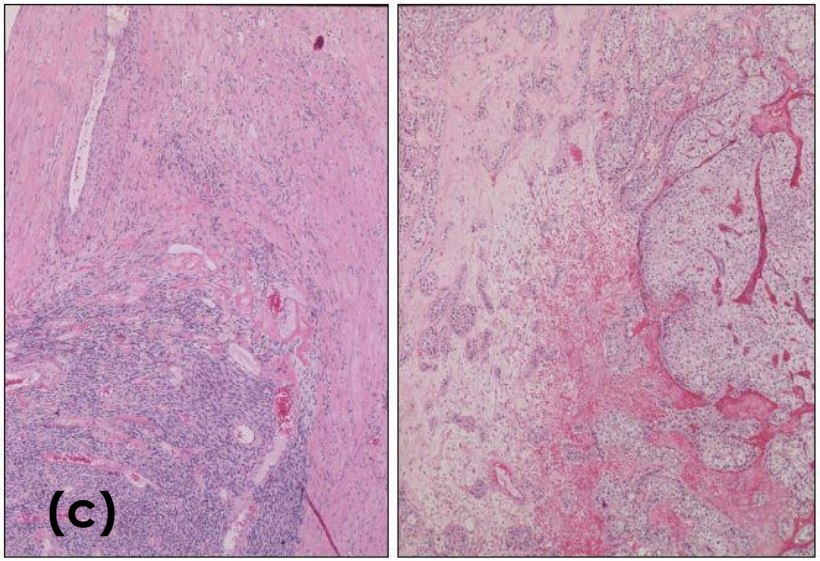

Blanes, Diaz-Cano. **Am J Clin Pathol** 2007;127:398-408

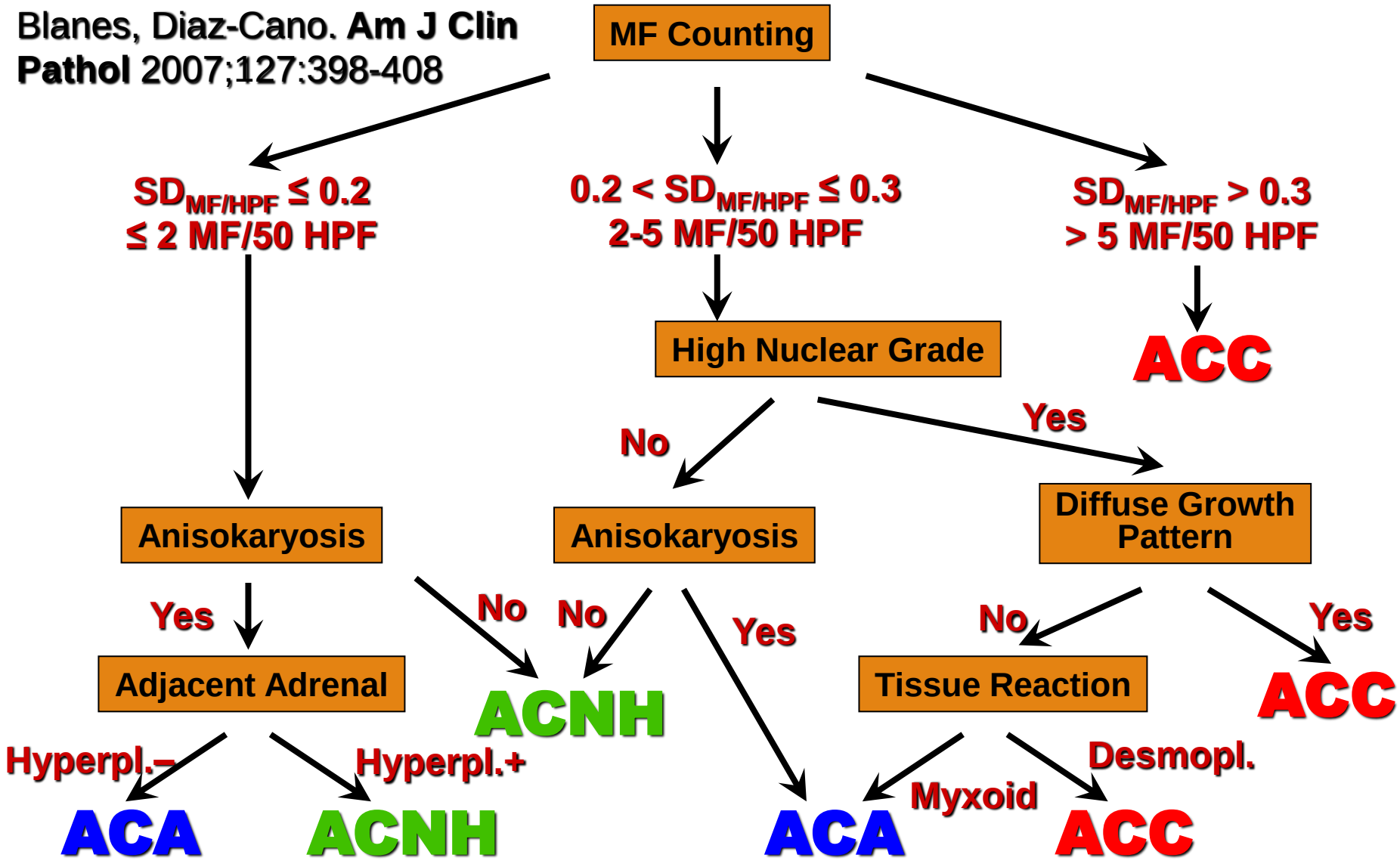
Blanes, Diaz-Cano. Am J Clin Pathol 2007;127:398-408
MF Counting
SD MF/HPF ≤ 0.2
≤ 2 MF/50 HPF
0.2 < SD MF/HPF ≤ 0.3
2-5 MF/50 HPF
SD MF/HPF > 0.3
> 5 MF/50 HPF
ACC
High Nuclear Grade
No
Yes
Anisokaryosis
Anisokaryosis
Diffuse Growth Pattern
Yes
No
No
Yes
No
Yes
Adjacent Adrenal
ACNH
Tissue Reaction
ACC
Hyperpl.–
Hyperpl.+
Desmopl.
Myxoid
ACA
ACNH
ACA
ACC

Gene Expression in ACPL

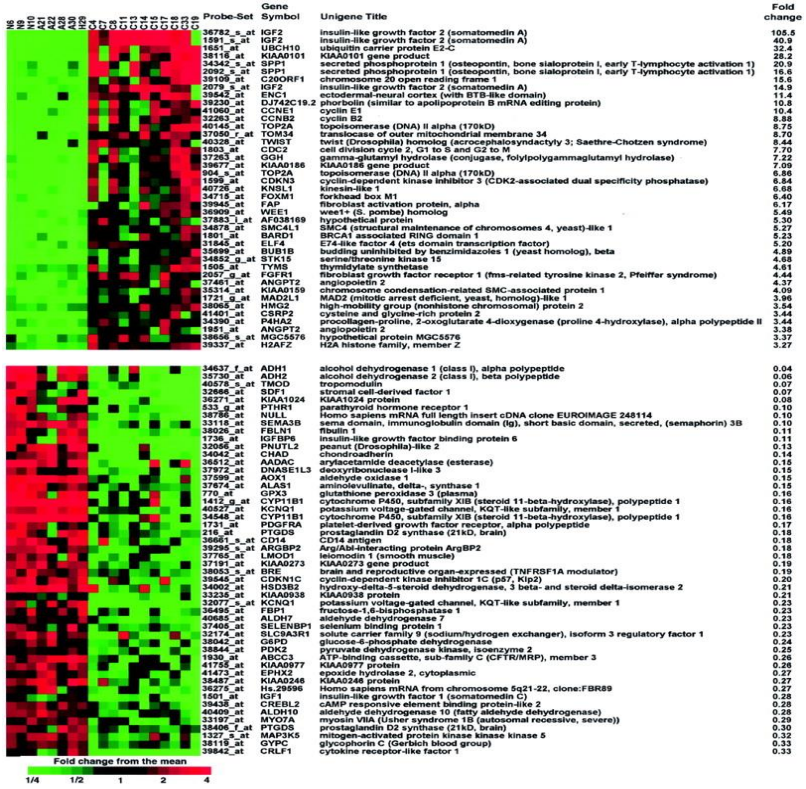

Probe-Set	Gene Symbol	Unigene Title	Fold change
36782_s_at	IGF2	insulin-like growth factor 2 (somatomedin A)	105.5
1591_s_at	IGF2	insulin-like growth factor 2 (somatomedin A)	40.9
1651_at	UBCH10	ubiquitin carrier protein E2-C	32.4
38118_at	KIAA0101	KIAA0101 gene product	28.2
34342_s_at	SPP1	secreted phosphoprotein 1 (osteopontin, bone sialoprotein I, early T-lymphocyte activation 1)	20.9
2092_s_at	SPP1	secreted phosphoprotein 1 (osteopontin, bone sialoprotein I, early T-lymphocyte activation 1)	16.6
39108_at	C20ORF1	chromosome 20 open reading frame 1	15.6
2079_s_at	IGF2	insulin-like growth factor 2 (somatomedin A)	14.9
39542_at	ENC1	ectodermal-neural cortex (with BTB-like domain)	11.4
39230_at	DJ742C19.2	phorbolin (similar to apolipoprotein B mRNA editing protein)	10.8
41060_at	CCNE1	cyclin E1	10.4
32263_at	CCNB2	cyclin B2	8.88
40145_at	TOP2A	topoisomerase (DNA) II alpha (170kD)	8.75
37050_r_at	TOM34	translocase of outer mitochondrial membrane 34	8.70
40328_at	TWIST	twist (Drosophila) homolog (acrocephalosyndactyly 3; Saethre-Chotzen syndrome)	8.44
1803_at	CDC2	cell division cycle 2, G1 to S and G2 to M	7.70
37263_at	GGH	gamma-glutamyl hydrolase (conjugase, folylpolygammaglutamyl hydrolase)	7.22
39677_at	KIAA0186	KIAA0186 gene product	7.09
904_s_at	TOP2A	topoisomerase (DNA) II alpha (170kD)	6.86
1598_at	CDKN3	cyclin-dependent kinase inhibitor 3 (CDK2-associated dual specificity phosphatase)	6.84
40728_at	KNSL1	kinesin-like 1	6.68
34715_at	FOXM1	forkhead box M1	6.40
39945_at	FAP	fibroblast activation protein, alpha	6.17
36909_at	WEE1	wee1+ (S. pombe) homolog	5.49
37883_i_at	AF038169	hypothetical protein	5.30
34878_at	SMC4L1	SMC4 (structural maintenance of chromosomes 4, yeast)-like 1	5.27
1801_at	BARD1	BRCA1 associated RING domain 1	5.23
31845_at	ELF4	E74-like factor 4 (ets domain transcription factor)	5.20
35699_at	BUB1B	budding uninhibited by benzimidazoles 1 (yeast homolog), beta	4.89
34852_g_at	STK15	serine/threonine kinase 15	4.68
1508_at	TYMS	thymidylate synthetase	4.61
2057_s_at	FGFR1	fibroblast growth factor receptor 1 (fms-related tyrosine kinase 2, Pfeiffer syndrome)	4.44
37461_at	ANGPT2	angiopoietin 2	4.37
35314_at	KIAA0159	chromosome condensation-related SMC-associated protein 1	4.09
1721_g_at	MAD2L1	MAD2 (mitotic arrest deficient, yeast, homolog)-like 1	3.96
38065_at	HMG2	high-mobility group (nonhistone chromosomal) protein 2	3.54
41401_at	CSRP2	cysteine and glycine-rich protein 2	3.44
34390_at	P4HA2	procollagen-proline, 2-oxoglutarate 4-dioxygenase (proline 4-hydroxylase), alpha polypeptide II	3.44
1851_at	ANGPT2	angiopoietin 2	3.38
38656_s_at	MGC5576	hypothetical protein MGC5576	3.37
39337_at	H2AFZ	H2A histone family, member Z	3.27
34637_f_at	ADH1	alcohol dehydrogenase 1 (class I), alpha polypeptide	0.04
35730_at	ADH2	alcohol dehydrogenase 2 (class I), beta polypeptide	0.06
40578_s_at	TMOD	tropomodulin	0.07
32866_at	SDF1	stromal cell-derived factor 1	0.07
36271_at	KIAA1024	KIAA1024 protein	0.08
533_g_at	PTHR1	parathyroid hormone receptor 1	0.10
38786_at	NULL	Homo sapiens mRNA full length insert cDNA clone EUROIMAGE 248114	0.10
33118_at	SEMA3B	sema domain, immunoglobulin domain (Ig), short basic domain, secreted, (semaphorin) 3B	0.10
38026_at	FBLN1	fibulin 1	0.11
1736_at	IGFBP6	insulin-like growth factor binding protein 6	0.11
32056_at	PNUTL2	peanut (Drosophila)-like 2	0.13
34042_at	CHAD	chondroadherin	0.14
36512_at	AADAC	arylacetamide deacetylase (esterase)	0.14
37972_at	DNASE1L3	deoxyribonuclease I-like 3	0.15
37599_at	AOX1	aldehyde oxidase 1	0.15
37674_at	ALAS1	aminolevulinate, delta-, synthase 1	0.15
770_at	GPX3	glutathione peroxidase 3 (plasma)	0.16
1412_g_at	CYP11B1	cytochrome P450, subfamily XIB (steroid 11-beta-hydroxylase), polypeptide 1	0.16
40527_at	KCNQ1	potassium voltage-gated channel, KQT-like subfamily, member 1	0.16
34548_at	CYP11B1	cytochrome P450, subfamily XIB (steroid 11-beta-hydroxylase), polypeptide 1	0.16
1731_at	PDGFRA	platelet-derived growth factor receptor, alpha polypeptide	0.17
216_at	PTGDS	prostaglandin D2 synthase (21kD, brain)	0.18
36681_s_at	CD14	CD14 antigen	0.18
39295_s_at	ARGBP2	Arg/Abl-interacting protein ArgBP2	0.18
37765_at	LMOD1	leiomodin 1 (smooth muscle)	0.18
37191_at	KIAA0273	KIAA0273 gene product	0.19
38053_s_at	BRE	brain and reproductive organ-expressed (TNFRSF1A modulator)	0.19
39546_at	CDKN1C	cyclin-dependent kinase inhibitor 1C (p57, Kip2)	0.20
34002_at	HSD3B2	hydroxy-delta-5-steroid dehydrogenase, 3 beta- and steroid delta-isomerase 2	0.21
33235_at	KIAA0938	KIAA0938 protein	0.21
32077_s_at	KCNQ1	potassium voltage-gated channel, KQT-like subfamily, member 1	0.23
36495_at	FBP1	fructose-1,6-biphosphatase 1	0.23
40685_at	ALDH7	aldehyde dehydrogenase 7	0.23
37406_at	SELENBP1	selenium binding protein 1	0.23
32174_at	SLC9A3R1	solute carrier family 9 (sodium/hydrogen exchanger), isoform 3 regulatory factor 1	0.23
38042_at	G6PD	glucose-6-phosphate dehydrogenase	0.24
38844_at	PDK2	pyruvate dehydrogenase kinase, isoenzyme 2	0.25
1930_at	ABCC3	ATP-binding cassette, sub-family C (CFTR/MRP), member 3	0.26
41758_at	KIAA0977	KIAA0977 protein	0.26
41473_at	EPHX2	epoxide hydrolase 2, cytoplasmic	0.27
38487_at	KIAA0248	KIAA0248 protein	0.27
36275_at	Hs.29596	Homo sapiens mRNA from chromosome 5q21-22, clone:FBR89	0.27
1501_at	IGF1	insulin-like growth factor 1 (somatomedin C)	0.28
39438_at	CREBL2	cAMP responsive element binding protein-like 2	0.28
40409_at	ALDH10	aldehyde dehydrogenase 10 (fatty aldehyde dehydrogenase)	0.28
33197_at	MYO7A	myosin VIIA (Usher syndrome 1B (autosomal recessive, severe))	0.29
38406_f_at	PTGDS	prostaglandin D2 synthase (21kD, brain)	0.30
1327_s_at	MAP3K5	mitogen-activated protein kinase kinase kinase 5	0.32
38119_at	GYPC	glycophorin C (Gerbich blood group)	0.33
39842_at	CRLF1	cytokine receptor-like factor 1	0.33

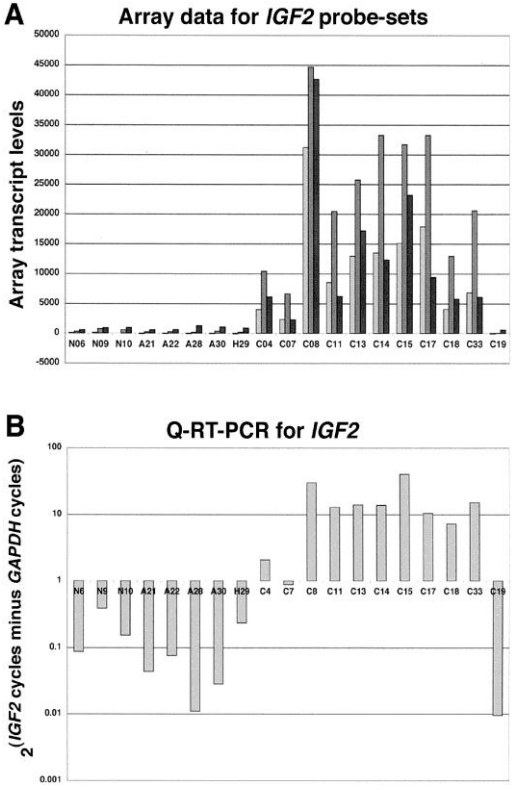

Am J Pathol 2003, 162:521–531

Gene Expression in ACPL

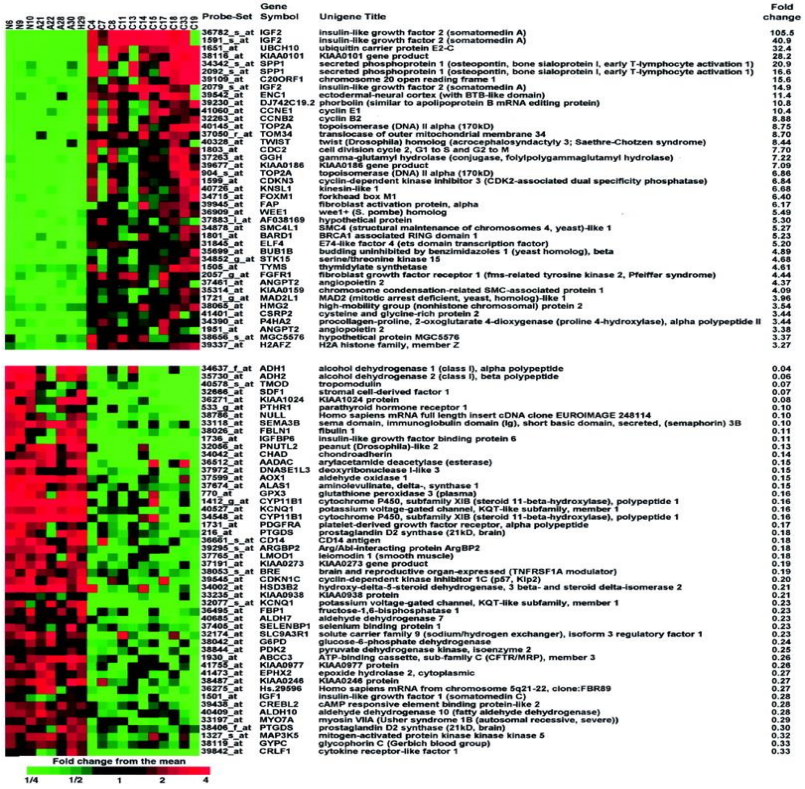

Probe-Set	Gene Symbol	Unigene Title	Fold change
36782_s_at	IGF2	insulin-like growth factor 2 (somatomedin A)	105.5
1591_s_at	IGF2	insulin-like growth factor 2 (somatomedin A)	40.9
1651_at	UBCH10	ubiquitin carrier protein E2-C	32.4
38118_at	KIAA0101	KIAA0101 gene product	28.2
34342_s_at	SPP1	secreted phosphoprotein 1 (osteopontin, bone sialoprotein I, early T-lymphocyte activation 1)	20.9
2092_s_at	SPP1	secreted phosphoprotein 1 (osteopontin, bone sialoprotein I, early T-lymphocyte activation 1)	16.6
39108_at	C20ORF1	chromosome 20 open reading frame 1	15.6
2079_s_at	IGF2	insulin-like growth factor 2 (somatomedin A)	14.9
39542_at	ENC1	ectodermal-neural cortex (with BTB-like domain)	11.4
39230_at	DJ742C19.2	phorbolin (similar to apolipoprotein B mRNA editing protein)	10.8
41060_at	CCNE1	cyclin E1	10.4
32263_at	CCNB2	cyclin B2	8.88
40145_at	TOP2A	topoisomerase (DNA) II alpha (170kD)	8.75
37090_r_at	TOM34	translocase of outer mitochondrial membrane 34	8.70
40328_at	TWIST	twist (Drosophila) homolog (acrocephalosyndactyly 3; Saethre-Chotzen syndrome)	8.44
1803_at	CDC2	cell division cycle 2, G1 to S and G2 to M	7.70
37253_at	GGH	gamma-glutamyl hydrolase (conjugase, folylpolygammaglutamyl hydrolase)	7.22
39677_at	KIAA0186	KIAA0186 gene product	7.09
904_s_at	TOP2A	topoisomerase (DNA) II alpha (170kD)	6.86
1598_at	CDKN3	cyclin-dependent kinase inhibitor 3 (CDK2-associated dual specificity phosphatase)	6.84
40728_at	KNSL1	kinesin-like 1	6.68
34715_at	FOXM1	forkhead box M1	6.40
39945_at	FAP	fibroblast activation protein, alpha	6.17
36909_at	WEE1	wee1+ (S. pombe) homolog	5.49
37883_i_at	AF038169	hypothetical protein	5.30
34870_at	SMC4L1	SMC4 (structural maintenance of chromosomes 4, yeast)-like 1	5.27
1801_at	BARD1	BRCA1 associated RING domain 1	5.23
31845_at	ELF4	E74-like factor 4 (ets domain transcription factor)	5.20
35699_at	BUB1B	budding uninhibited by benzimidazoles 1 (yeast homolog), beta	4.89
34852_g_at	STK15	serine/threonine kinase 15	4.68
1508_at	TYMS	thymidylate synthetase	4.61
2057_s_at	FGFR1	fibroblast growth factor receptor 1 (fms-related tyrosine kinase 2, Pfeiffer syndrome)	4.44
37461_at	ANGPT2	angiopoietin 2	4.37
35314_at	KIAA0159	chromosome condensation-related SMC-associated protein 1	4.09
1721_g_at	MAD2L1	MAD2 (mitotic arrest deficient, yeast, homolog)-like 1	3.96
38065_at	HMG2	high-mobility group (nonhistone chromosomal) protein 2	3.54
41401_at	CSRP2	cysteine and glycine-rich protein 2	3.44
34390_at	P4HA2	procollagen-proline, 2-oxoglutarate 4-dioxygenase (proline 4-hydroxylase), alpha polypeptide II	3.44
1851_at	ANGPT2	angiopoietin 2	3.38
38656_s_at	MGC5576	hypothetical protein MGC5576	3.37
39337_at	H2AFZ	H2A histone family, member Z	3.27
34637_f_at	ADH1	alcohol dehydrogenase 1 (class I), alpha polypeptide	0.04
35730_at	ADH2	alcohol dehydrogenase 2 (class I), beta polypeptide	0.06
40578_s_at	TMOD	tropomodulin	0.07
32866_at	SDF1	stromal cell-derived factor 1	0.07
36271_at	KIAA1024	KIAA1024 protein	0.08
533_g_at	PTHR1	parathyroid hormone receptor 1	0.10
38786_at	NULL	Homo sapiens mRNA full length insert cDNA clone EUROIMAGE 248114	0.10
33118_at	SEMA3B	sema domain, immunoglobulin domain (Ig), short basic domain, secreted, (semaphorin) 3B	0.10
38026_at	FBLN1	fibulin 1	0.11
1736_at	IGFBP6	insulin-like growth factor binding protein 6	0.11
32056_at	PNUTL2	peanut (Drosophila)-like 2	0.13
34042_at	CHAD	chondroadherin	0.14
36512_at	AADAC	arylacetamide deacetylase (esterase)	0.16
37972_at	DNASE1L3	deoxyribonuclease I-like 3	0.15
37599_at	AOX1	aldehyde oxidase 1	0.15
37674_at	ALAS1	aminolevulinate, delta-, synthase 1	0.15
770_at	GPX3	glutathione peroxidase 3 (plasma)	0.16
1412_g_at	CYP11B1	cytochrome P450, subfamily XIB (steroid 11-beta-hydroxylase), polypeptide 1	0.16
40527_at	KCNQ1	potassium voltage-gated channel, KQT-like subfamily, member 1	0.16
34548_at	CYP11B1	cytochrome P450, subfamily XIB (steroid 11-beta-hydroxylase), polypeptide 1	0.16
1731_at	PDGFRA	platelet-derived growth factor receptor, alpha polypeptide	0.17
216_at	PTGDS	prostaglandin D2 synthase (21kD, brain)	0.18
36661_s_at	CD14	CD14 antigen	0.18
39295_s_at	ARGBP2	Arg/Abl-interacting protein ArgBP2	0.18
37765_at	LMOD1	leiomodin 1 (smooth muscle)	0.18
37191_at	KIAA0273	KIAA0273 gene product	0.19
38053_s_at	BRE	brain and reproductive organ-expressed (TNFRSF1A modulator)	0.19
39546_at	CDKN1C	cyclin-dependent kinase inhibitor 1C (p57, Kip2)	0.20
34002_at	HSD3B2	hydroxy-delta-5-steroid dehydrogenase, 3 beta- and steroid delta-isomerase 2	0.21
33236_at	KIAA0938	KIAA0938 protein	0.21
32077_s_at	KCNQ1	potassium voltage-gated channel, KQT-like subfamily, member 1	0.23
34695_at	FBP1	fructose-1,6-bisphosphatase 1	0.23
40685_at	ALDH7	aldehyde dehydrogenase 7	0.23
37406_at	SELENBP1	selenium binding protein 1	0.23
32174_at	SLC9A3R1	solute carrier family 9 (sodium/hydrogen exchanger), isoform 3 regulatory factor 1	0.23
38042_at	G6PD	glucose-6-phosphate dehydrogenase	0.24
38844_at	PDK2	pyruvate dehydrogenase kinase, isoenzyme 2	0.25
1930_at	ABCC3	ATP-binding cassette, sub-family C (CFTR/MRP), member 3	0.26
41758_at	KIAA0977	KIAA0977 protein	0.26
41473_at	EPHX2	epoxide hydrolase 2, cytoplasmic	0.27
38487_at	KIAA0248	KIAA0248 protein	0.27
36275_at	Hs.29596	Homo sapiens mRNA from chromosome 5q21-22, clone:FBR89	0.27
1501_at	IGF1	insulin-like growth factor 1 (somatomedin C)	0.28
39438_at	CREBL2	cAMP responsive element binding protein-like 2	0.28
40409_at	ALDH10	aldehyde dehydrogenase 10 (fatty aldehyde dehydrogenase)	0.28
33197_at	MYO7A	myosin VIIA (Usher syndrome 1B (autosomal recessive, severe))	0.29
38406_f_at	PTGDS	prostaglandin D2 synthase (21kD, brain)	0.30
1327_s_at	MAP3K5	mitogen-activated protein kinase kinase kinase 5	0.32
38119_at	GYPC	glycophorin C (Gerbich blood group)	0.33
39842_at	CRLF1	cytokine receptor-like factor 1	0.33

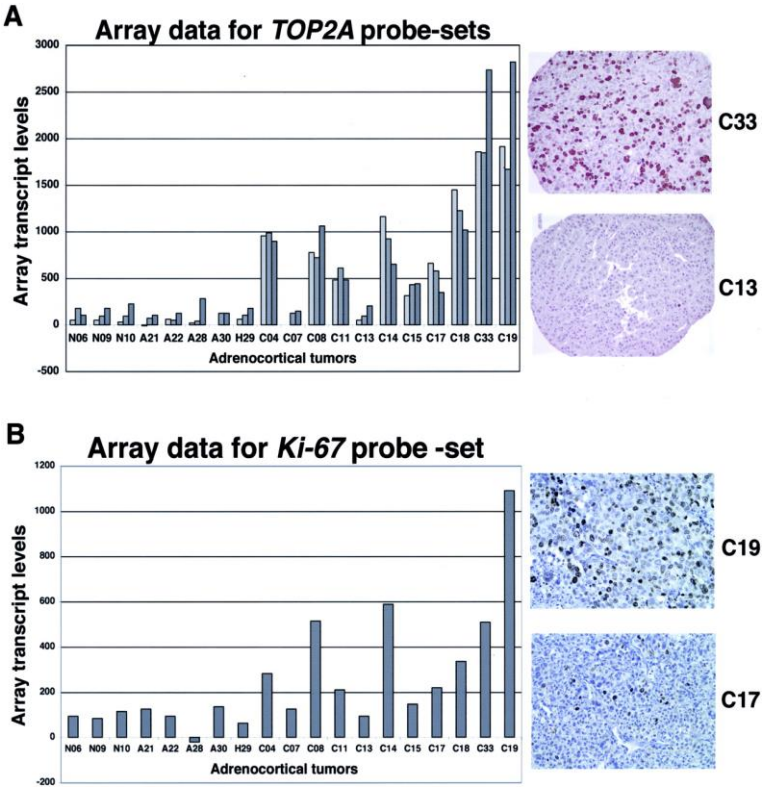

Am J Pathol 2003, 162:521–531

Gene Expression in ACPL

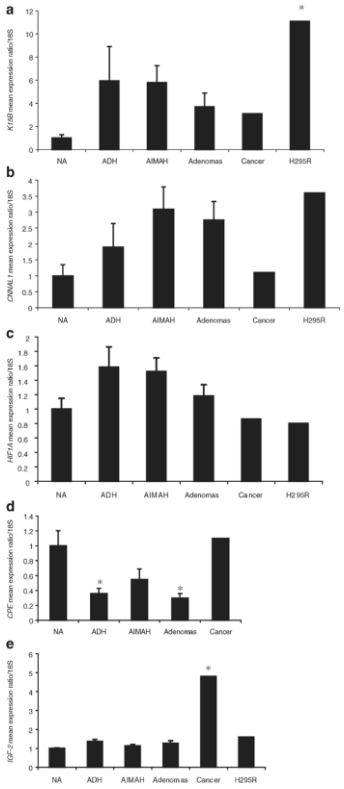

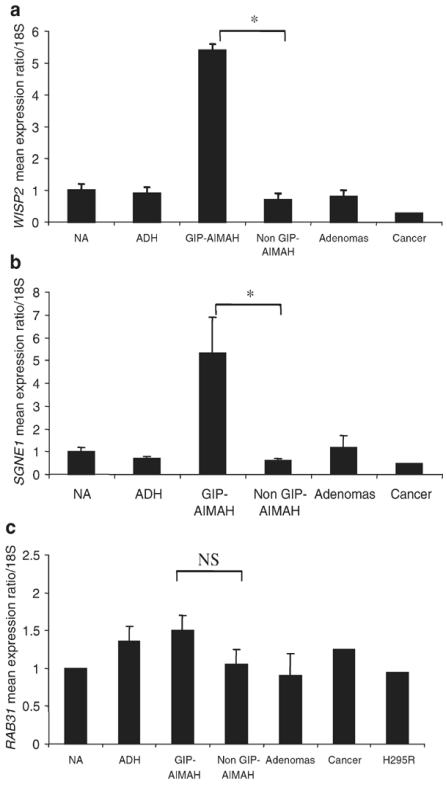

Oncogene (2004) 23, 1575–1585

ACC – Genomic Profiles

- **Standardized molecular data from 91 cases of adrenocortical carcinoma**
- **Driver genes including *TP53*, *ZNFR3*, *CTNNB1*, *PRKAR1A*, *CCNE1*, and *TERF2***
- **Whole-genome doubling event is a marker for ACC progression**
- **Three prognostic molecular subtypes captured by a DNA-methylation signature**

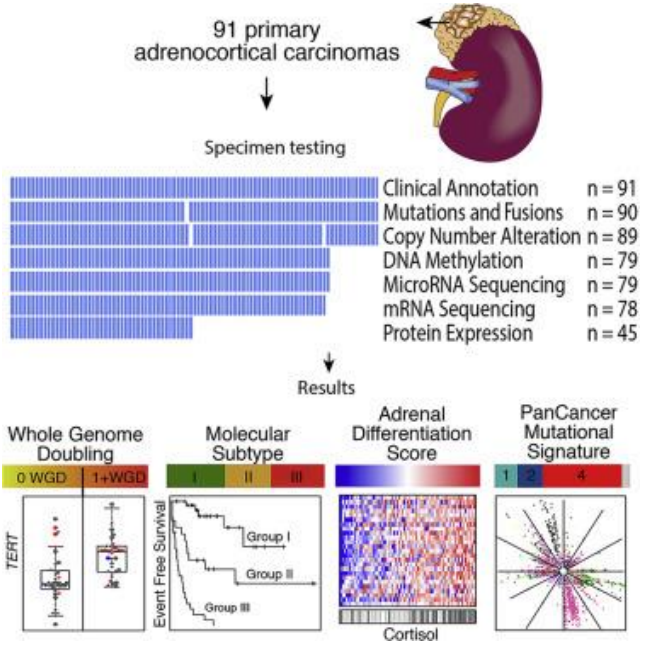

Cancer Cell. 2016 May 9;29(5):723-36.

Clonality and DNA - Kinetic Heterogeneity

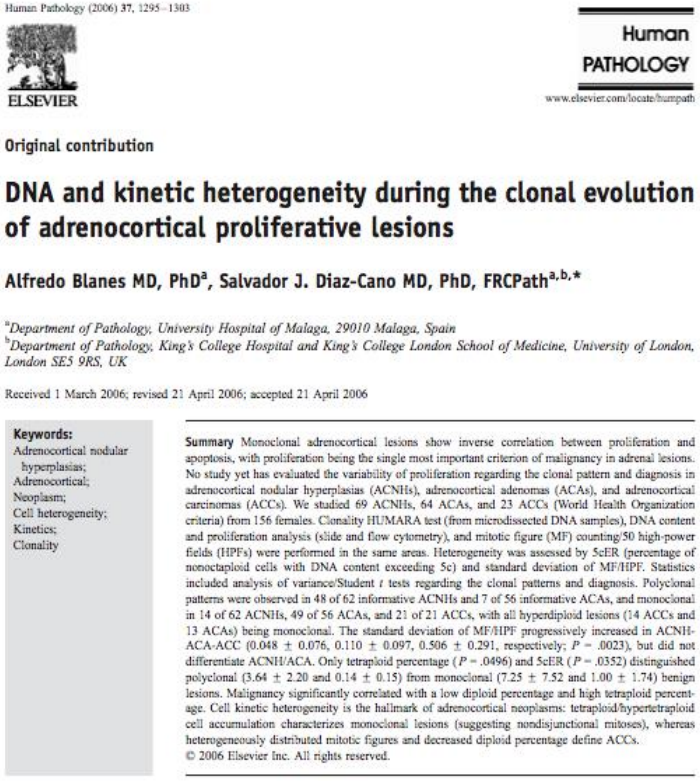

Human Pathology (2006) 37, 1295–1303

ELSEVIER

Human PATHOLOGY

www.elsevier.com/locate/humpath

Original contribution

DNA and kinetic heterogeneity during the clonal evolution of adrenocortical proliferative lesions

Alfredo Blanes MD, PhD[a], Salvador J. Diaz-Cano MD, PhD, FRCPath[a,b,*]

[a]*Department of Pathology, University Hospital of Malaga, 29010 Malaga, Spain*
[b]*Department of Pathology, King's College Hospital and King's College London School of Medicine, University of London, London SE5 9RS, UK*

Received 1 March 2006; revised 21 April 2006; accepted 21 April 2006

Keywords:
Adrenocortical nodular hyperplasias;
Adrenocortical;
Neoplasm;
Cell heterogeneity;
Kinetics;
Clonality

Summary Monoclonal adrenocortical lesions show inverse correlation between proliferation and apoptosis, with proliferation being the single most important criterion of malignancy in adrenal lesions. No study yet has evaluated the variability of proliferation regarding the clonal pattern and diagnosis in adrenocortical nodular hyperplasias (ACNHs), adrenocortical adenomas (ACAs), and adrenocortical carcinomas (ACCs). We studied 69 ACNHs, 64 ACAs, and 23 ACCs (World Health Organization criteria) from 156 females. Clonality HUMARA test (from microdissected DNA samples), DNA content and proliferation analysis (slide and flow cytometry), and mitotic figure (MF) counting/50 high-power fields (HPFs) were performed in the same areas. Heterogeneity was assessed by 5cER (percentage of nonoctaploid cells with DNA content exceeding 5c) and standard deviation of MF/HPF. Statistics included analysis of variance/Student *t* tests regarding the clonal patterns and diagnosis. Polyclonal patterns were observed in 48 of 62 informative ACNHs and 7 of 56 informative ACAs, and monoclonal in 14 of 62 ACNHs, 49 of 56 ACAs, and 21 of 21 ACCs, with all hyperdiploid lesions (14 ACCs and 13 ACAs) being monoclonal. The standard deviation of MF/HPF progressively increased in ACNH-ACA-ACC (0.048 ± 0.076, 0.110 ± 0.097, 0.506 ± 0.291, respectively; $P = .0023$), but did not differentiate ACNH/ACA. Only tetraploid percentage ($P = .0496$) and 5cER ($P = .0352$) distinguished polyclonal (3.64 ± 2.20 and 0.14 ± 0.15) from monoclonal (7.25 ± 7.52 and 1.00 ± 1.74) benign lesions. Malignancy significantly correlated with a low diploid percentage and high tetraploid percentage. Cell kinetic heterogeneity is the hallmark of adrenocortical neoplasms: tetraploid/hypertetraploid cell accumulation characterizes monoclonal lesions (suggesting nondisjunctional mitoses), whereas heterogeneously distributed mitotic figures and decreased diploid percentage define ACCs.
© 2006 Elsevier Inc. All rights reserved.

HUMARA

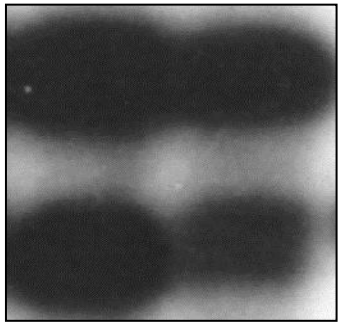

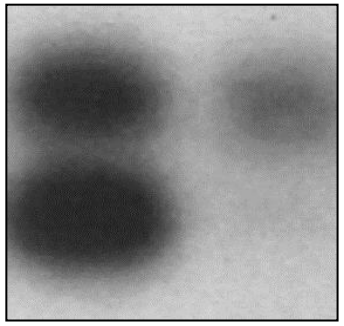

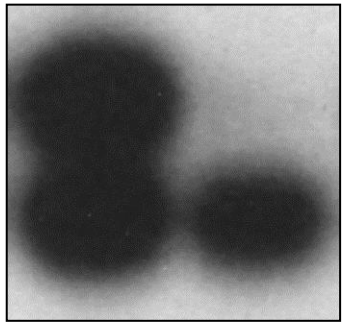

DNA Ploidy

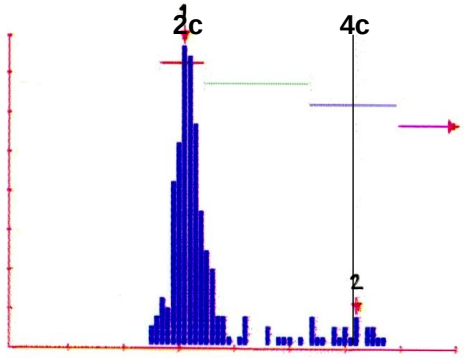

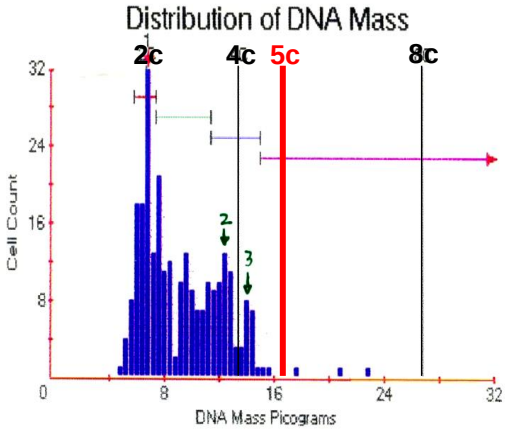

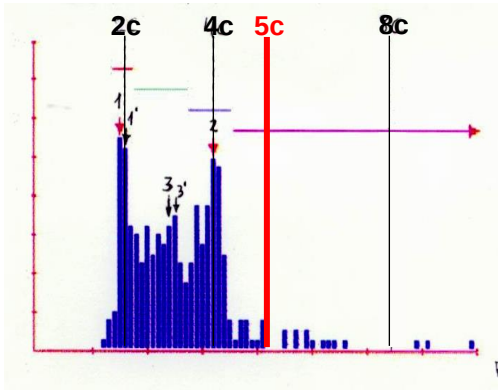

$SD_{MF/HPF}$

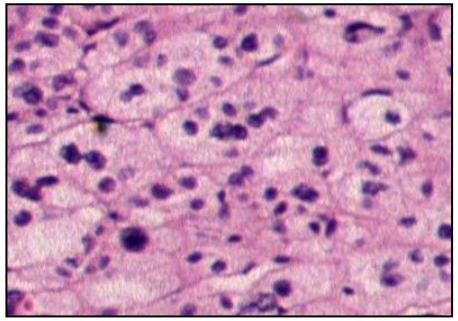

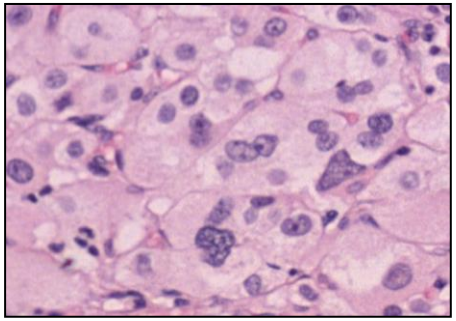

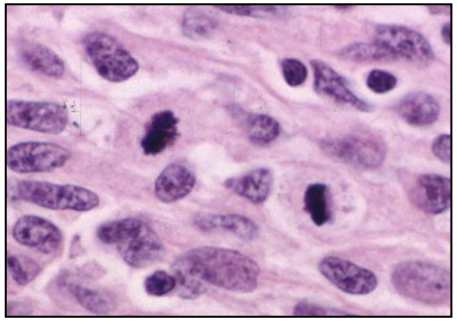

Polyclonal benign | **Monoclonal benign** | **Monoclonal malignant**

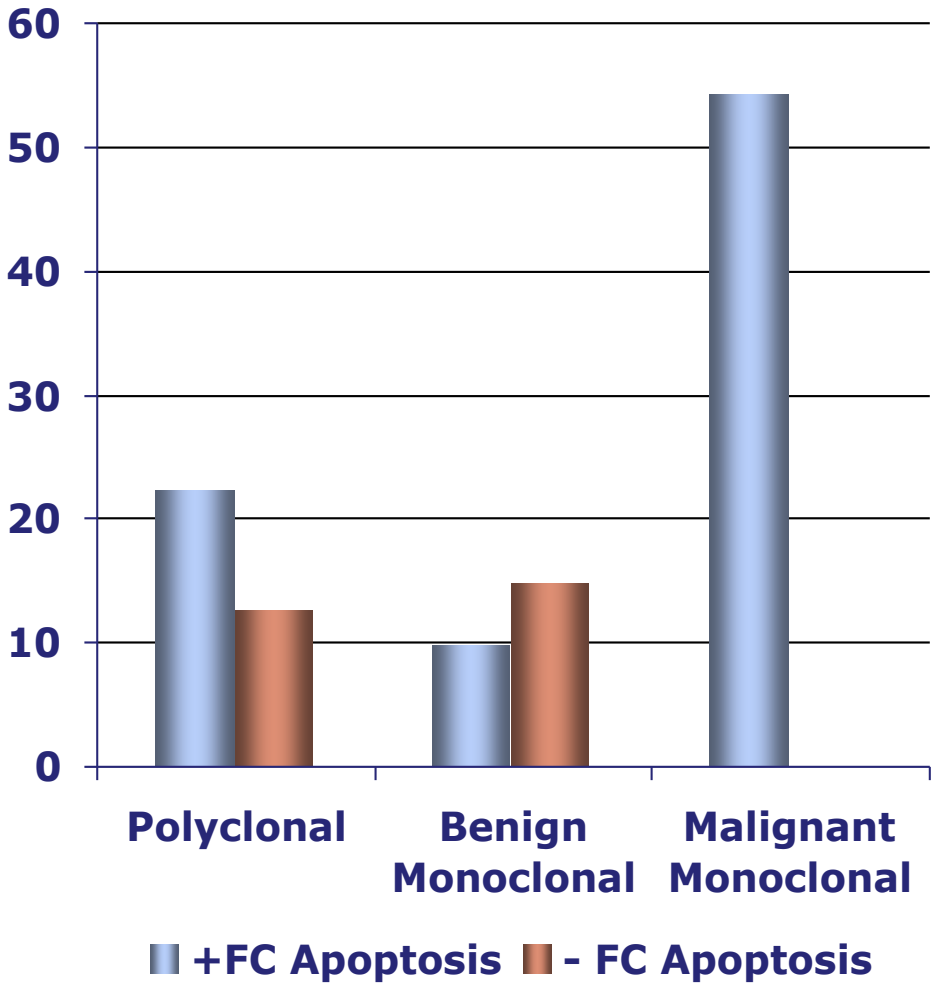

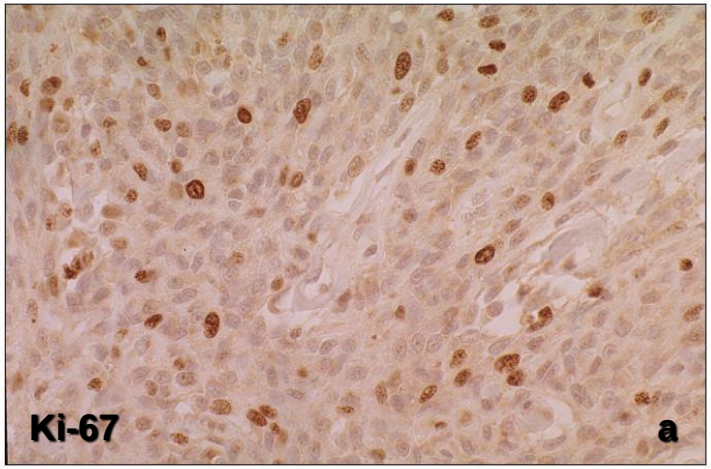

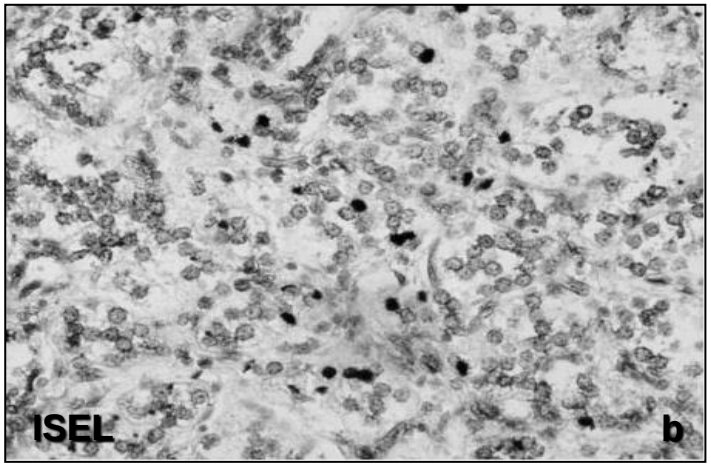

Blanes, Diaz-Cano. **Hum Pathol** 2006;37(10):1295-303.

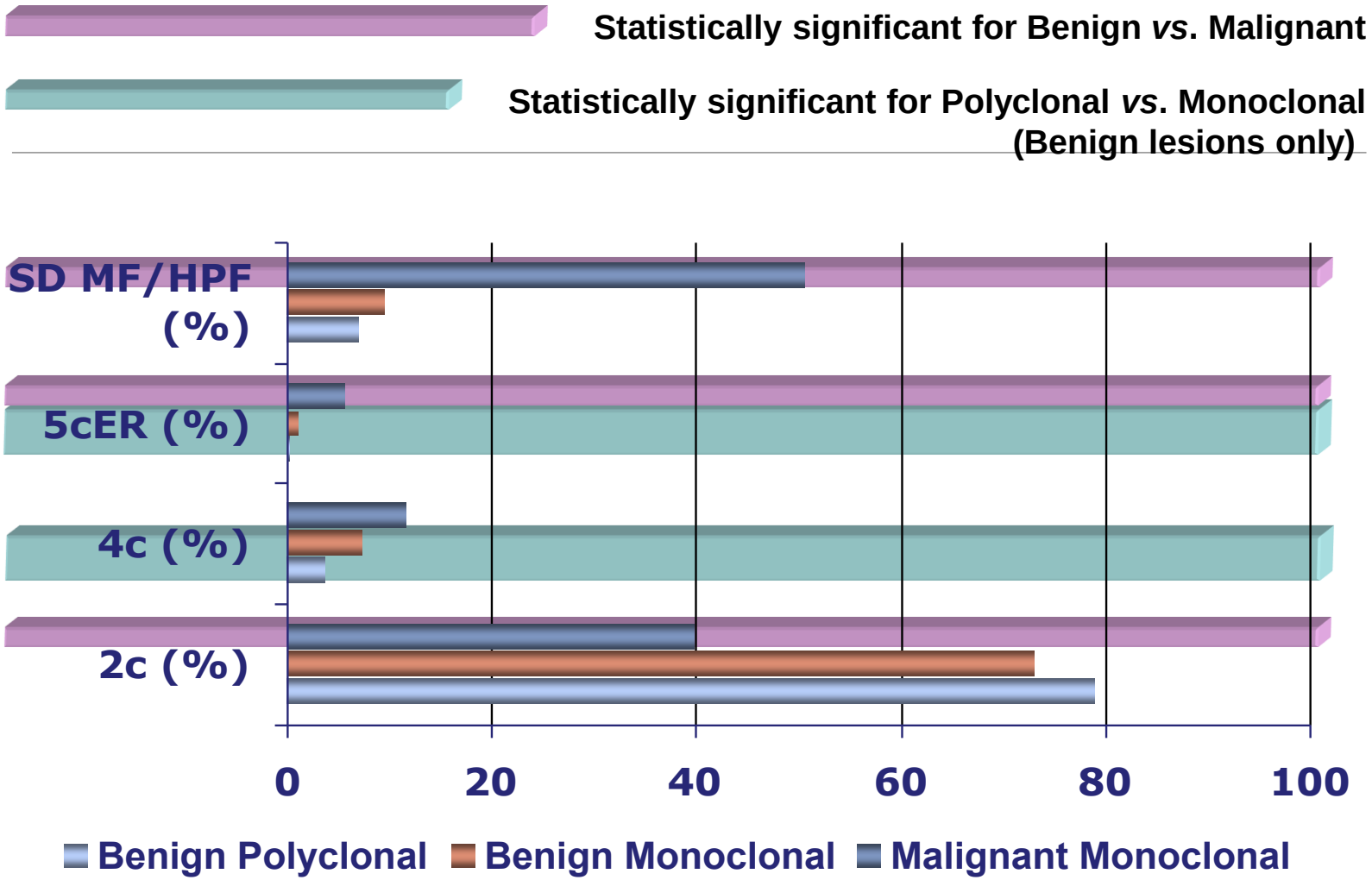

Blanes, Diaz-Cano. **Hum Pathol** 2006;37(10):1295-303.

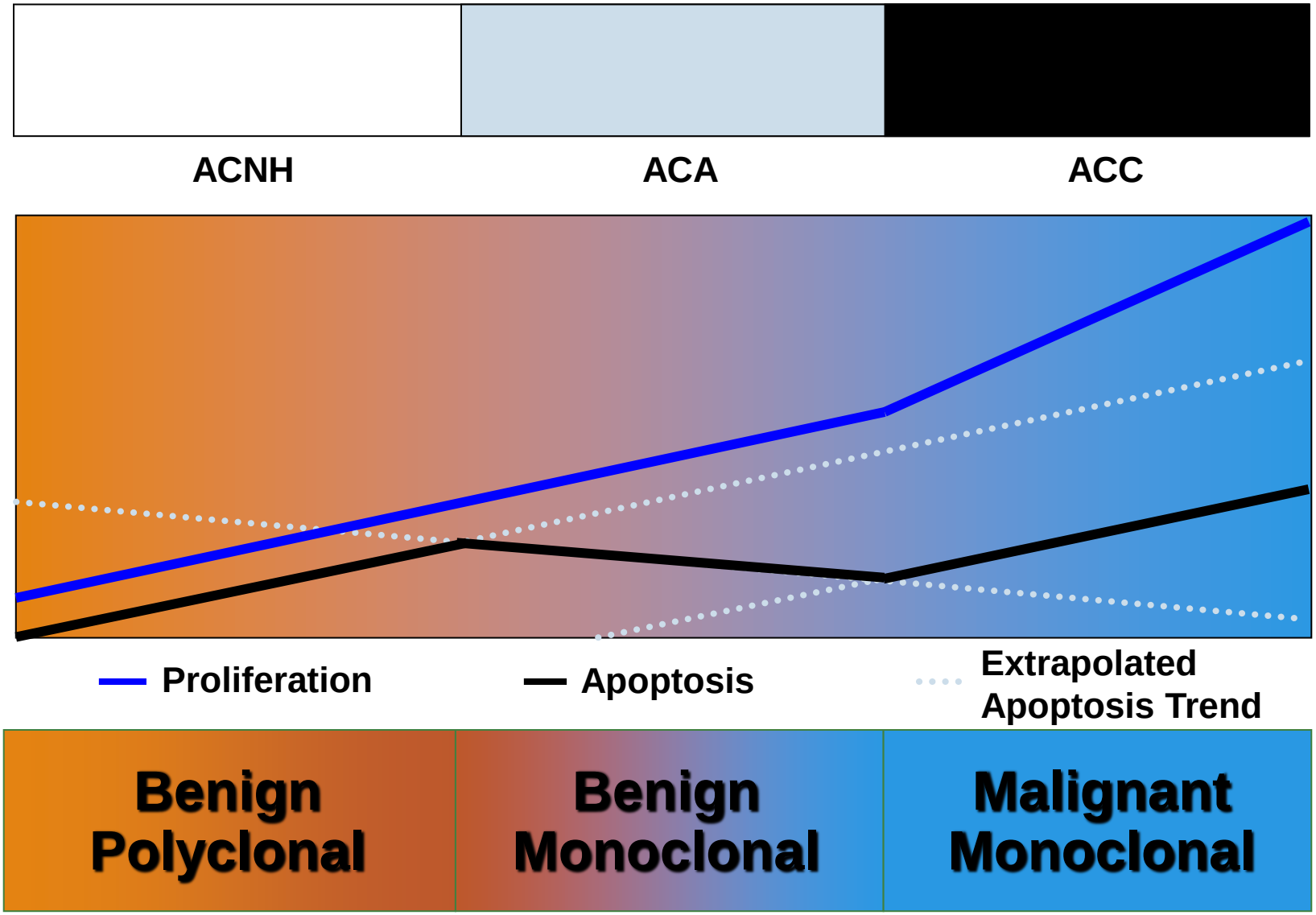

Blanes, Diaz-Cano. **Hum Pathol** 2006;37(10):1295-303.

Blanes, Diaz-Cano. **Hum Pathol** 2006;37(10):1295-303

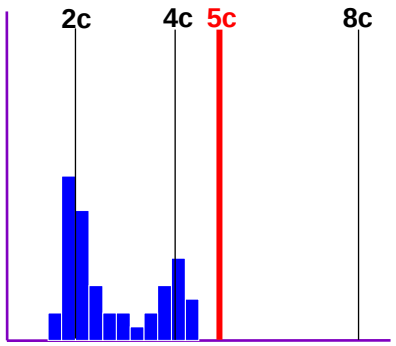

G_2 Arrest

Prophase

Metaphase

Anaphase

Apoptosis

G_2 Cell

2n/4c

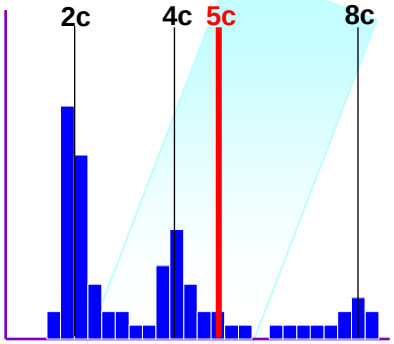

Cycling Tetraploid Cells

4n/4c

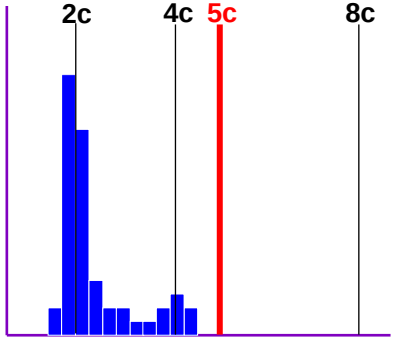

Normal Histogram

G_1 Cell

2n/2c

Cytokinesis

ACC - Molecular Genomic

- **Whole Genome Doubling is a hallmark of disease progression**
  - **Increased *TERT* expression,**
  - **Decreased telomere length, and**
  - **Activation of cell-cycle programs.**

Cancer Cell. 2016 May 9;29(5):723-36.

Cell Kinetic and Clonal Cell Segregation

American Journal of Pathology, Vol. 156, No. 1, January 2000
Copyright © American Society for Investigative Pathology

Clonality as Expression of Distinctive Cell Kinetics Patterns in Nodular Hyperplasias and Adenomas of the Adrenal Cortex

Salvador J. Díaz-Cano,*† Manuel de Miguel,‡ Alfredo Blanes,§ Robert Tashjian,* Hugo Galera,‡ and Hubert J. Wolfe*

From the Department of Pathology, Tufts University–New England Medical Center, Boston, Massachusetts; the Department of Pathology,† St Bartholomew's and the Royal London School of Medicine and Dentistry, London, United Kingdom; the Department of Pathology,‡ University Hospital of Seville, Seville, Spain; and the Department of Pathology,§ University Hospital of Malaga, Malaga, Spain*

gen receptor alleles in ACNHs and ACAs. ***(Am J Pathol 2000, 156:311–319)***

Neoplasms result from the progressive and convergent selection of cell populations, but several factors should be considered. On one hand, selection will determine tumor progression and cellular heterogeneity. On the other hand, cellular selection must be related to cell kinetics process.[1,2] All genetic abnormalities seen in tumors should be fixed on the transformed cell before ending in a fully established malignancy. These genetic changes must be cooperative and resistant to the cellular repair systems, and they must not activate the apoptosis

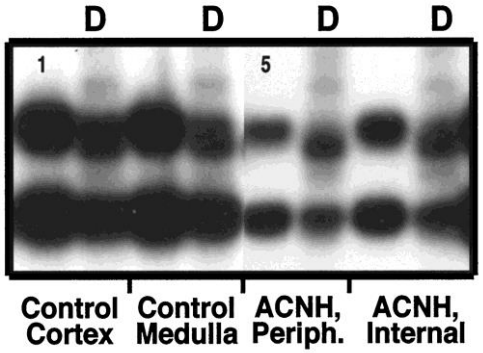

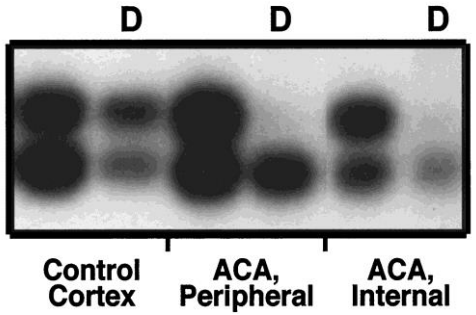

a

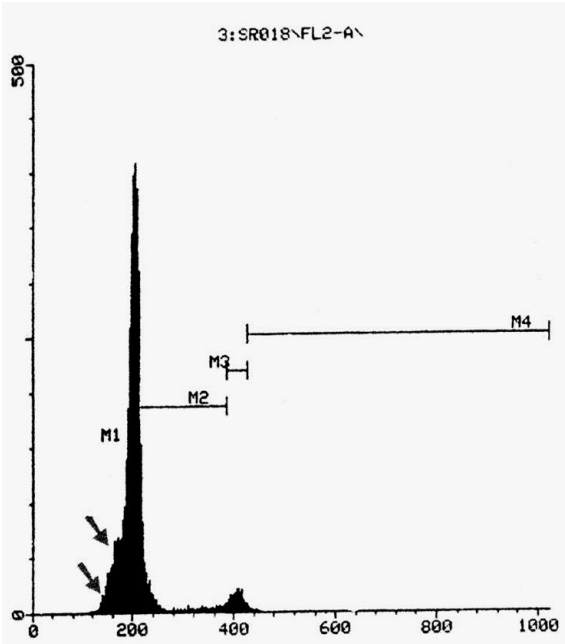

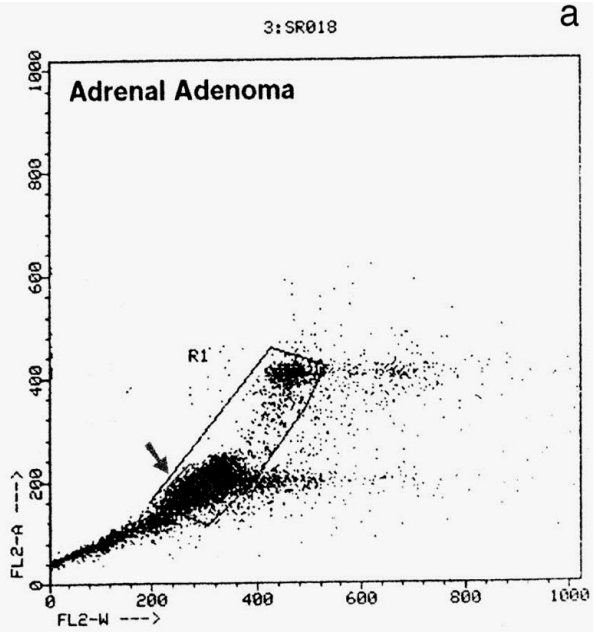

b

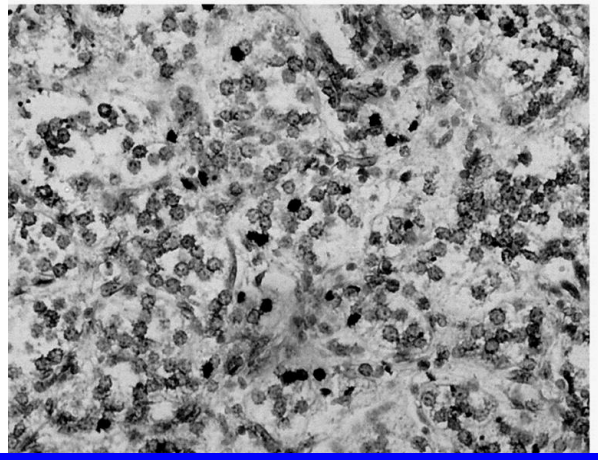

Clonality and Kinetics in Adrenal Cortex
Diaz-Cano et al. **Am J Pathol** 2000;156:311-319

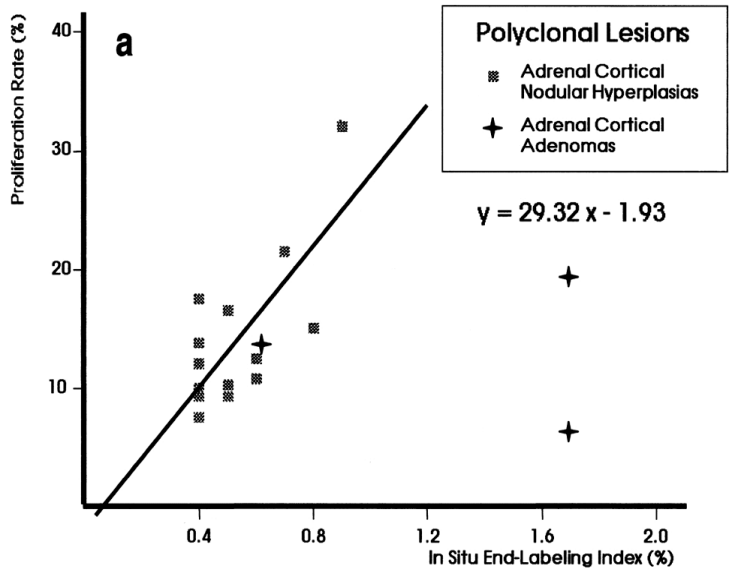
a
Polyclonal Lesions
Adrenal Cortical Nodular Hyperplasias
Adrenal Cortical Adenomas
y = 29.32 x - 1.93
Proliferation Rate (%)
In Situ End-Labeling Index (%)
40
30
20
10
0.4
0.8
1.2
1.6
2.0

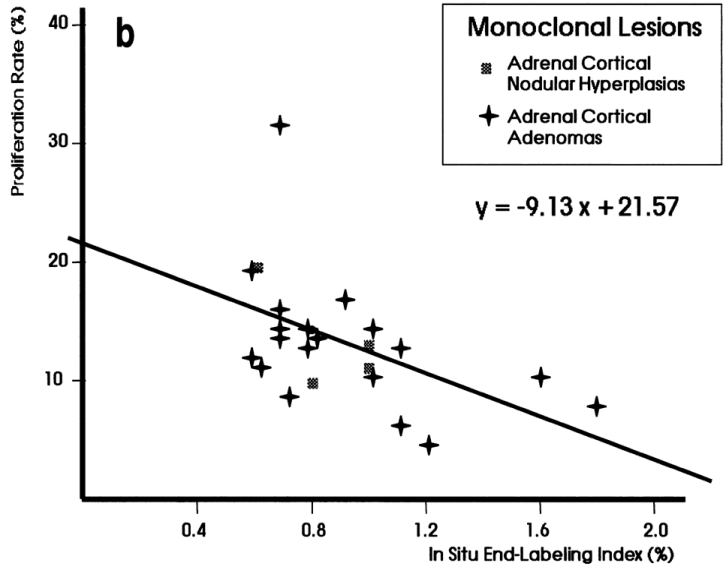
b
Monoclonal Lesions
Adrenal Cortical Nodular Hyperplasias
Adrenal Cortical Adenomas
y = -9.13 x + 21.57
Proliferation Rate (%)
In Situ End-Labeling Index (%)
40
30
20
10
0.4
0.8
1.2
1.6
2.0

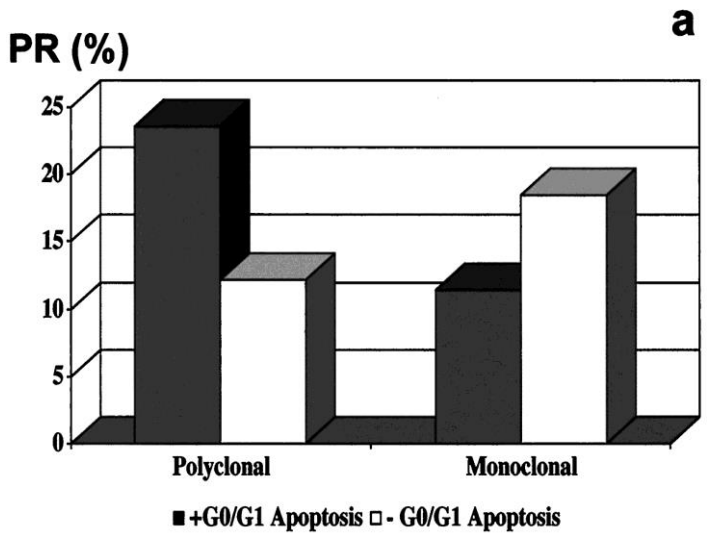
a
PR (%)
25
20
15
10
5
0
Polyclonal
Monoclonal
■ +G0/G1 Apoptosis □ - G0/G1 Apoptosis

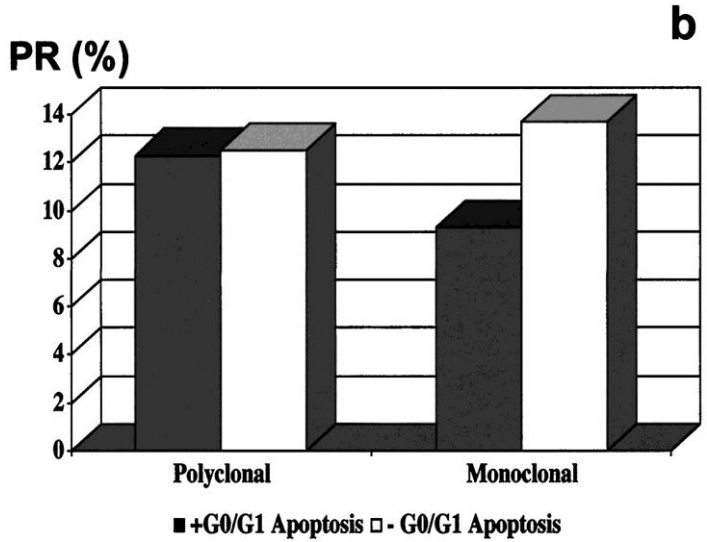
b
PR (%)
14
12
10
8
6
4
2
0
Polyclonal
Monoclonal
■ +G0/G1 Apoptosis □ - G0/G1 Apoptosis

Clonality as Expression of Distinctive Cell Kinetics

- **A distinctive correlation between proliferation and apoptosis, direct for ACNHs and inverse for ACAs, helps explain clone selection.**
- **The inverse correlation of kinetic parameters would provide the best selective mechanism resulting in dominant clone expansion (monoclonal) in ACAs, whereas direct correlation gives a less selective mechanism, allowing balanced expansion of clones (polyclonal) in ACNHs**

Clonality and Microvessels

Contribution of the Microvessel Network to the Clonal and Kinetic Profiles of Adrenal Cortical Proliferative Lesions

SALVADOR J. DIAZ-CANO, MD, PHD, MANUEL DE MIGUEL, PHD, ALFREDO BLANES, MD, PHD, HUGO GALERA, MD, PHD, AND HUBERT J. WOLFE, MD

Monoclonal adrenocortical lesions have been characterized by an inverse correlation between proliferation and apoptosis, and polyclonal lesions show a direct correlation. Their relationship with the vascular pattern remains unknown in adrenocortical nodular hyperplasias (ACNHs), adenomas (ACAs), and carcinomas (ACCs). We studied 20 ACNHs, 25 ACAs, and 10 ACCs (World Health Organization classification criteria) from 55 women. The analysis included X-chromosome inactivation assay (on microdissected samples), slide and flow cytometry, and in situ end labeling. Endothelial cells were stained with anti-CD31, and the blood vessel area and density were quantified by image analysis in the same areas. Appropriate tissue controls were run in every case. Regression analyses between kinetic and vascular features were performed in both polyclonal and monoclonal lesions. Polyclonal patterns were observed in 14 of 18 informative ACNHs and 3 of 22 informative ACAs, and monoclonal patterns were seen in 4 of 18 ACNHs, 19 of 22 ACAs, and 9 of 9 ACCs. A progressive increase in microvessel area was observed in the ACNH–ACA–ACC transition but was statistically significant between benign and malignant lesions only (191.36 ± 168.32 *v* 958.07 ± 1279.86 μm^2; $P < .0001$). In addition, case stratification by clonal pattern showed significant differences between polyclonal and monoclonal benign lesions; 6% of polyclonal and 57% of monoclonal lesions had microvessel area >186 μm^2 ($P = .0000008$). Monoclonal lesions showed parallel trends (but with opposite signs) for microvessel area and density in comparison with proliferation and apoptosis, whereas polyclonal lesions showed inverse trends. In conclusion, the kinetic advantage of monoclonal adrenal cortical lesions (increased proliferation, decreased apoptosis) is maintained by parallel increases in microvessel area and density. HUM PATHOL 32:1232-1239. Copyright © 2001 by W.B. Saunders Company

Key words: adrenal cortex, nodular hyperplasia, adenoma, carcinoma, clonality, proliferation, apoptosis, microvessel density.

Abbreviations: ACA, adrenocortical adenoma; ACC, adrenocortical carcinoma; ACNH, adrenocortical nodular hyperplasia; H&E, hematoxylin and eosin; PCR, polymerase chain reaction; HUMARA, human androgen receptor gene; ISEL, in situ end labeling.

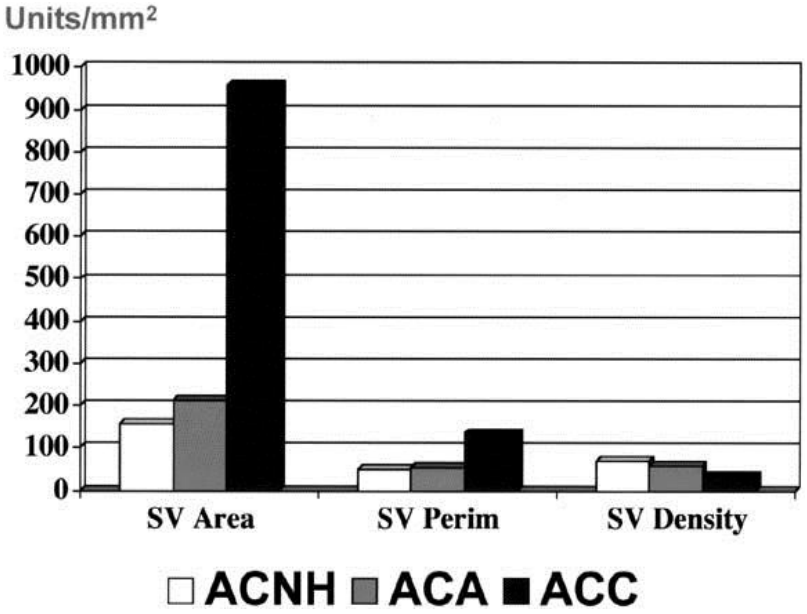

Clonality and Cell Kinetics

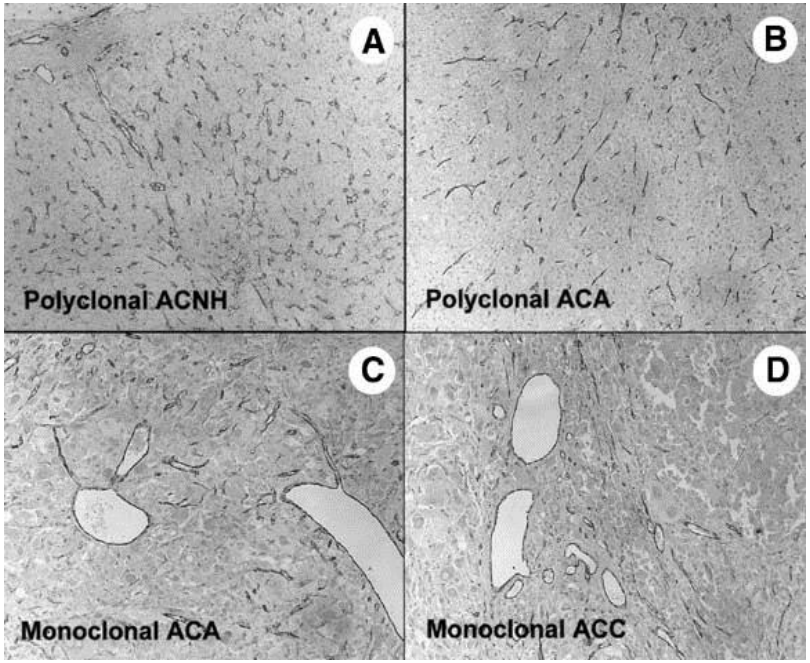

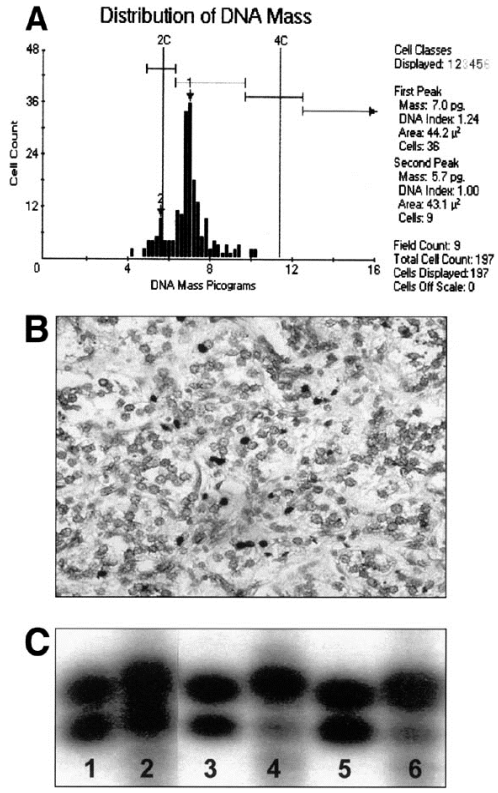

Cell Kinetics and Microvessels

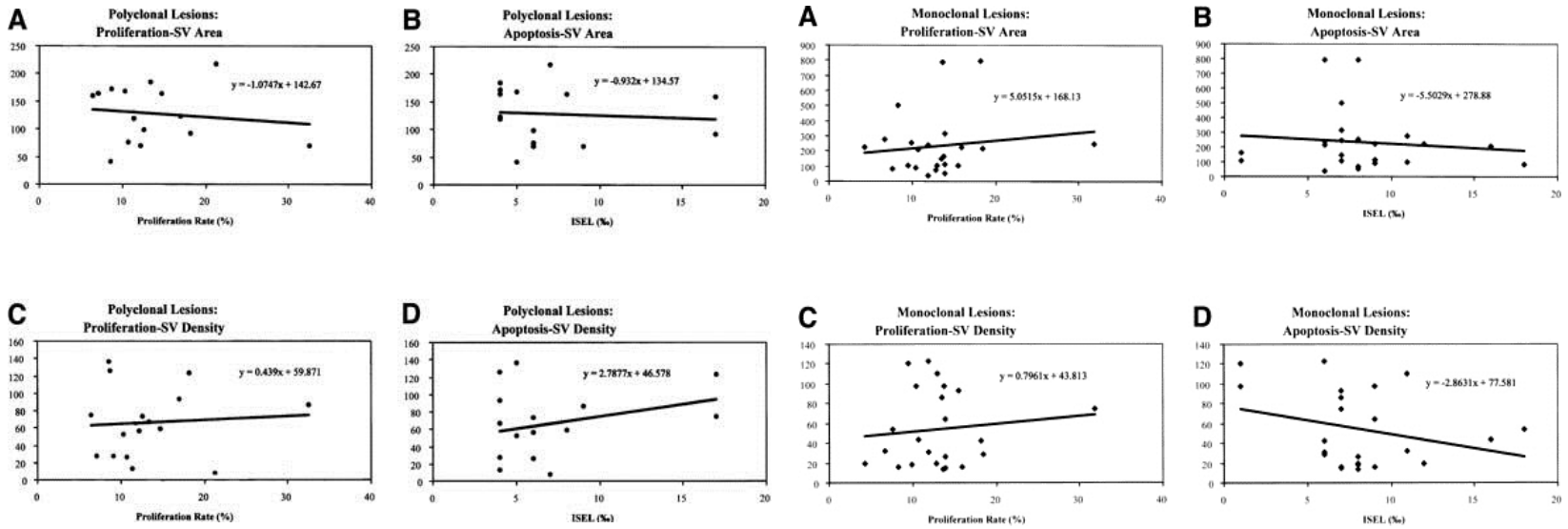

Clonality, Cell Kinetics, and Microvessel Network

The microvessel profile of monoclonal adrenocortical lesions is characterized by parallel increases in microvessel area and density that correlate directly with proliferation and inversely with apoptosis.

This distinctive microvessel pattern certainly helps maintain the kinetic advantage (high proliferation and low apoptosis), clonal cell selection, and eventually cellular progression in those lesions

Adrenocortical Proliferative Lesions

MORPHOLOGY AND FUNCTION

Control of Adrenal Cortical Secretion

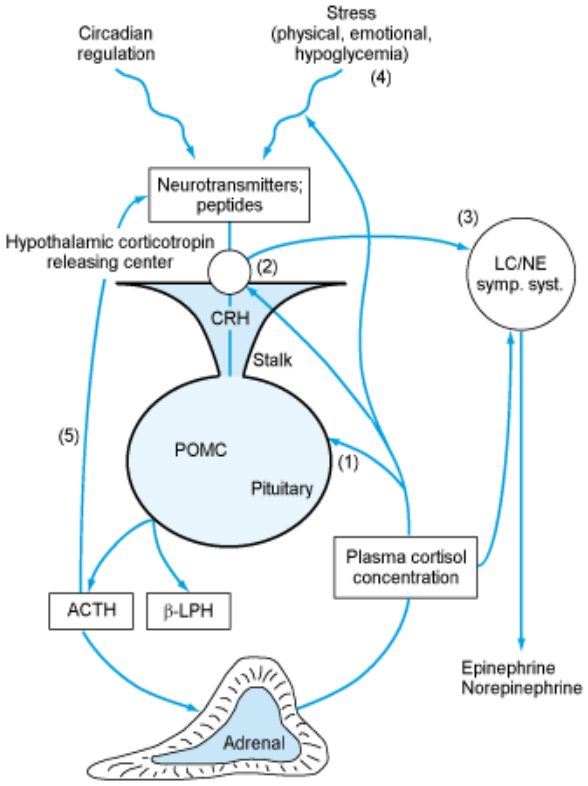

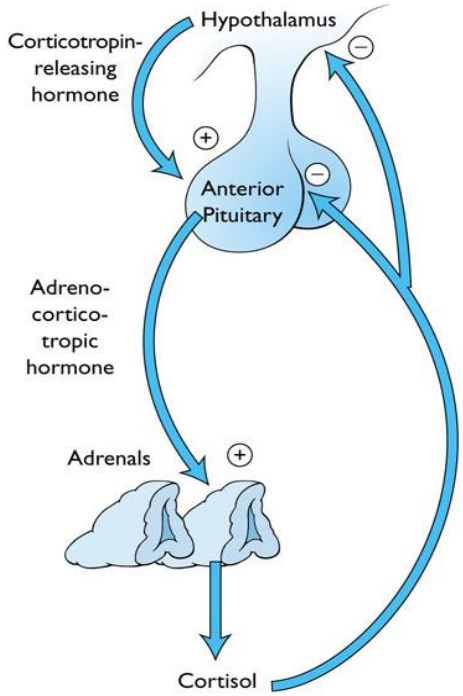

Hypothalamic-pituitary-adrenal axis in ACTH-dependent Cushing's syndrome

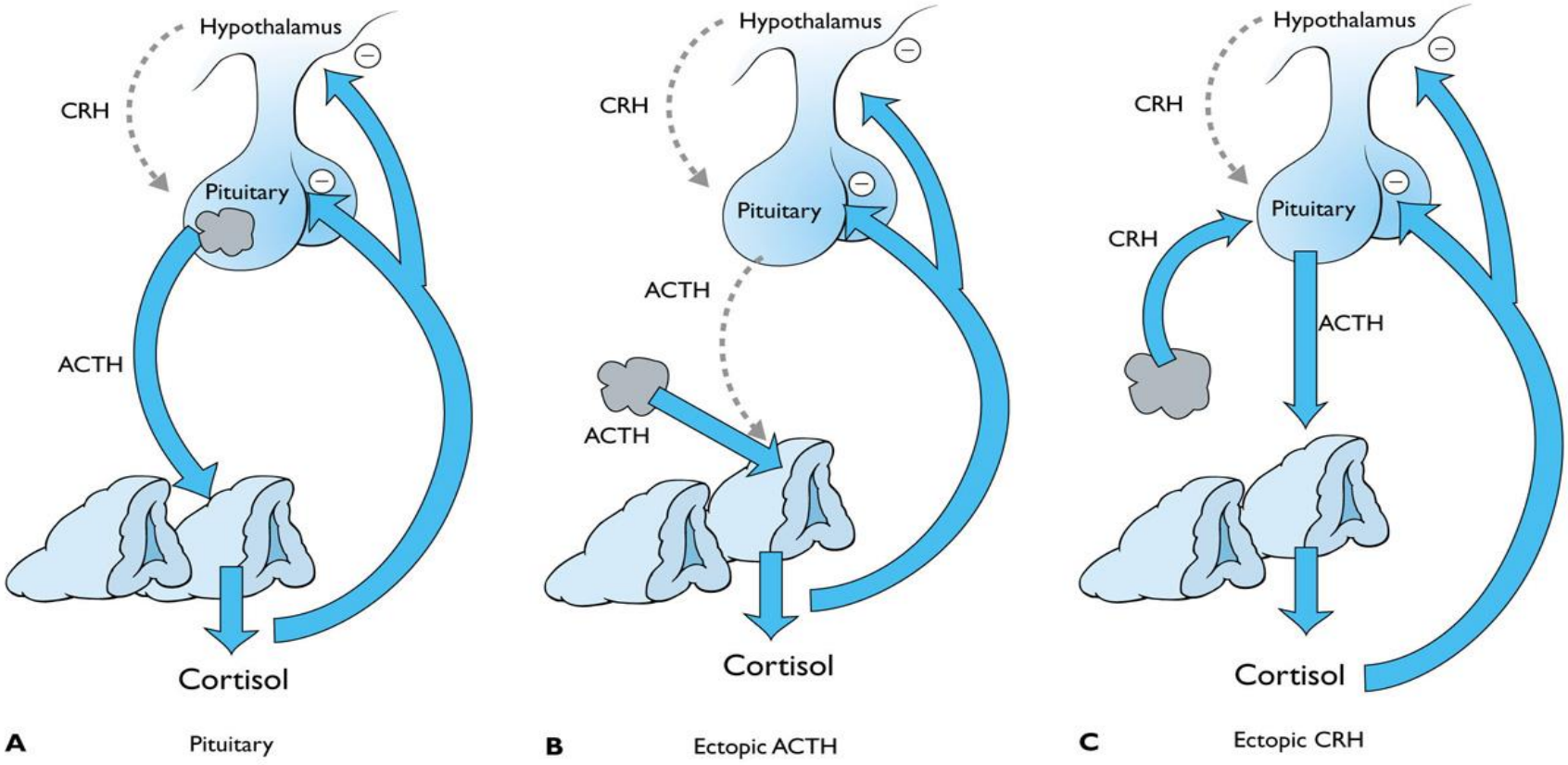

Hypothalamic-pituitary-adrenal axis in ACTH-independent Cushing's syndrome

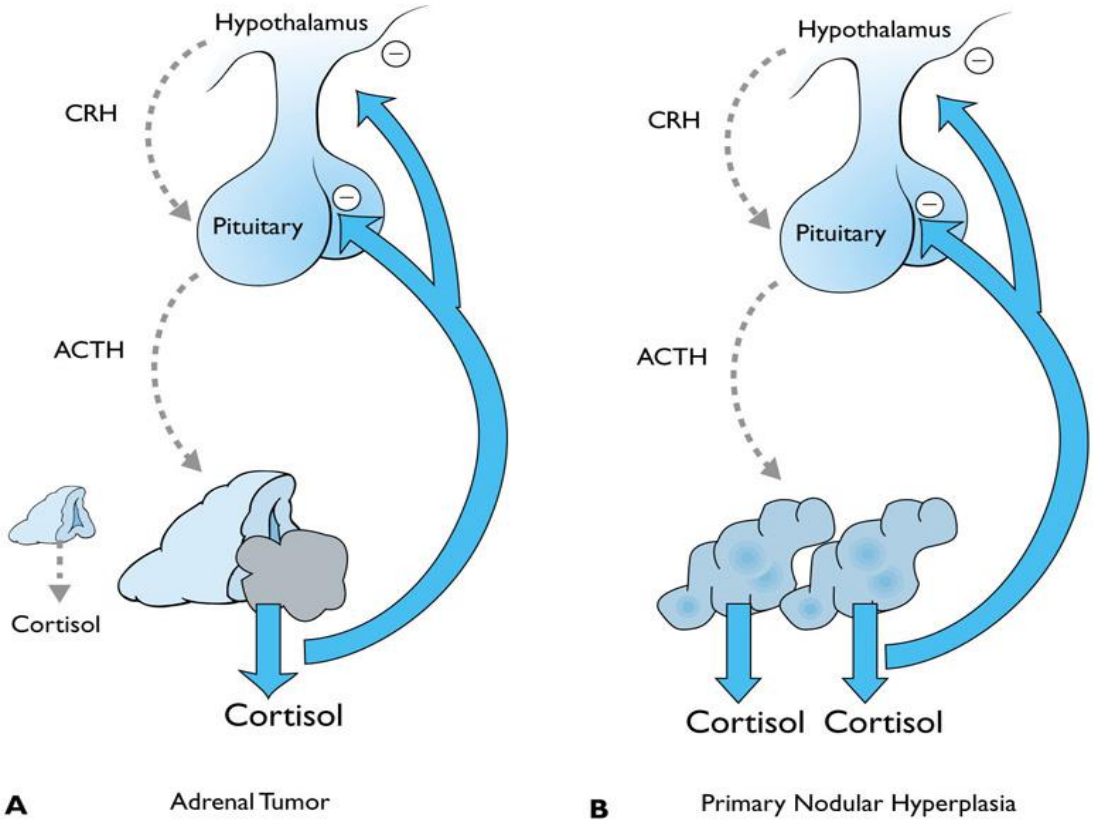

Benign Adrenal Cortical Proliferative Lesions

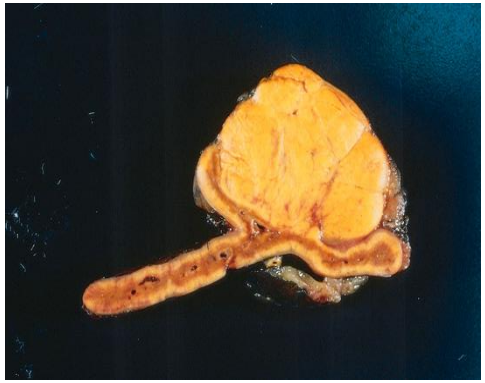

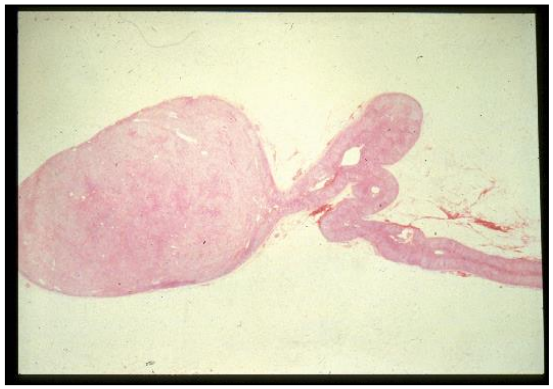

Etiologic Diagnosis of Cushing

Test	ACTH - Pituitary	ACTH - Ectopic	Primary adrenal
ACTH	↑	↑↑	↓
CRH stimulation test	↑	--	--
HDDST	+	- (80%)	-
Metyrapone stimulation test	+	-/±	-

Hyperaldosteronism

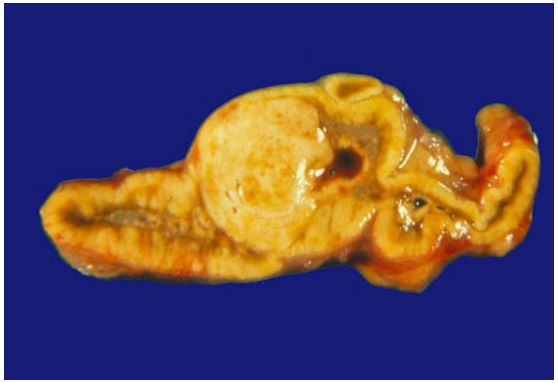

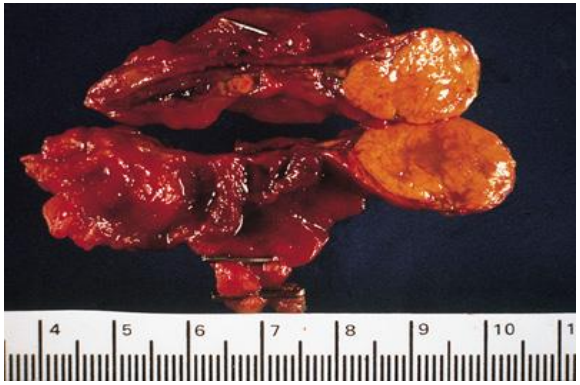

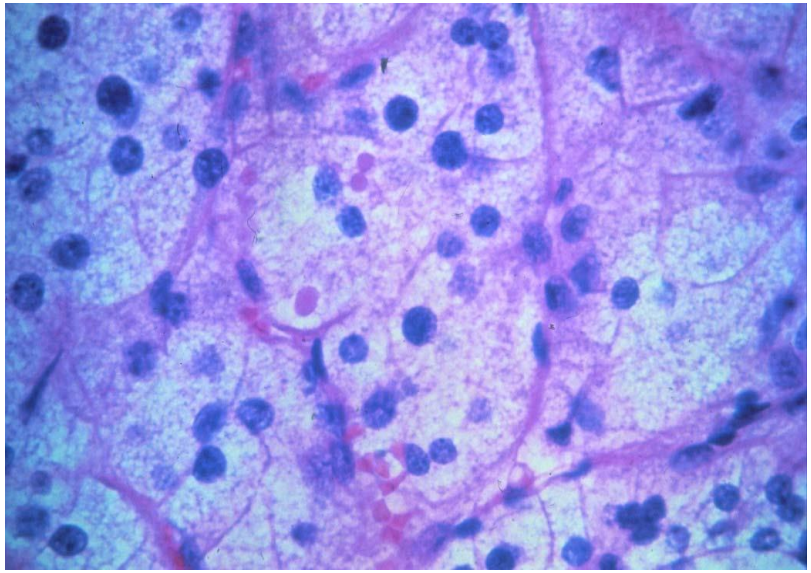

Adrenal Medullary Lesions

- **Pheochromocytomas in familial syndromes**
- **Precursor lesions: Criteria, clonality, and kinetic**
- **Malignancy and topographic heterogeneity**

Molecular Pathways in PCC

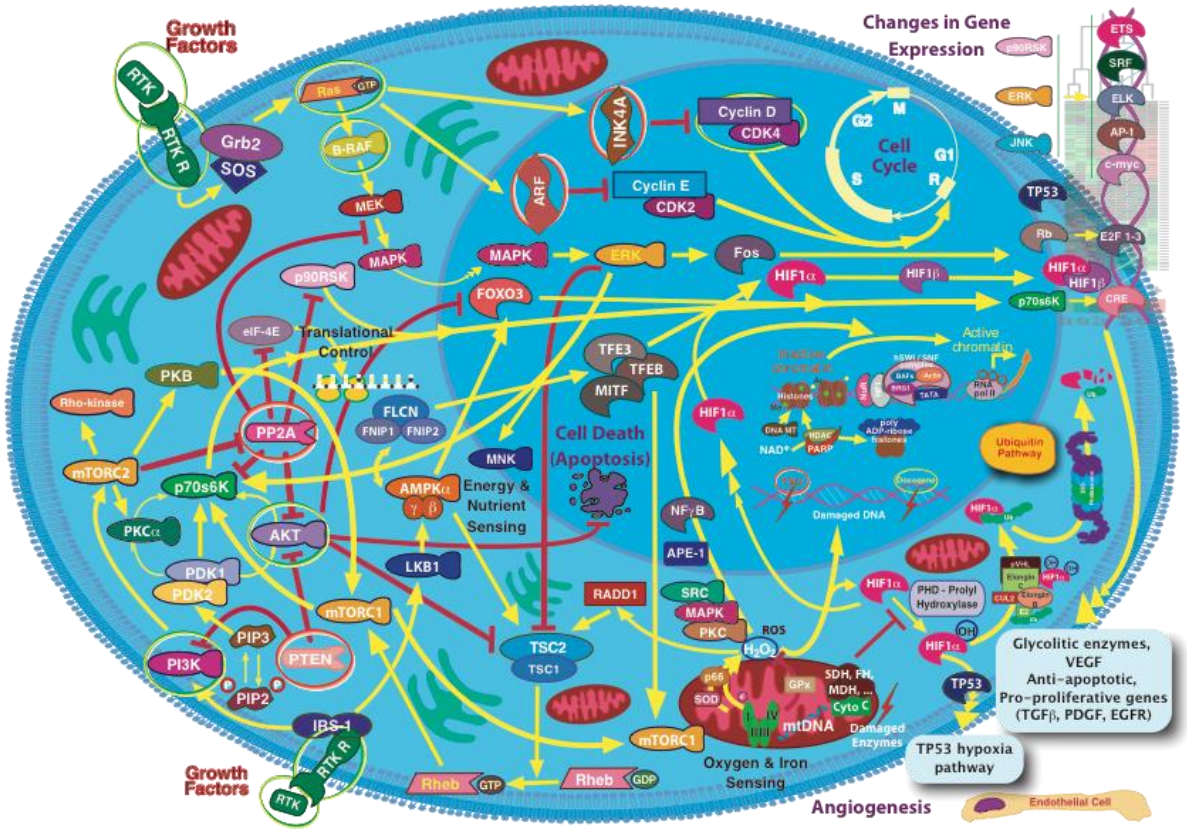

Familial PCC

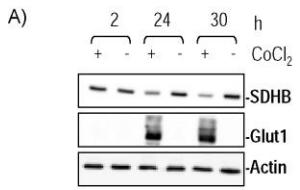

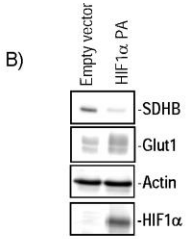

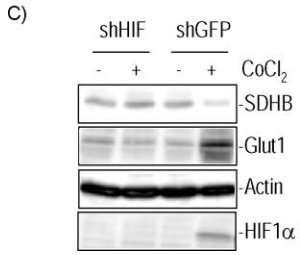

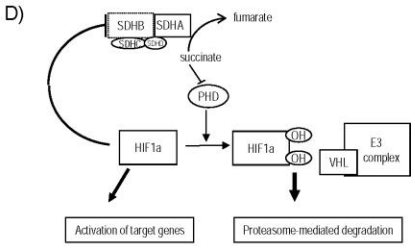

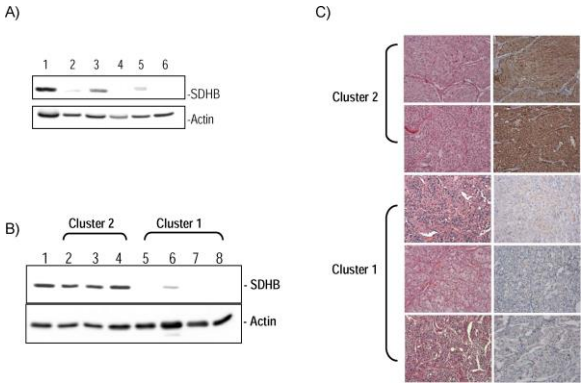

Suppl. Data 3. Validation by real time PCR and Western analyses of genes differentially expressed in pheochromocytomas

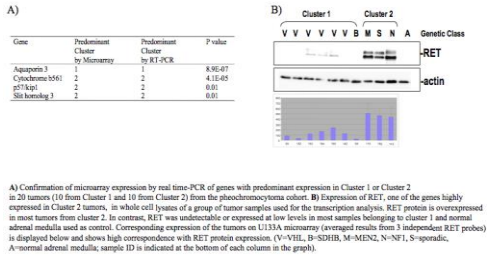

Gene	Predominant Cluster by Microarray	Predominant Cluster by RT-PCR	P value
Aquaporin 3	1	1	8.9E-07
Cytochrome b561	2	2	4.1E-05
p57kip1	2	2	0.01
Slit homolog 3	2	2	0.01

A) Confirmation of microarray expression by real time-PCR of genes with predominant expression in Cluster 1 or Cluster 2 in 20 tumors (10 from Cluster 1 and 10 from Cluster 2) from the pheochromocytoma cohort. B) Expression of RET, one of the genes highly expressed in Cluster 2 tumors, in whole cell lysates of a group of tumor samples used for the transcription analysis. RET protein is overexpressed in most tumors from cluster 2. In contrast, RET was undetectable or expressed at low levels in most samples belonging to cluster 1 and normal adrenal medulla used as control. Corresponding expression of the tumors on U133A microarray (averaged results from 3 independent RET probes) is displayed below and shows high correspondence with RET protein expression. (V=VHL, B=SDHB, M=MEN2, N=NF1, S=sporadic, A=normal adrenal medulla; sample ID is indicated at the bottom of each column in the graph).

Familial PCC - Gene Expression

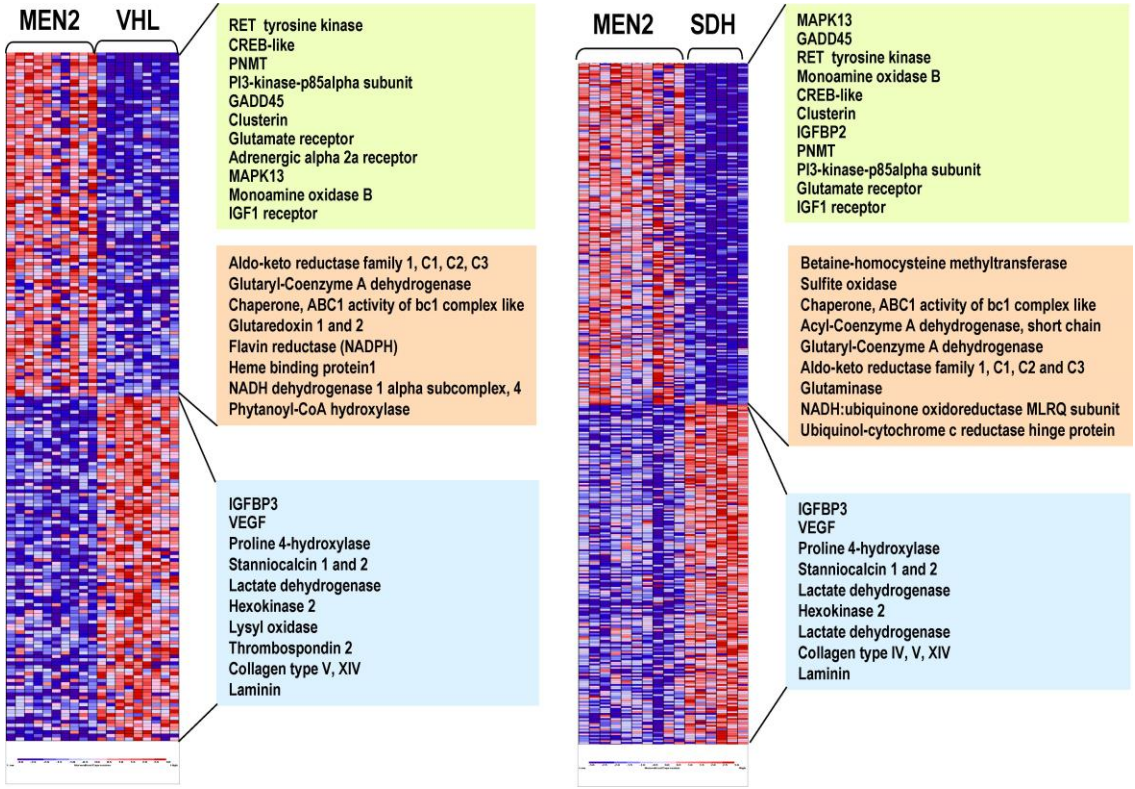

Familial PCC

	Extra-adrenal	Bilateral	AMH	Capsule	Metastasis
MEN 2	-	+	+	-	Very rare
VHL type2	-	+	-	+, Vascular	Rare
NF1	±	<25%	-	+	Rare
PGL-PCC	+	±	-	-	40%

NF1 Pheochromocytomas

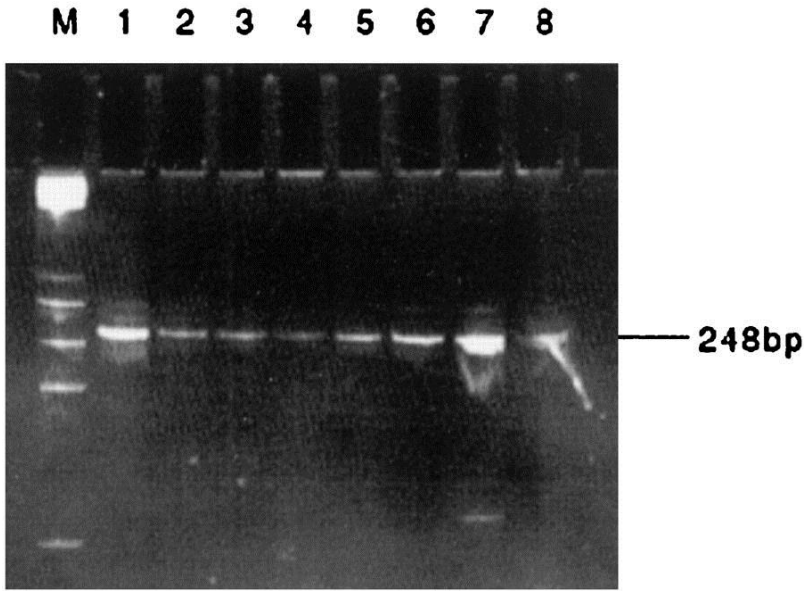

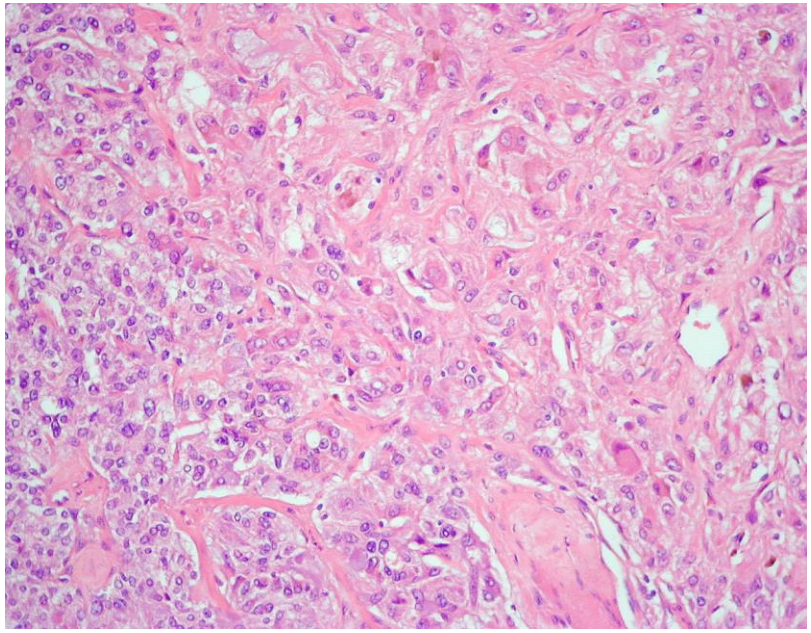

VHL Pheochromocytomas

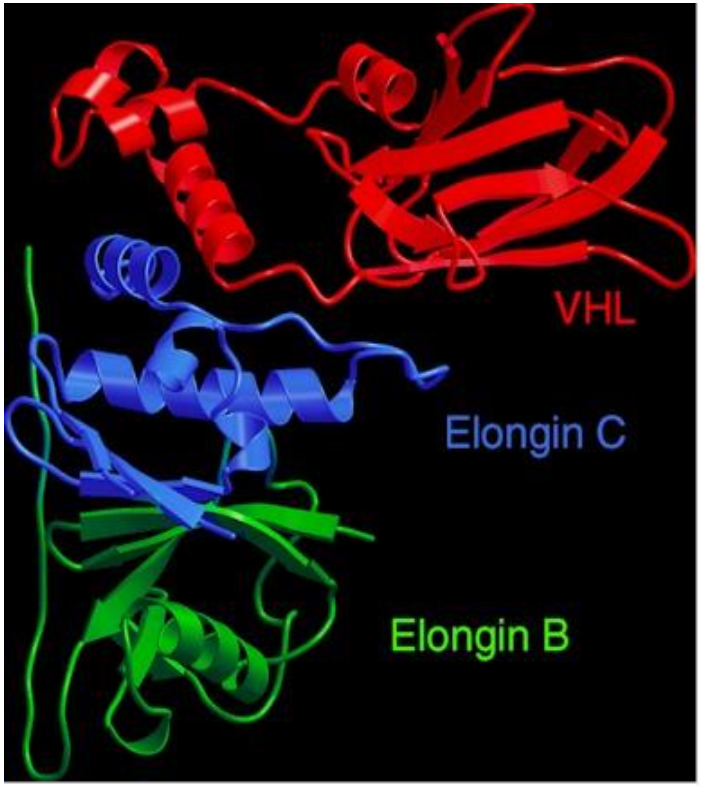

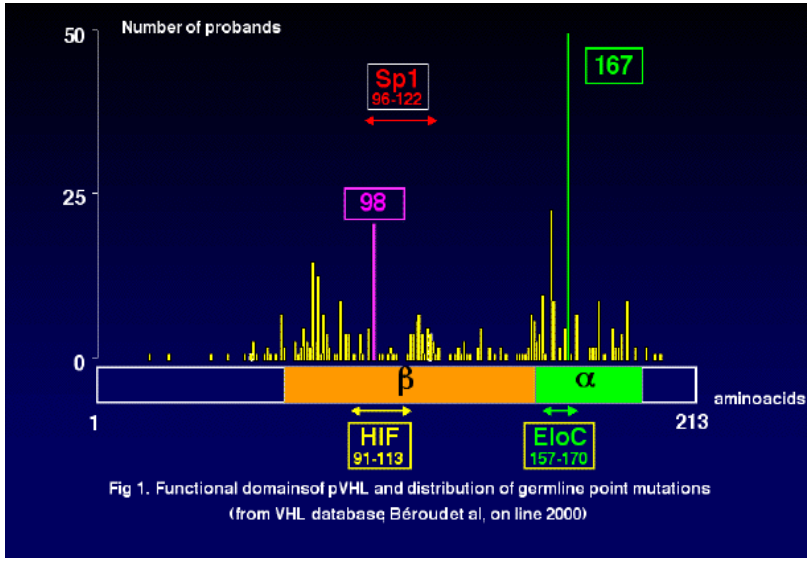

VHL Pheochromocytomas

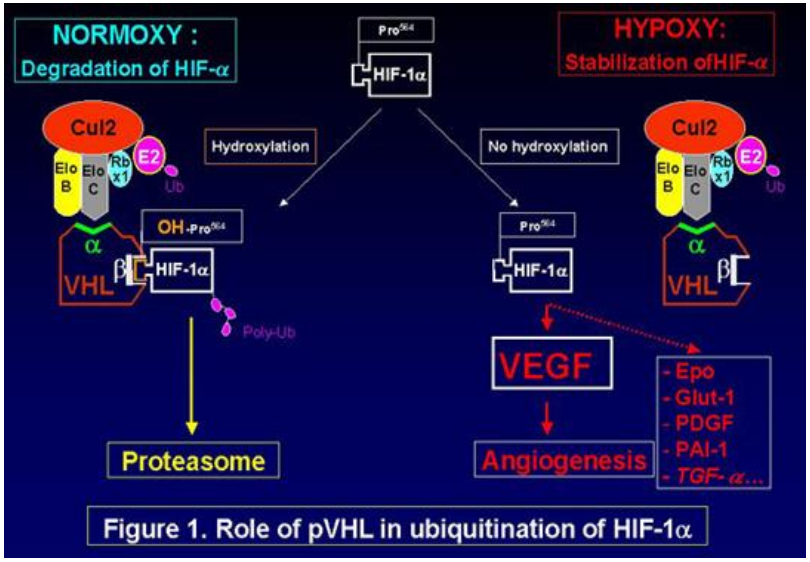

Figure 1. Role of pVHL in ubiquitination of HIF-1α

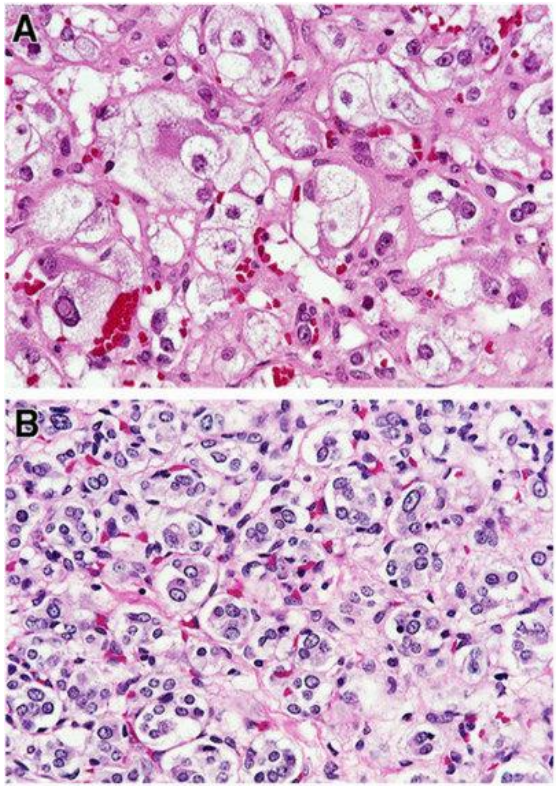

VHL Syndrome

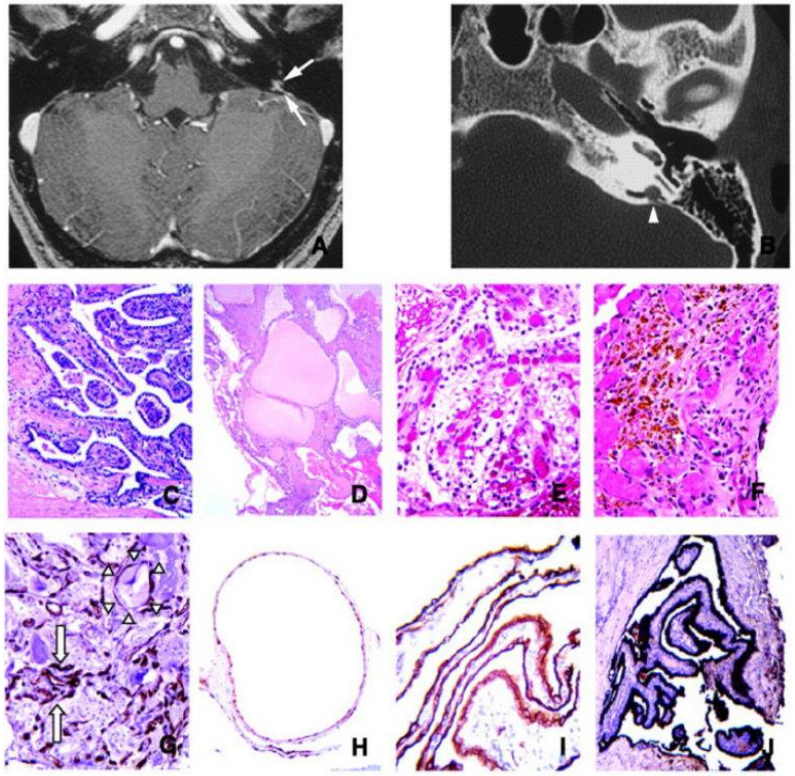

Familial PCC/PGL

Syndrome	Gene	PCC unilat	PCC bilat	PGL symp	PGL paras
MEN 2	*RET*	+	++	-	-
VHL	*VHL*	+	++	±	-
NF1	*NF1*	+	±	-	-
PGL4	*SDHB*	+	-	++	+
PGL3	*SDHC*	-	-	-	+
PGL1	*SDHD*	±	-	±	++

PCC-PGL – Genetic Profiles

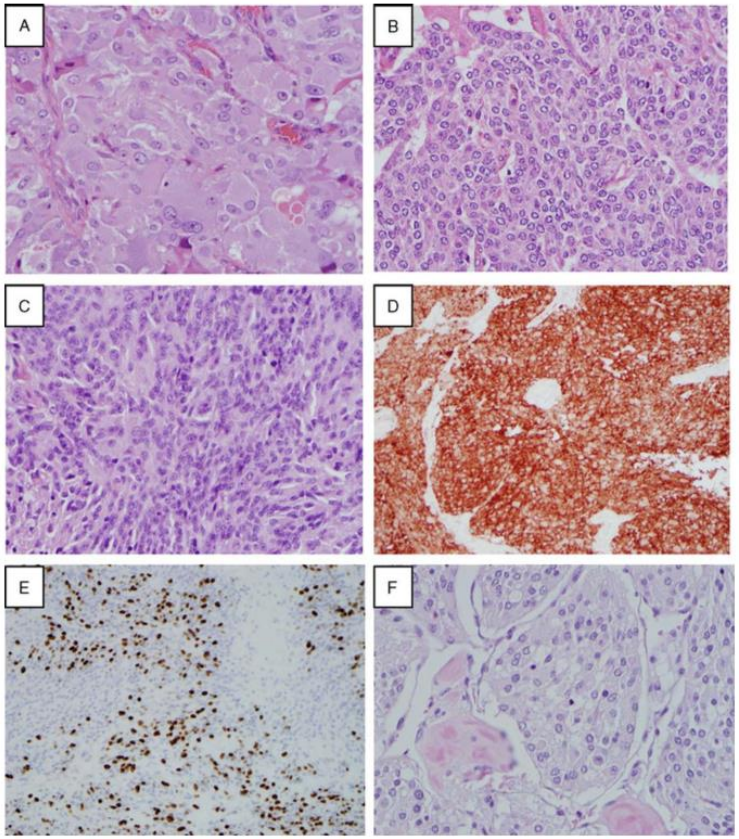

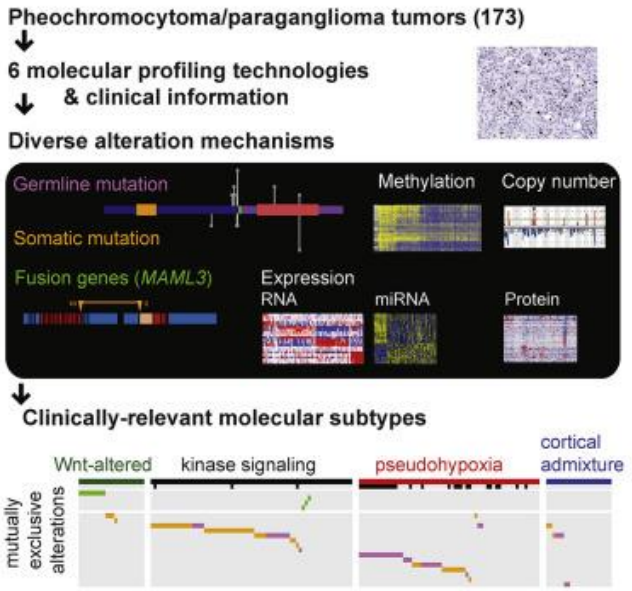

Cancer Cell. 2017 Feb 13;31(2):181-193.

PCC-PGL – Molecular Pathways

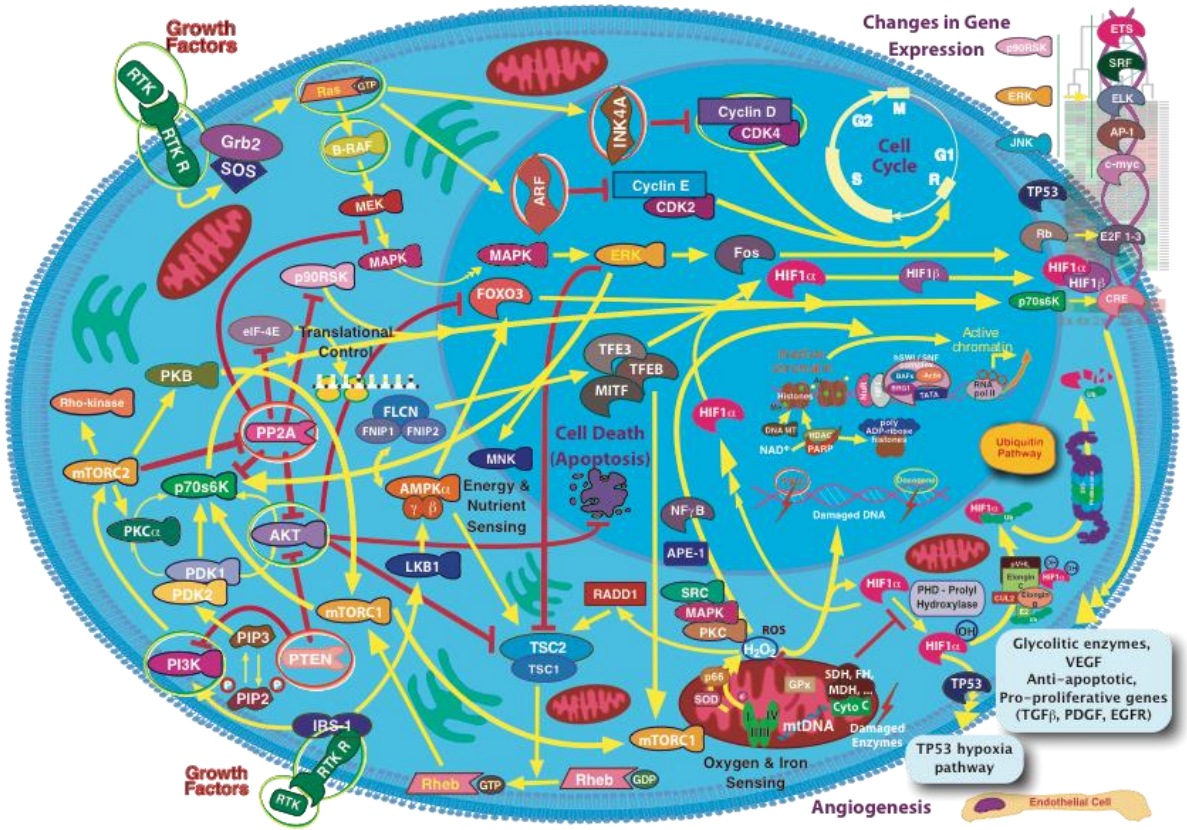

Pseudohypoxia

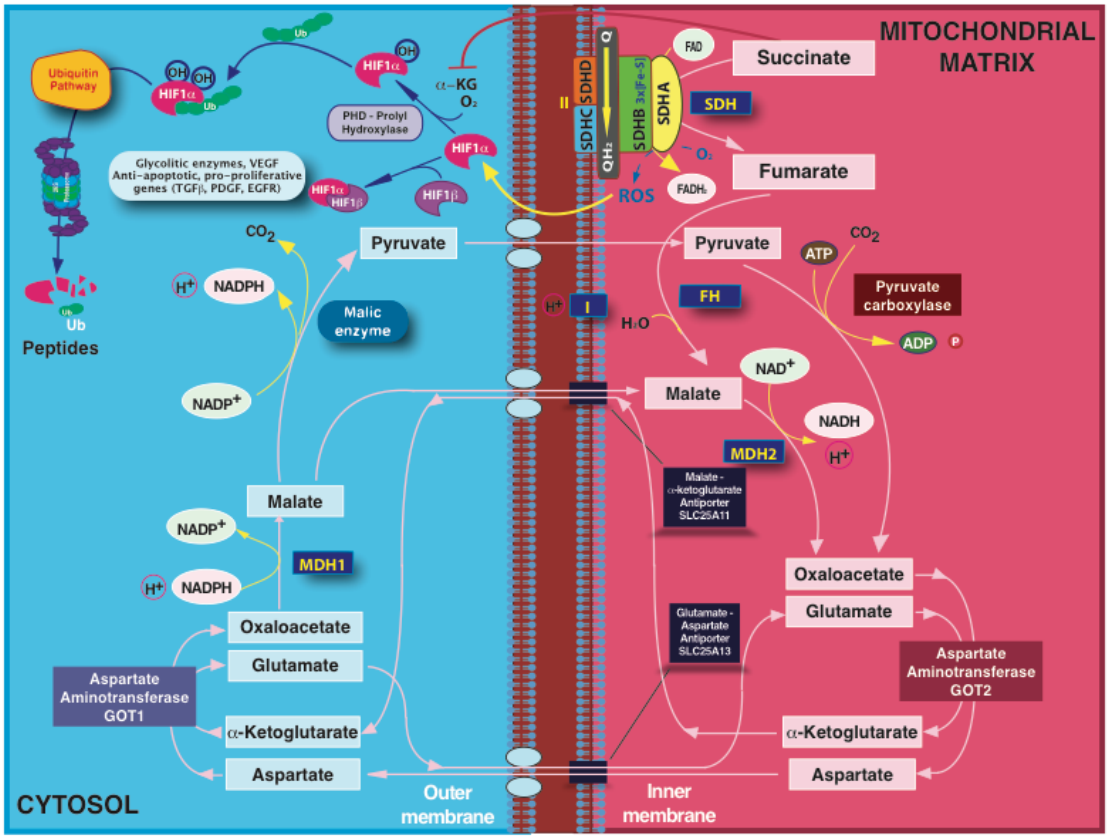

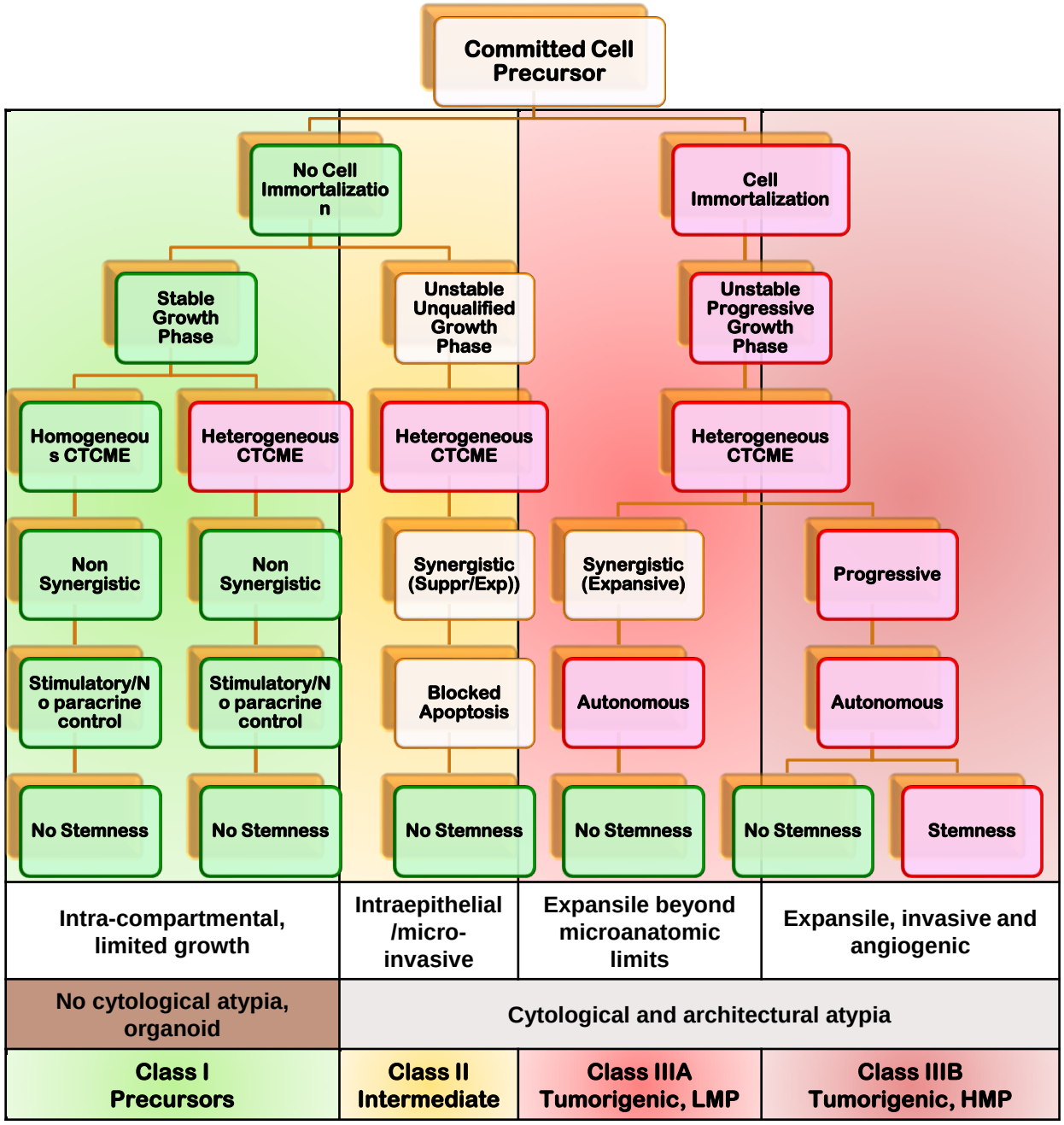

Driving Forces

Cell Selection Pressure

- Kinetics, cellular (homologous and heterologous) and ECM interactions, and gradients (O_2, nutrients, GF)

Mutations

- Neutral, deleterious, and promoting

SPATIAL HETEROGENEITY

PCC-PGL – Molecular Genomic

- Comprehensive molecular profiling of 173 pheochromocytoma and paraganglioma tumors
- Single drivers in tumors by germline mutation, somatic mutation, or fusion gene
- *MAML3* fusion gene and *CSDE1* somatic mutation define a Wnt-altered subtype
- Prognostic markers of metastatic disease include the *MAML3* fusion gene

- **Four molecularly defined groups:**
  - Kinase signaling subtype,
  - Pseudohypoxia subtype,
  - Wnt-altered subtype, driven by *MAML3* and *CSDE1*, and
  - Cortical admixture subtype.

Multifocal or Multicentric?

SINGLE CLONE PROLIFERATION *VERSUS* NEOPLASTIC FIELD CHANGE

Multifocal or Multicentric?

Familial tumor syndromes are good models due to:

- **Synchronic and metachronic tumors**
- **Range of precursor lesions and established neoplasms are frequent**

Germline *RET* mutation (multiple endocrine neoplasia 2) has high penetrance and shows AMH-PCC and CCH-MTC

Molecular Genetics in CCH & AMH Patients

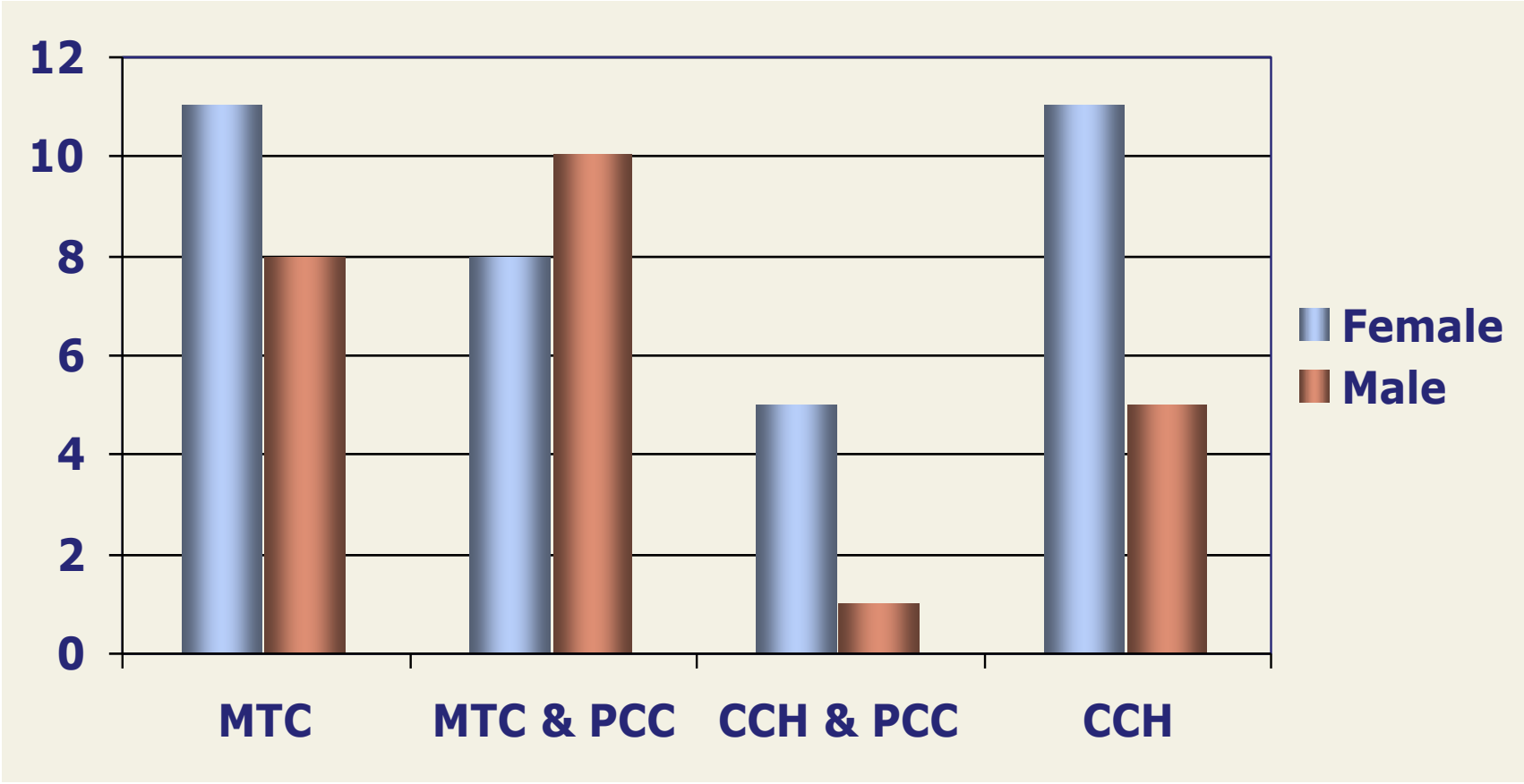

AR Allele Pattern in MEN-2A

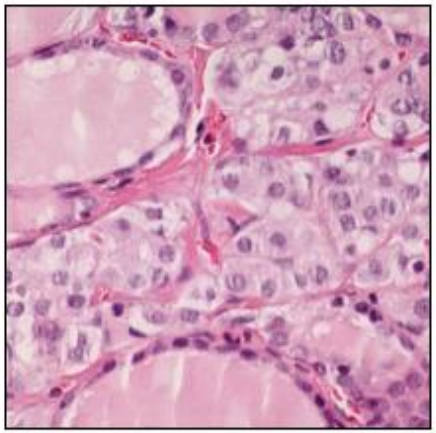

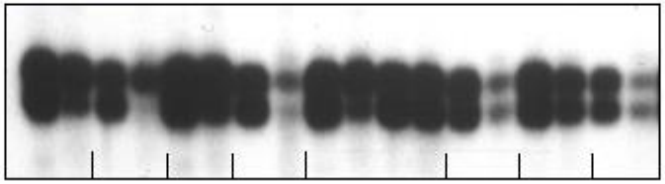

C * C * C * C *

* = CCH

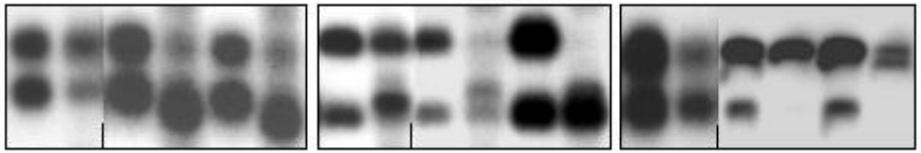

C CCH C CCH C CCH

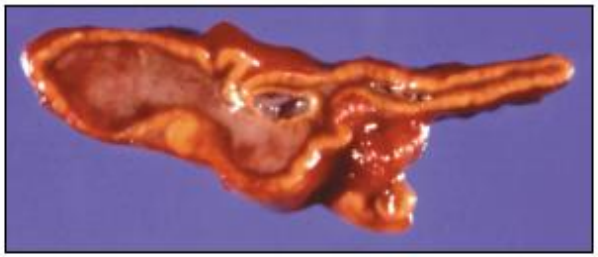

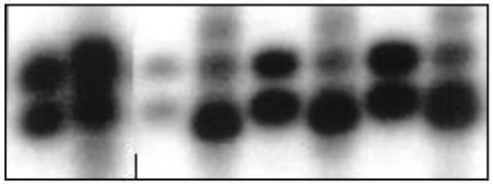

C AMH Nodules

Early Monoclonal Expansions in MEN-2A Results

p(AR pattern in tissue) = 1/3
No of AR Allele (informative patients) = 2
n = No of lesions compared
x = No of patients
p(concordant AR pattern) = $2\ [(1/3)^n]^x$

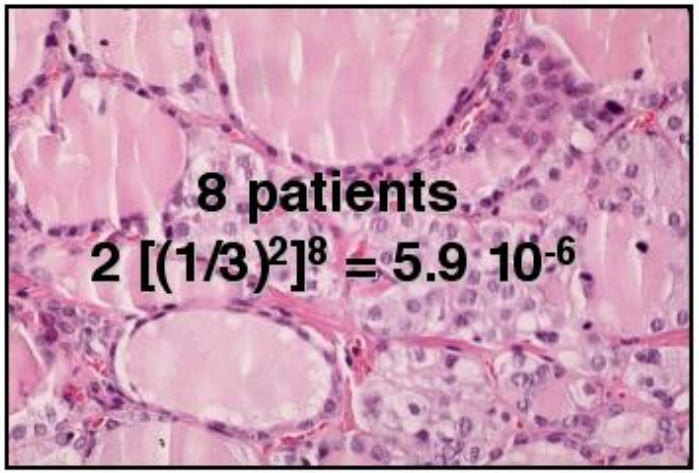

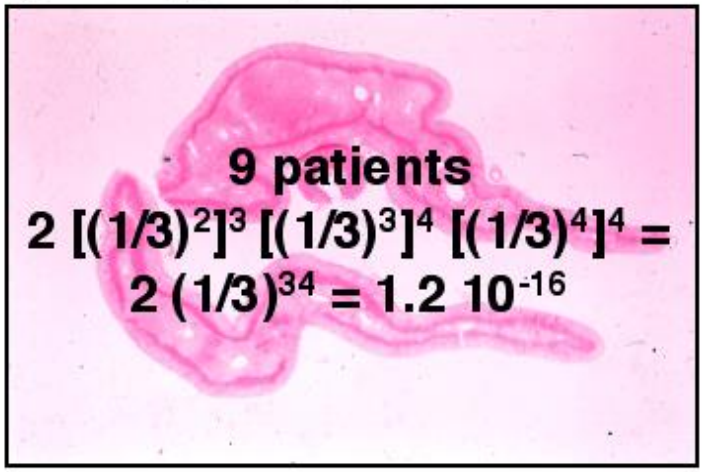

Clonality Assays - Cell and Tissue Comparisons

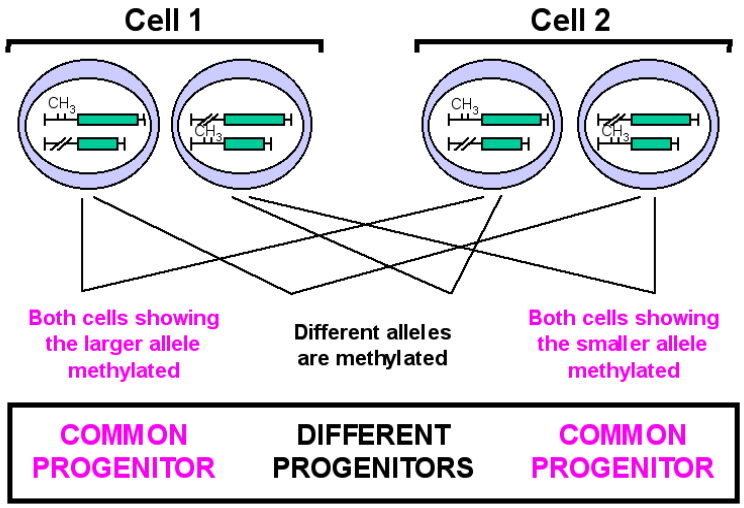

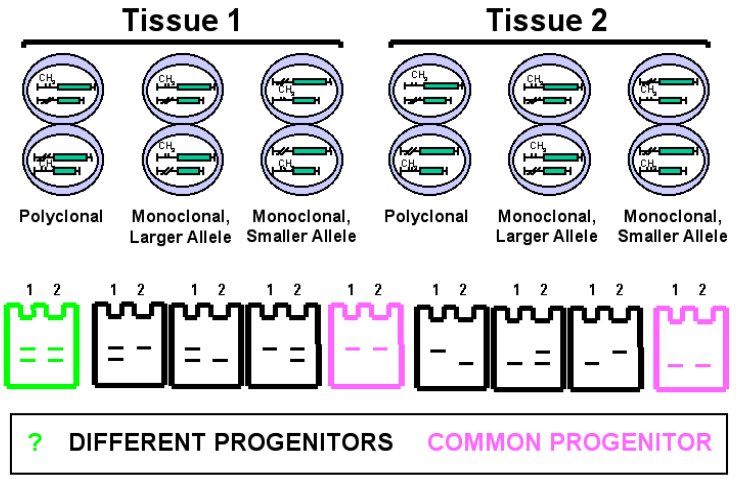

Journal of Pathology
J Pathol 2000; **192**: 221–228.
DOI: 10.1002/1096-9896(2000)9999:9999<::AID-PATH679>3.0.CO;2-B

Original Paper

Clonal patterns in phaeochromocytomas and MEN-2A adrenal medullary hyperplasias: histological and kinetic correlates†

Salvador J. Diaz-Cano[1,2]*, Manuel de Miguel[3], Alfredo Blanes[4], Robert Tashjian[2], Hugo Galera[3] and Hubert J. Wolfe[2]

[1] *Department of Pathology, St Bartholomew's and the Royal London School of Medicine and Dentistry, London, UK*
[2] *Department of Pathology, Tufts University – New England Medical Center, Boston, MA, USA*
[3] *Department of Pathology, University Hospital of Seville, Spain*
[4] *Department of Pathology, University Hospital of Málaga, Spain*

*Correspondence to: Salvador J. Diaz-Cano, Department of Histopathology and Morbid Anatomy, The Royal London Hospital, Whitechapel, London E1 1BB, UK.
E-mail: s.j.diaz-cano@mds.qmw.ac.uk

Received: 3 September 1999
Revised: 7 December 1999
Accepted: 24 March 2000
Published online: 26 June 2000

Abstract

The relationship among histological features, cell kinetics, and clonality has not been studied in adrenal medullary hyperplasias (AMHs) and phaeochromocytomas (PCCs). Thirty-four PCCs (23 sporadic and 11 MEN-2A (multiple endocrine neoplasia type 2A)-related tumours, the latter associated with AMH) from females were included in this study. Representative samples were histologically evaluated and microdissected to extract DNA and evaluate the methylation pattern of the androgen receptor alleles. At least two tissue samples (from the peripheral and internal zones in each tumour) were analysed with appropriate tissue controls run in every case. The same areas were selected for MIB-1 staining and *in situ* end labelling (ISEL). Malignant PCCs were defined by histologically confirmed distant metastases. All monoclonal AMH nodules from the same patient showed the same X-chromosome inactivated. Six sporadic PCCs revealed liver metastases (malignant PCC) and eight additional sporadic PCCs showed periadrenal infiltration (locally invasive PCC). All informative PCCs were monoclonal, except for five locally invasive PCCs and one benign PCC that revealed polyclonal patterns. Those cases also showed a fibroblastic stromal reaction with prominent blood vessels, focal smooth muscle differentiation, and significantly higher MIB-1 (126.8±29.9) and ISEL (50.9±12.8) indices. Concordant X-chromosome inactivation in nodules from a given patient suggests that MEN-2A AMH is a multifocal monoclonal condition. A subgroup of PCCs characterized by balanced methylation of androgen receptor alleles, high cellular turnover, and stromal proliferation also shows locally invasive features. **Copyright © 2000 John Wiley & Sons, Ltd.**

Keywords: **phaeochromocytomas; adrenal medullary hyperplasias; MEN-2A; X-chromosome inactivation; proliferation; apoptosis; stromal reaction**

Early Monoclonal Expansions in MEN 2A AMH

AMH is a multifocal monoclonal condition with concordant methylation of androgen receptor alleles in a given MEN-2A patient (*RET* point mutation at codon 634)

The multifocal nature and the concordant methylation pattern suggest an early clonal expansion of precursors at certain point during embryogenesis

Diaz-Cano et al. **J Pathol** 2000; 192: 221-228

Neoplastic or not?

DIVERGENT GENETIC EVOLUTION OF C-CELL AND ADRENAL MEDULLARY HYPERPLASIAS IN MEN 2A

TSG Microsatellite Pattern in MEN-2A CCH

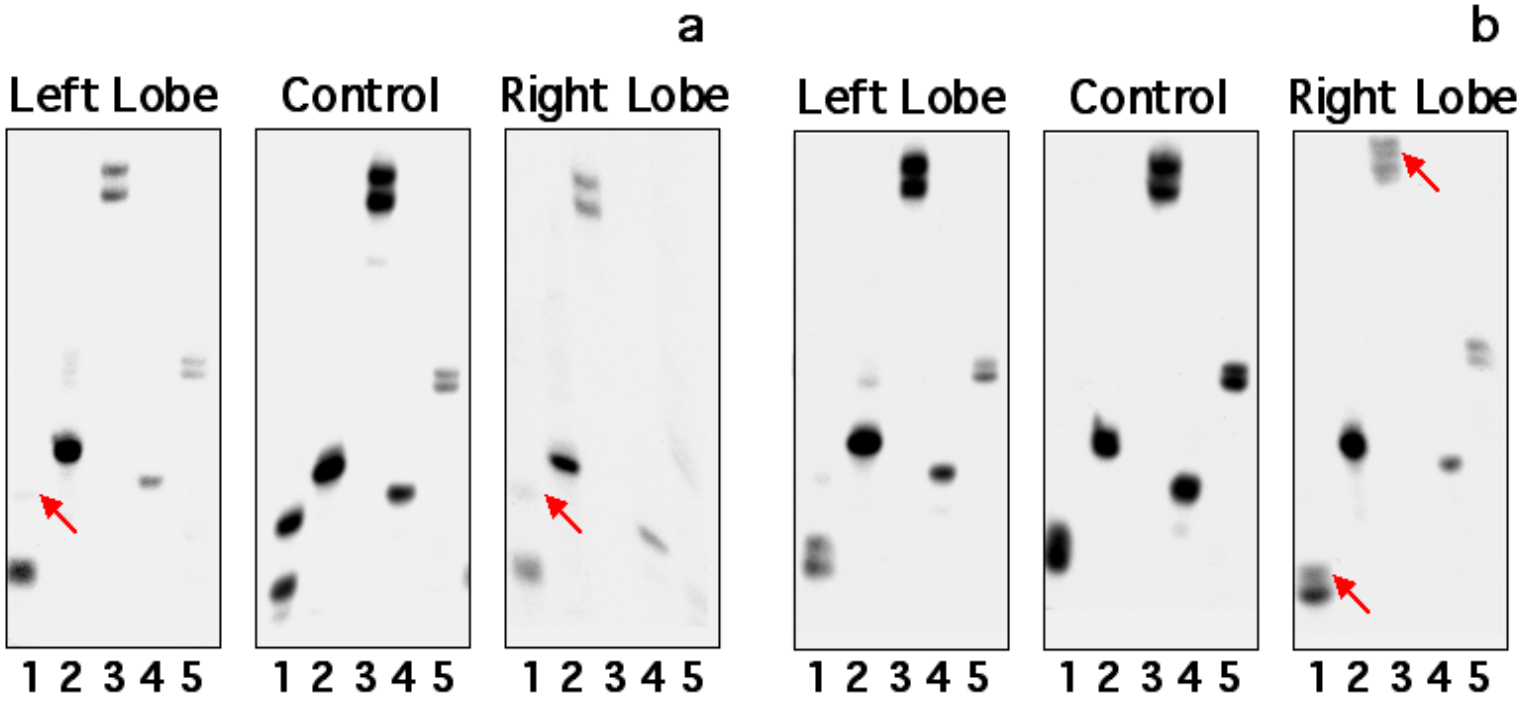

1 & 2 = *TP53*, 3 = *RB1*, 4 = *WT1*, 5 = *NF1*

Microsatellite Patterns in CCH

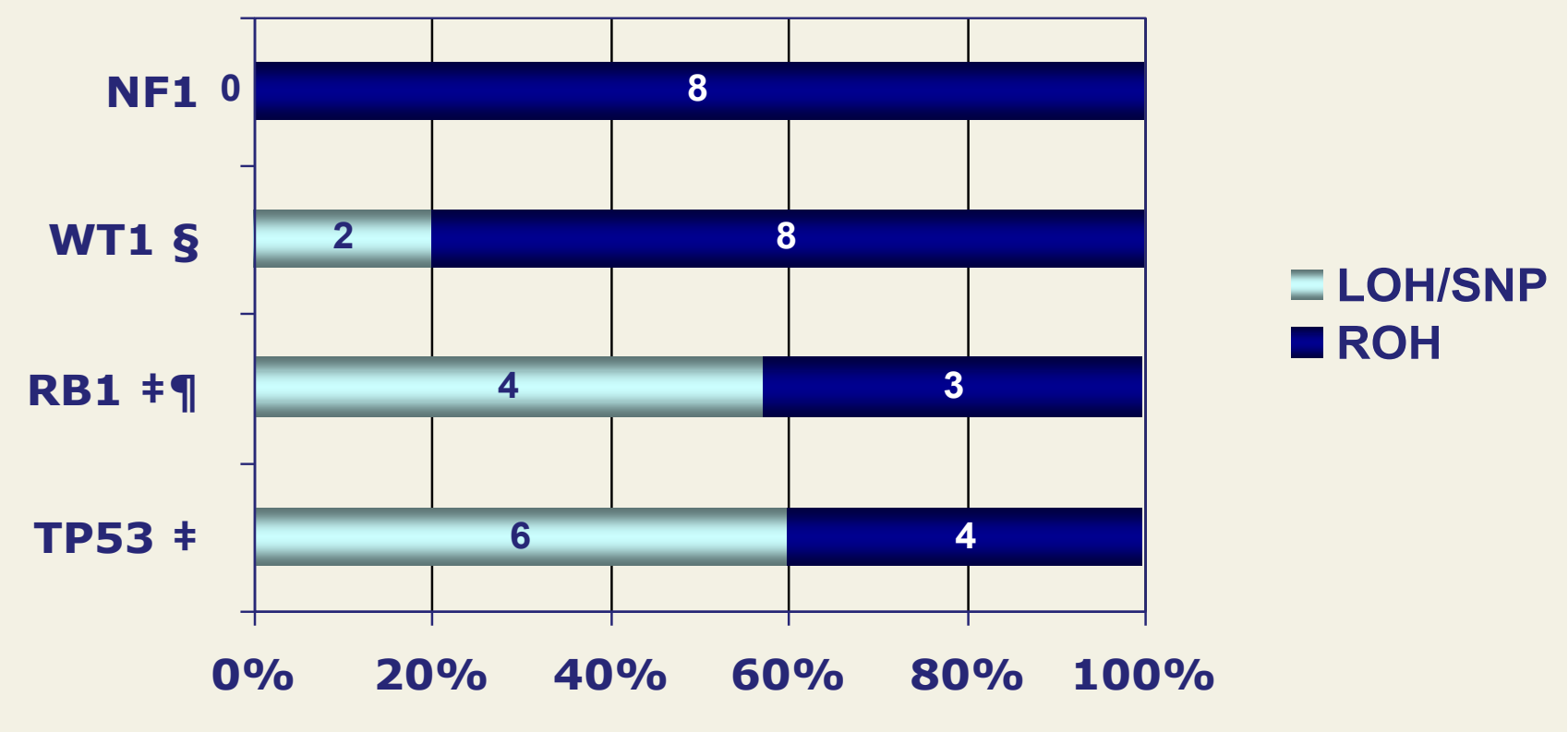

§ = Discordant LOH patterns in both lobes.
‡ = Concordant LOH patterns in both lobes.
¶ = Discordant SNP patterns in both lobes with concordant TP53 LOH patterns in 2 cases.

Microsatellite Patterns in AMH

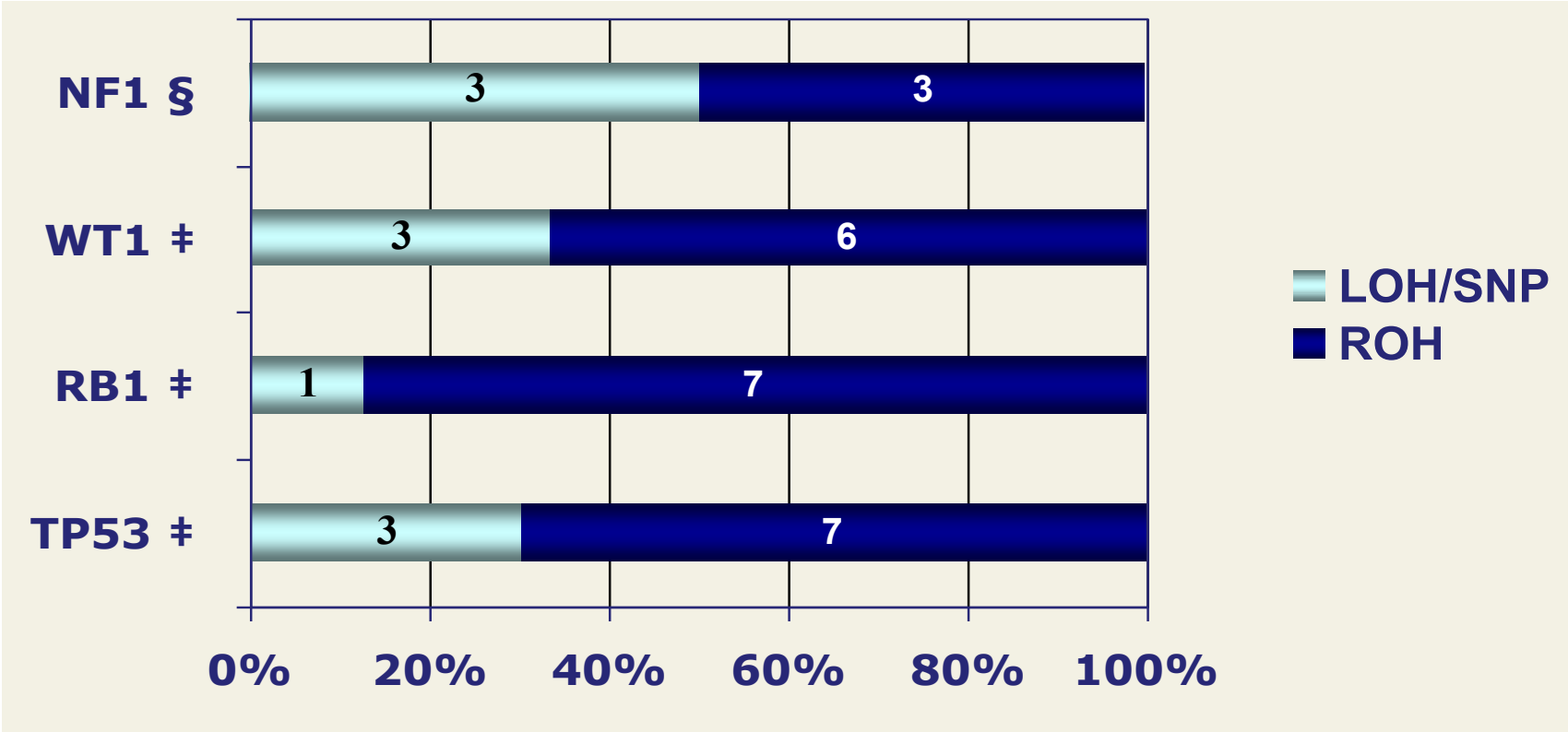

§ = Discordant LOH patterns in nodules from 2 patients (67%).
‡ = Concordant LOH patterns in nodules from 3 patients (42%), but in different TSG in each patient

Molecular Genetics in CCH & AMH Conclusions

MEN 2A CCH and AMH are mainly monoclonal lesions, but with divergent genetic evolution

- **CCH shows early concordant *TP53* and *RB1* loci abnormalities, supporting the neoplastic nature of this lesion**
- **AMH is genetically heterogeneous and reveals low incidence of microsatellite abnormalities and discordant patterns, especially at *NF1* locus. These results are not consistent with a fully established neoplasm**

Journal of Pathology
J Pathol 2000; **192**: 221–228.
DOI: 10.1002/1096-9896(2000)9999:9999<::AID-PATH679>3.0.CO;2-B

Original Paper

Clonal patterns in phaeochromocytomas and MEN-2A adrenal medullary hyperplasias: histological and kinetic correlates†

Salvador J. Diaz-Cano[1,2]*, Manuel de Miguel[3], Alfredo Blanes[4], Robert Tashjian[2], Hugo Galera[3] and Hubert J. Wolfe[2]

[1] *Department of Pathology, St Bartholomew's and the Royal London School of Medicine and Dentistry, London, UK*
[2] *Department of Pathology, Tufts University – New England Medical Center, Boston, MA, USA*
[3] *Department of Pathology, University Hospital of Seville, Spain*
[4] *Department of Pathology, University Hospital of Málaga, Spain*

*Correspondence to: Salvador J. Diaz-Cano, Department of Histopathology and Morbid Anatomy, The Royal London Hospital, Whitechapel, London E1 1BB, UK.
E-mail: s.j.diaz-cano@mds.qmw.ac.uk

Received: 3 September 1999
Revised: 7 December 1999
Accepted: 24 March 2000
Published online: 26 June 2000

Abstract

The relationship among histological features, cell kinetics, and clonality has not been studied in adrenal medullary hyperplasias (AMHs) and phaeochromocytomas (PCCs). Thirty-four PCCs (23 sporadic and 11 MEN-2A (multiple endocrine neoplasia type 2A)-related tumours, the latter associated with AMH) from females were included in this study. Representative samples were histologically evaluated and microdissected to extract DNA and evaluate the methylation pattern of the androgen receptor alleles. At least two tissue samples (from the peripheral and internal zones in each tumour) were analysed with appropriate tissue controls run in every case. The same areas were selected for MIB-1 staining and *in situ* end labelling (ISEL). Malignant PCCs were defined by histologically confirmed distant metastases. All monoclonal AMH nodules from the same patient showed the same X-chromosome inactivated. Six sporadic PCCs revealed liver metastases (malignant PCC) and eight additional sporadic PCCs showed periadrenal infiltration (locally invasive PCC). All informative PCCs were monoclonal, except for five locally invasive PCCs and one benign PCC that revealed polyclonal patterns. Those cases also showed a fibroblastic stromal reaction with prominent blood vessels, focal smooth muscle differentiation, and significantly higher MIB-1 (126.8±29.9) and ISEL (50.9±12.8) indices. Concordant X-chromosome inactivation in nodules from a given patient suggests that MEN-2A AMH is a multifocal monoclonal condition. A subgroup of PCCs characterized by balanced methylation of androgen receptor alleles, high cellular turnover, and stromal proliferation also shows locally invasive features. **Copyright © 2000 John Wiley & Sons, Ltd.**

Keywords: **phaeochromocytomas; adrenal medullary hyperplasias; MEN-2A; X-chromosome inactivation; proliferation; apoptosis; stromal reaction**

Locally Invasive PCC. Clonality

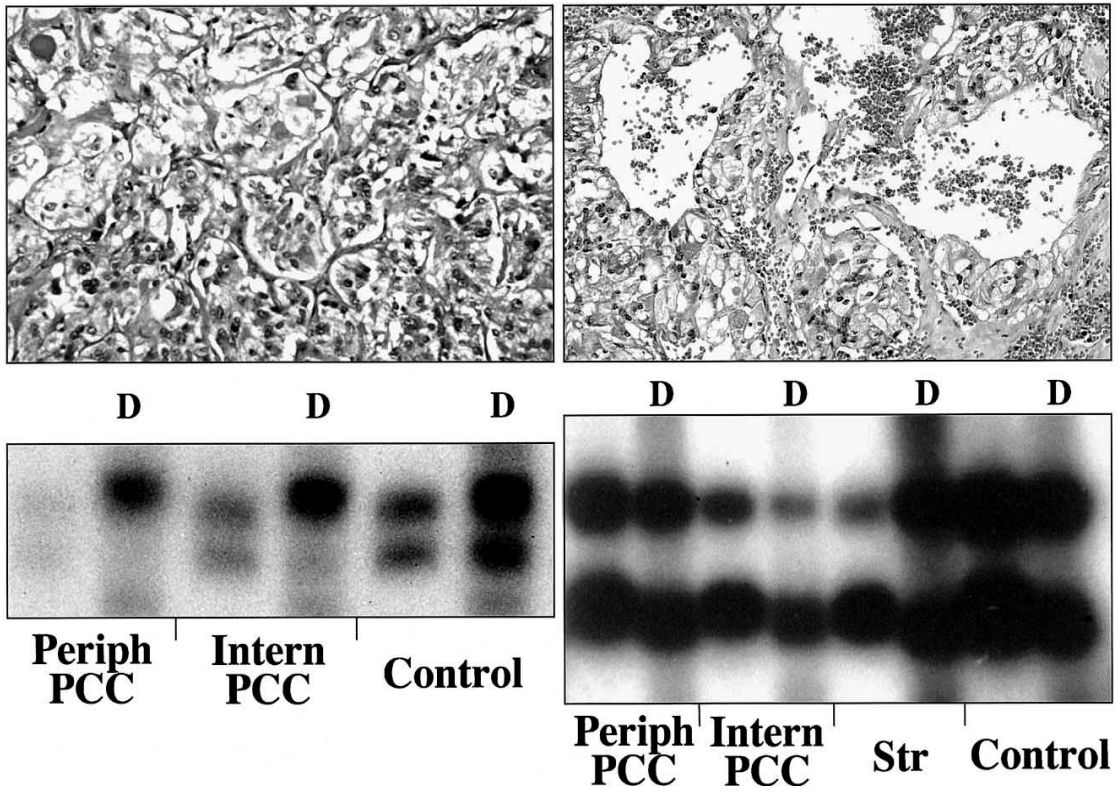

Diaz-Cano et al. **J Pathol** 2000; 192: 221-228

PCC - Histology and Clonality

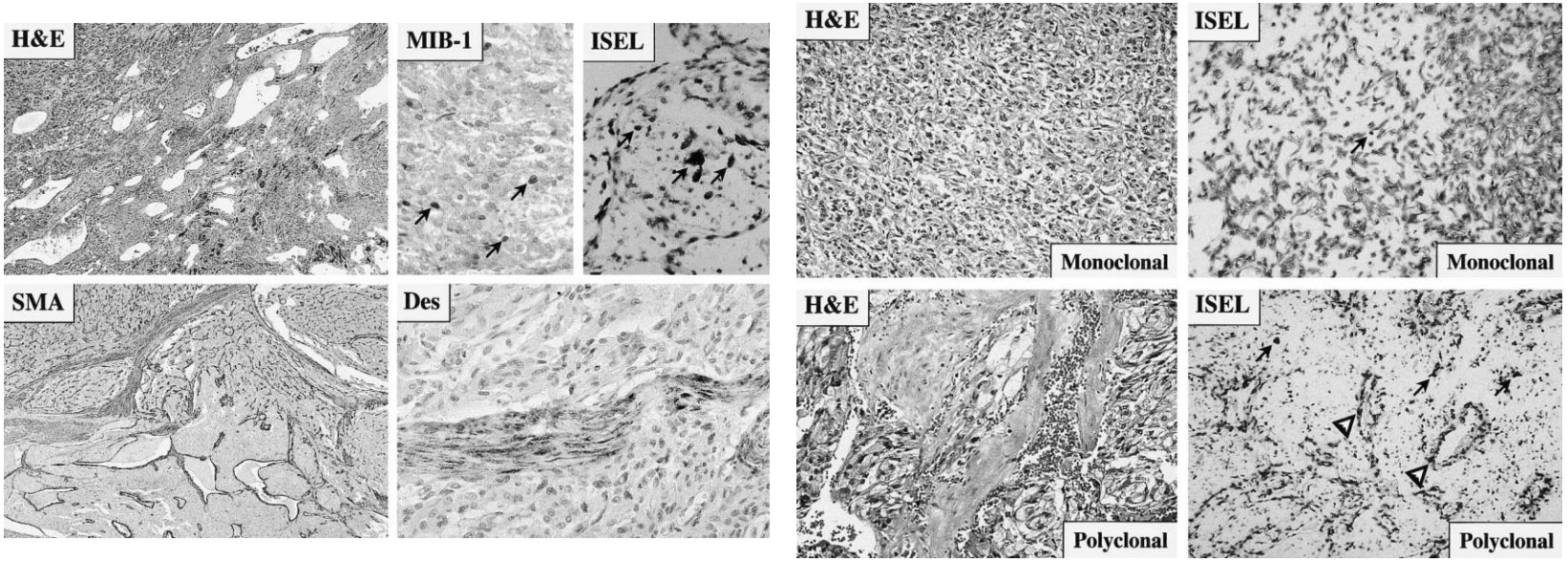

Diaz-Cano et al. **J Pathol** 2000; 192: 221-228

Apoptosis in PCC

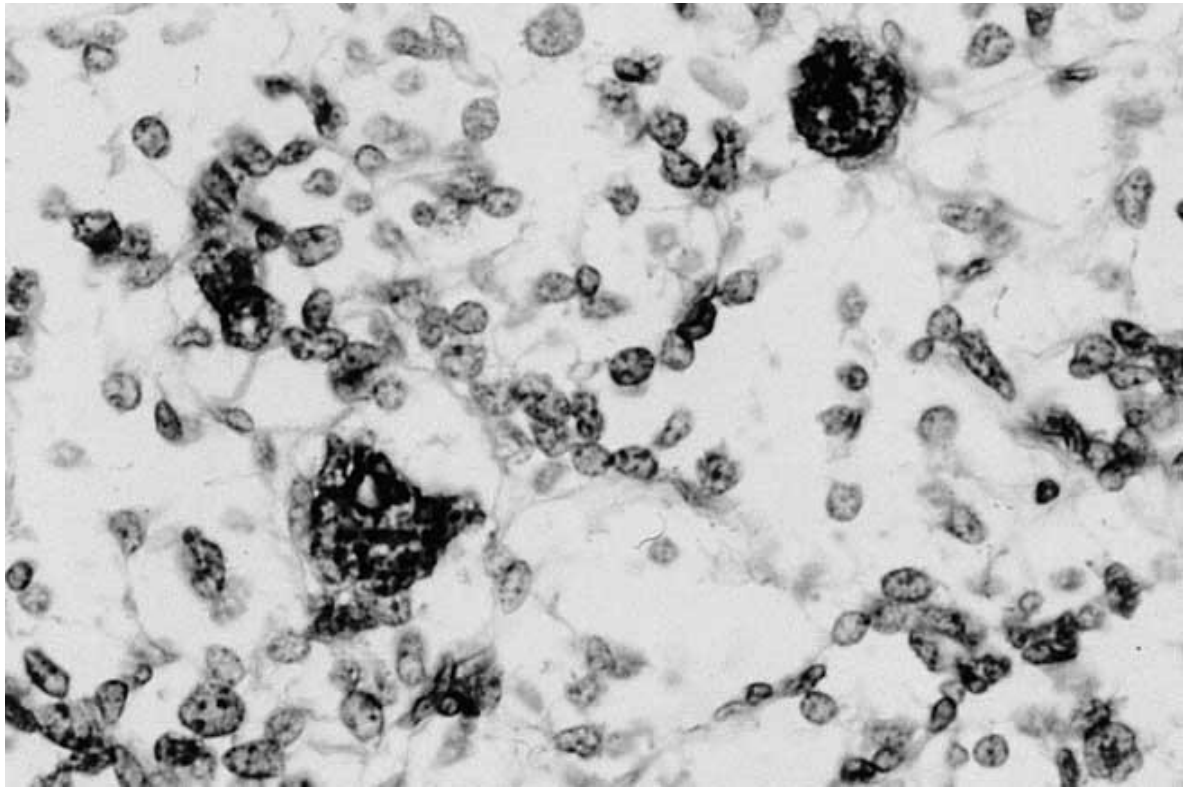

Diaz-Cano et al. **J Pathol** 2000; 192: 221-228

Clonality and Kinetics in PCC

Sporadic and MEN 2A PCC are mainly monoclonal.

A subgroup of PCC characterized by balanced methylation of androgen receptor alleles, high cellular turnover, and stromal proliferation also shows locally invasive features.

Intratumor Heterogeneity

DO GENETIC AND KINETIC CHANGES CORRELATE WITH TOPOGRAPHY?

: Cancer 1993 Feb 1;71(3):820-4 Related Articles, Books

Paragangliomas. Static cytometric studies of nuclear DNA patterns.

Gonzalez-Campora R, Diaz Cano S, Lerma-Puertas E, Rios Martin JJ, Salguero Villadiego M, Villar Rodriguez JL, Bibbo M, Davidson HG.

Department of Pathology, Hospital Universitario Virgen Macarena, University of Seville, Spain.

BACKGROUND. The biologic behavior of most paragangliomas cannot be predicted from their histologic appearance. Recently, cytometric studies have found an association between an aggressive clinical behavior and the presence of a hyperdiploid or tetraploid range in the DNA nuclear content. METHODS. The authors have studied morphometric (nuclear area and nuclear form factor) and DNA densitometric (integral optical density and DNA ploidy) features of 23 cases of paraganglioma by means of slide cytophotometry with the microTICAS system (University of Chicago, Chicago, IL). The samples were selected from paraffin-embedded tissue, and representative sections were stained with the Feulgen technique. The differences between groups (cervical versus extracervical paragangliomas) were investigated with the Mann-Whitney test and Fisher discriminant linear function. RESULTS. The densitometric study showed aneuploid cell lines in 15 of 16 noncervical paragangliomas (with a DNA index within the tetraploid range), whereas 3 of 7 cervical paragangliomas were aneuploid and only 1 case did not have not a diploid cell line (with a DNA index within the peridiploid range). Mean ploidy (4.33 arbitrary units [AU] and 2.72 AU, respectively), nuclear area (58.74 microns 2 and 32.08 microns 2, respectively), the minor and major DNA indices (1.09-1.24 and 1.83-1.96, respectively), and DNA content variability (2c deviation indices [2cDI] of 8.62 and 1.88 AU, respectively) were higher in noncervical paragangliomas. With Fisher linear discriminant function, mean nuclear area ($P = 0.0008$), 2cDI ($P = 0.0030$), and the minor DNA index of each cell proliferation were correlated with location. None of the variables established statistically significant differences in comparisons of malignant and benign paragangliomas. CONCLUSIONS. Karyometric and DNA densitometric parameters have limited value in determining the prognosis of paragangliomas, although they are correlated with tumoral location, which is still an indicator in establishing the prognosis of these neoplasms.

PMID: 8431863 [PubMed - indexed for MEDLINE]

Intratumor Heterogeneity

TOPOGRAPHIC DISTRIBUTION OF GENETIC CHANGES

Genetic Heterogeneity by Topographic Compartments in PCC Suggests a Convergent Cell Selection in the Peripheral Area

Topographic Heterogeneity in PCC

Adrenal pheochromocytomas (PCC) are histologically and biologically heterogeneous neoplasms

PCCs present as sporadic or familial tumors, the latter being associated with adrenal medullary hyperplasias

Topographic heterogeneity is associated with accumulation of genetic abnormalities in the peripheral compartment

PCC - Malignancy Criteria?

Feature	Score if present (no. of points assigned)
Large nests or diffuse growth (>10% of tumor volume)	2
Central (middle of large nests) or confluent tumor necrosis (not degenerative change)	2
High cellularity	2
Cellular monotony	2
Tumor cel spindling (even if focal)	2
Mitotic figures >3/10 HPF	2
Atypical mitotic figure(s)	2
Extension into adipose tissue	2
Vascular invasion	1
Capsular invasion	1
profound nuclear pleomorphism	1
Nuclear hyperchromasia	1
Total	**20**

HPF = high-power field.

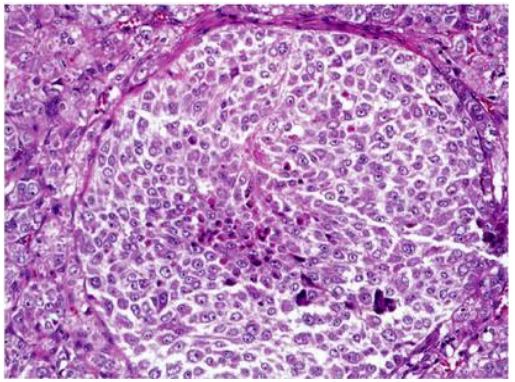

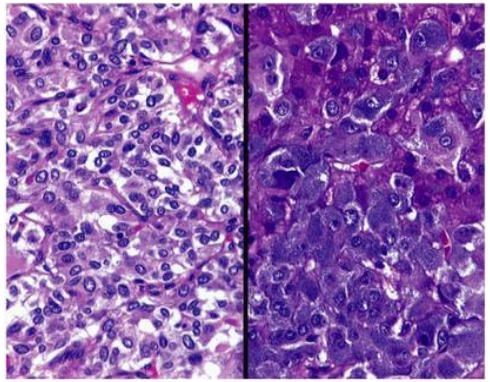

PCC - Malignancy Criteria?

Feature	Score if present (no. of points assigned)
Large nests or diffuse growth (>10% of tumor volume)	2
Central (middle of large nests) or confluent tumor necrosis (not degenerative change)	2
High cellularity	2
Cellular monotony	2
Tumor cel spindling (even if focal)	2
Mitotic figures >3/10 HPF	2
Atypical mitotic figure(s)	2
Extension into adipose tissue	2
Vascular invasion	1
Capsular invasion	1
profound nuclear pleomorphism	1
Nuclear hyperchromasia	1
Total	**20**

HPF = high-power field.

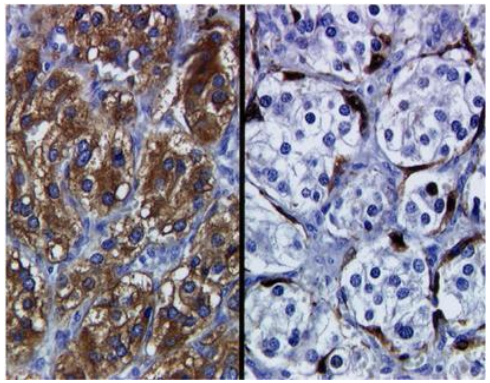

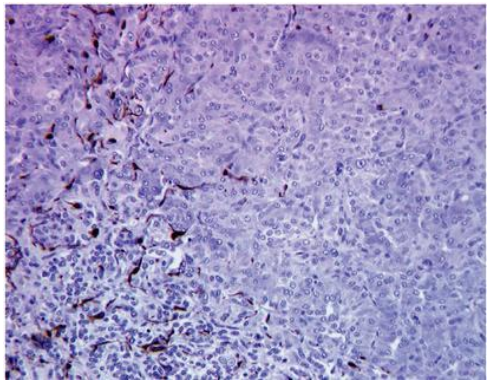

PCC - Malignancy Criteria?

Feature	Score if present (no. of points assigned)
Large nests or diffuse growth (>10% of tumor volume)	2
Central (middle of large nests) or confluent tumor necrosis (not degenerative change)	2
High cellularity	2
Cellular monotony	2
Tumor cel spindling (even if focal)	2
Mitotic figures >3/10 HPF	2
Atypical mitotic figure(s)	2
Extension into adipose tissue	2
Vascular invasion	1
Capsular invasion	1
profound nuclear pleomorphism	1
Nuclear hyperchromasia	1
Total	**20**

HPF = high-power field.

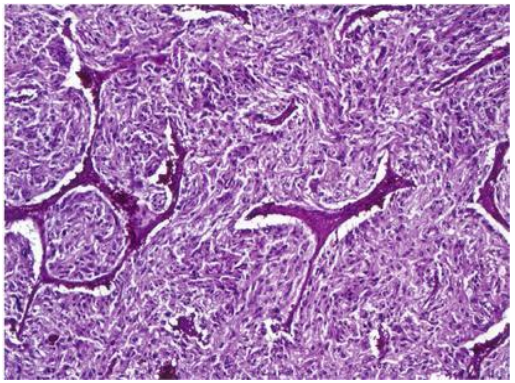

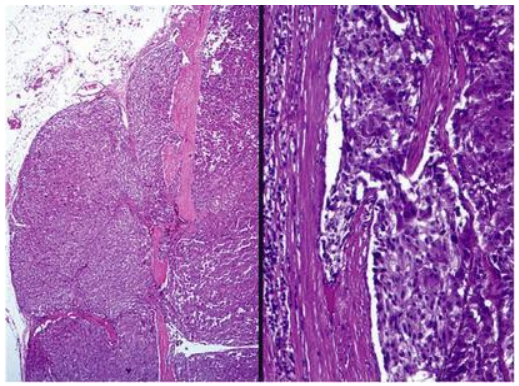

PCC - Malignancy Criteria?

Feature	Score if present (no. of points assigned)
Large nests or diffuse growth (>10% of tumor volume)	2
Central (middle of large nests) or confluent tumor necrosis (not degenerative change)	2
High cellularity	2
Cellular monotony	2
Tumor cel spindling (even if focal)	2
Mitotic figures >3/10 HPF	2
Atypical mitotic figure(s)	2
Extension into adipose tissue	2
Vascular invasion	1
Capsular invasion	1
profound nuclear pleomorphism	1
Nuclear hyperchromasia	1
Total	**20**

HPF = high-power field.

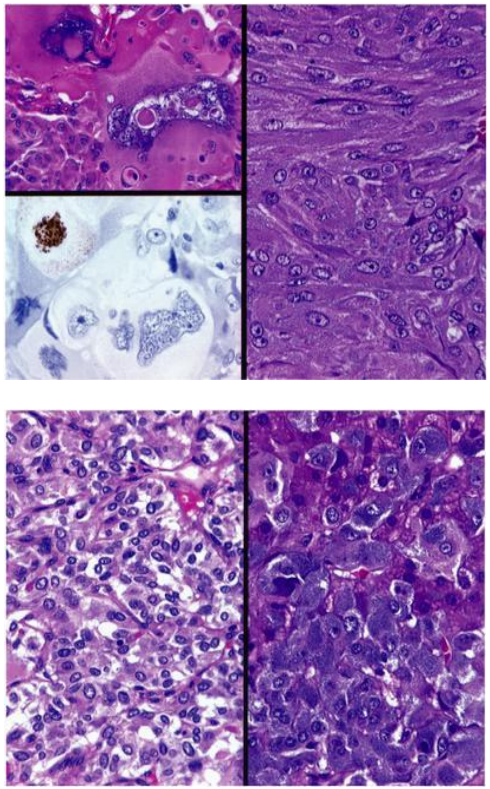

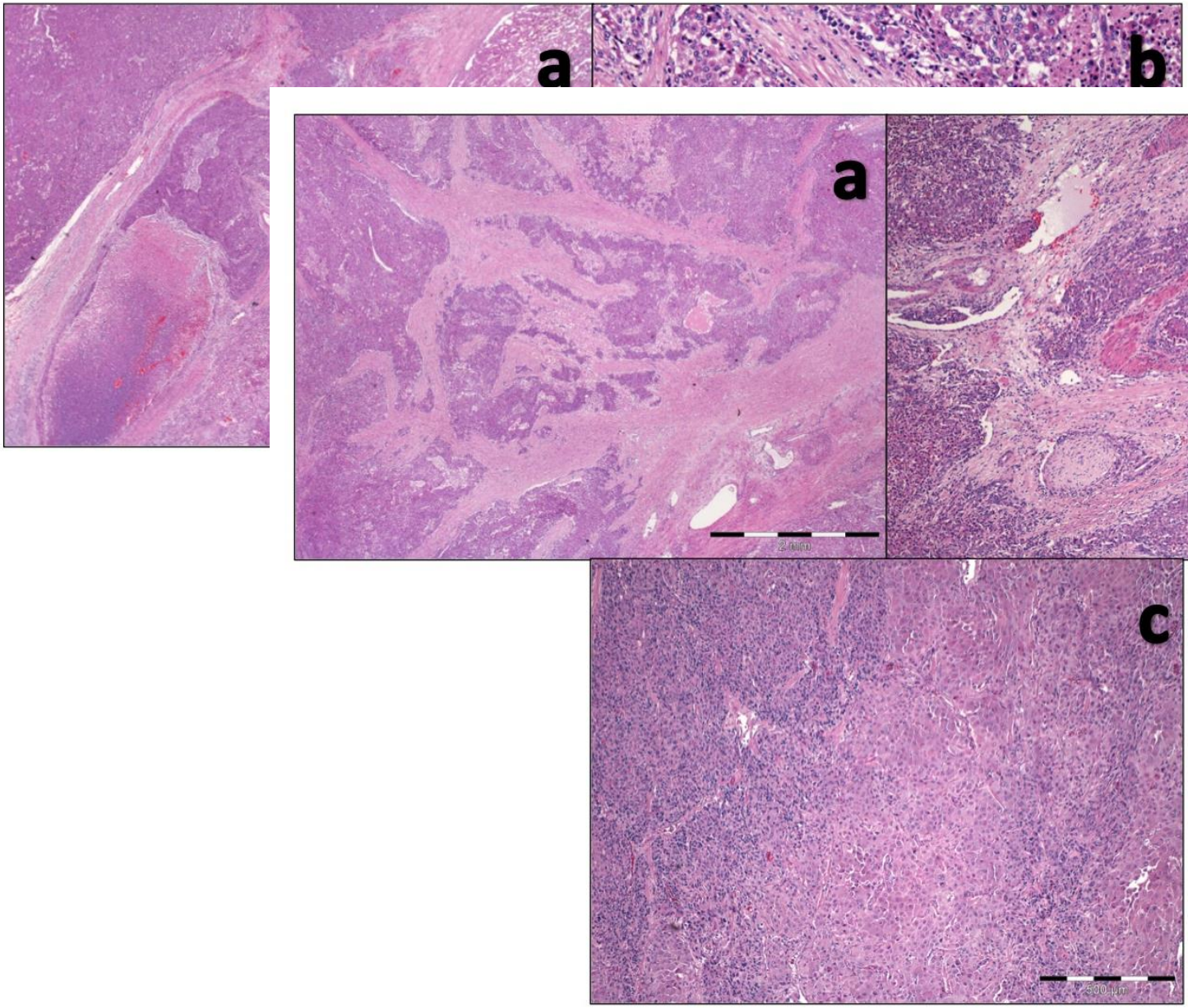
a
b
a
b
c

	PGL-PCC Low Risk	PGL-PCC High Risk
Criteria	Tumor with not enough invasive / tumorigenic features	At least one feature of invasive capacity and two features of tumorigenic expansion (±mitogenic activity)
Lymph nodes	N0	N0 / N1
Distant metastases	M0	M0 /M1

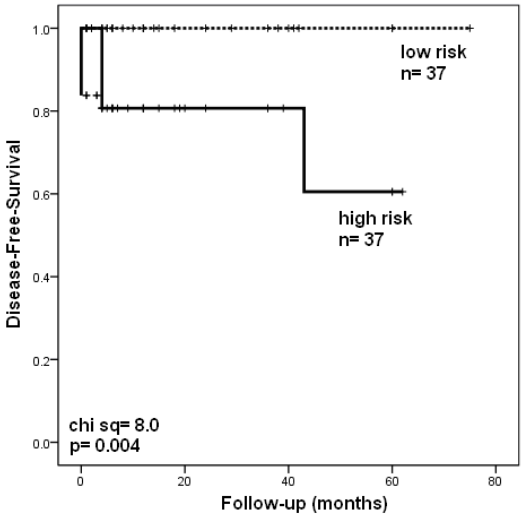

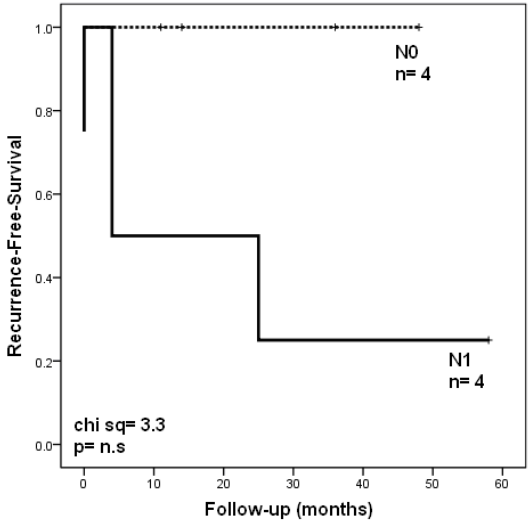

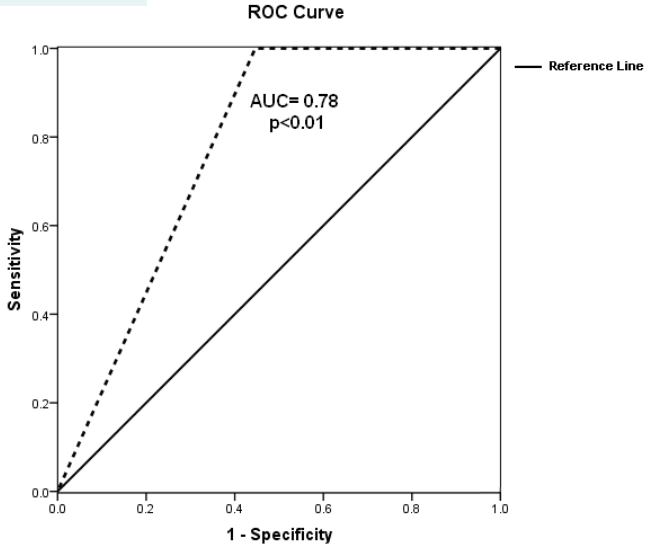

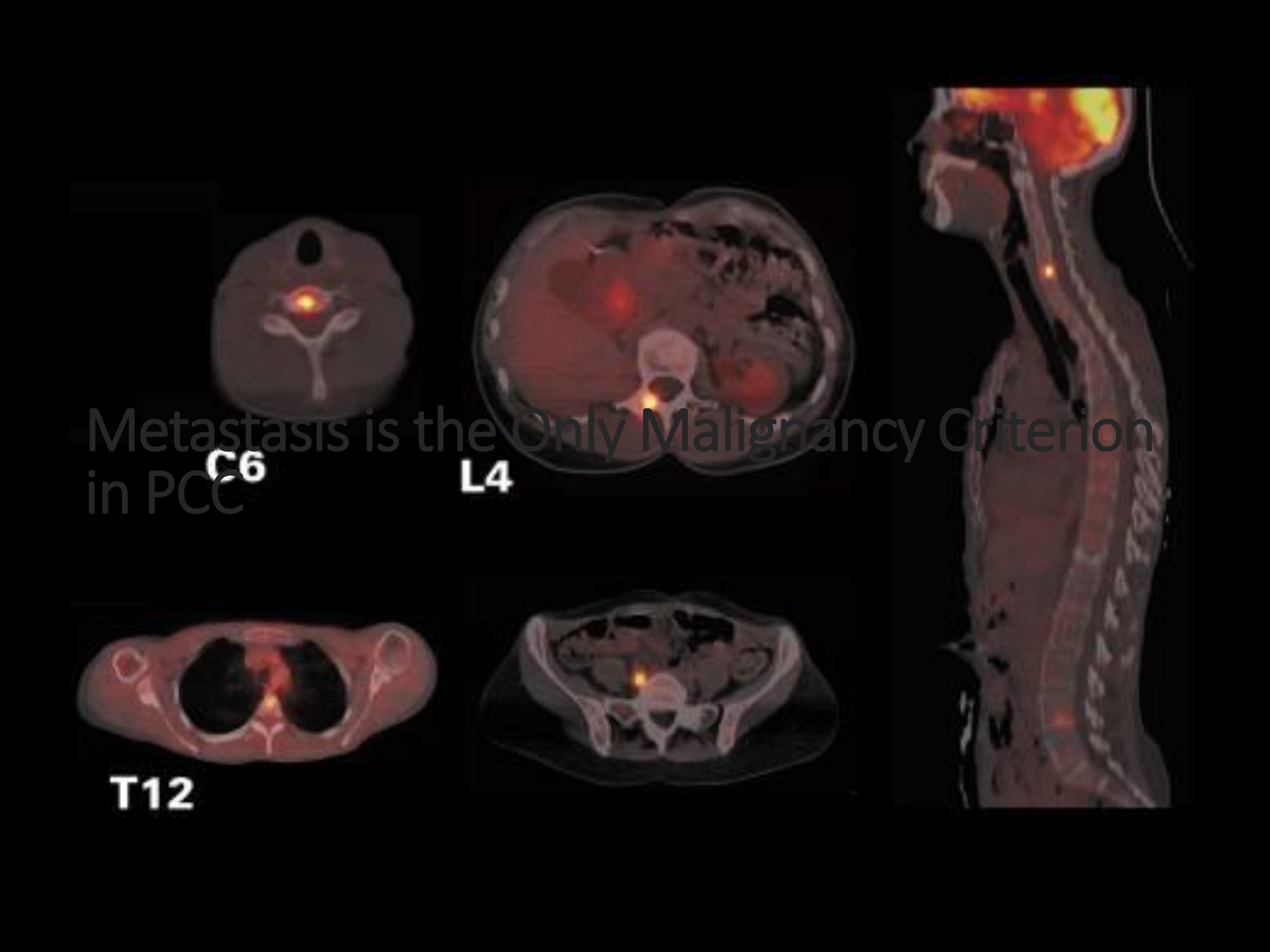

Metastasis is the Only Malignancy Criterion in PCC

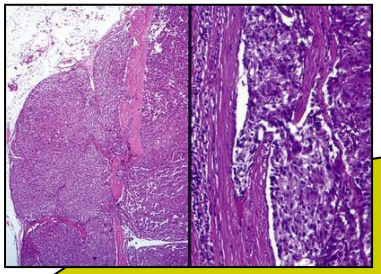

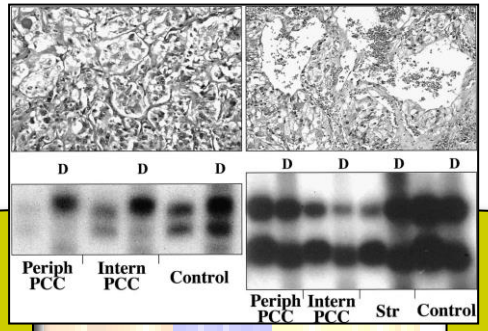
D D D
Periph PCC
Intern PCC
Control
D D D D
Periph PCC
Intern PCC
Str
Control

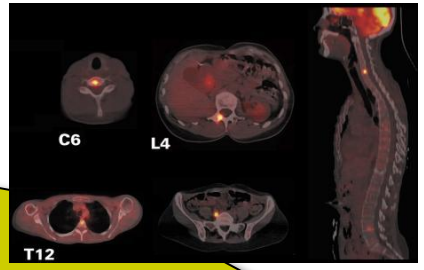
C6
L4
T12

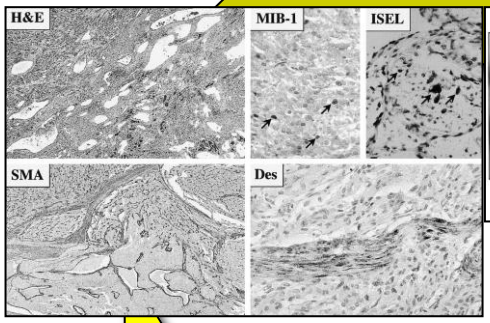
H&E
MIB-1
ISEL
SMA
Des

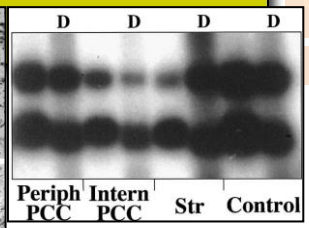
D D D D
Periph PCC
Intern PCC
Str
Control

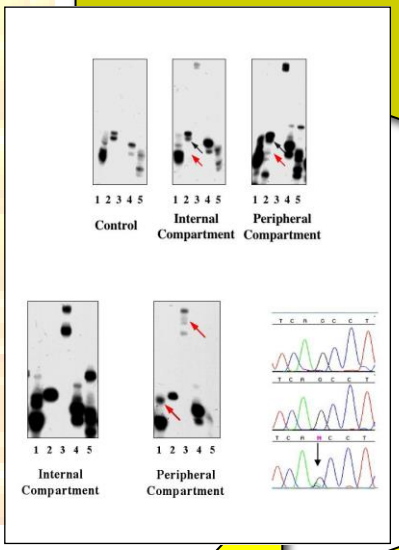
1 2 3 4 5
Control
1 2 3 4 5
Internal Compartment
1 2 3 4 5
Peripheral Compartment
1 2 3 4 5
Internal Compartment
1 2 3 4 5
Peripheral Compartment

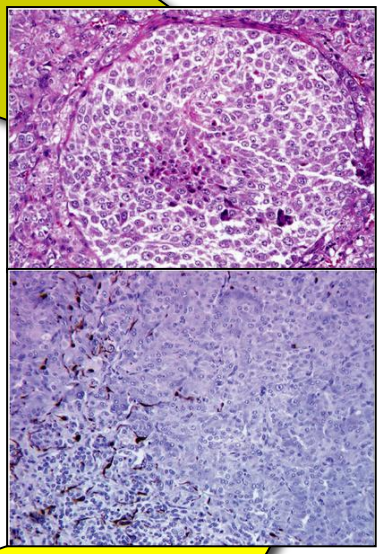

Microsatellite Profile of PCC by Tumor Compartment

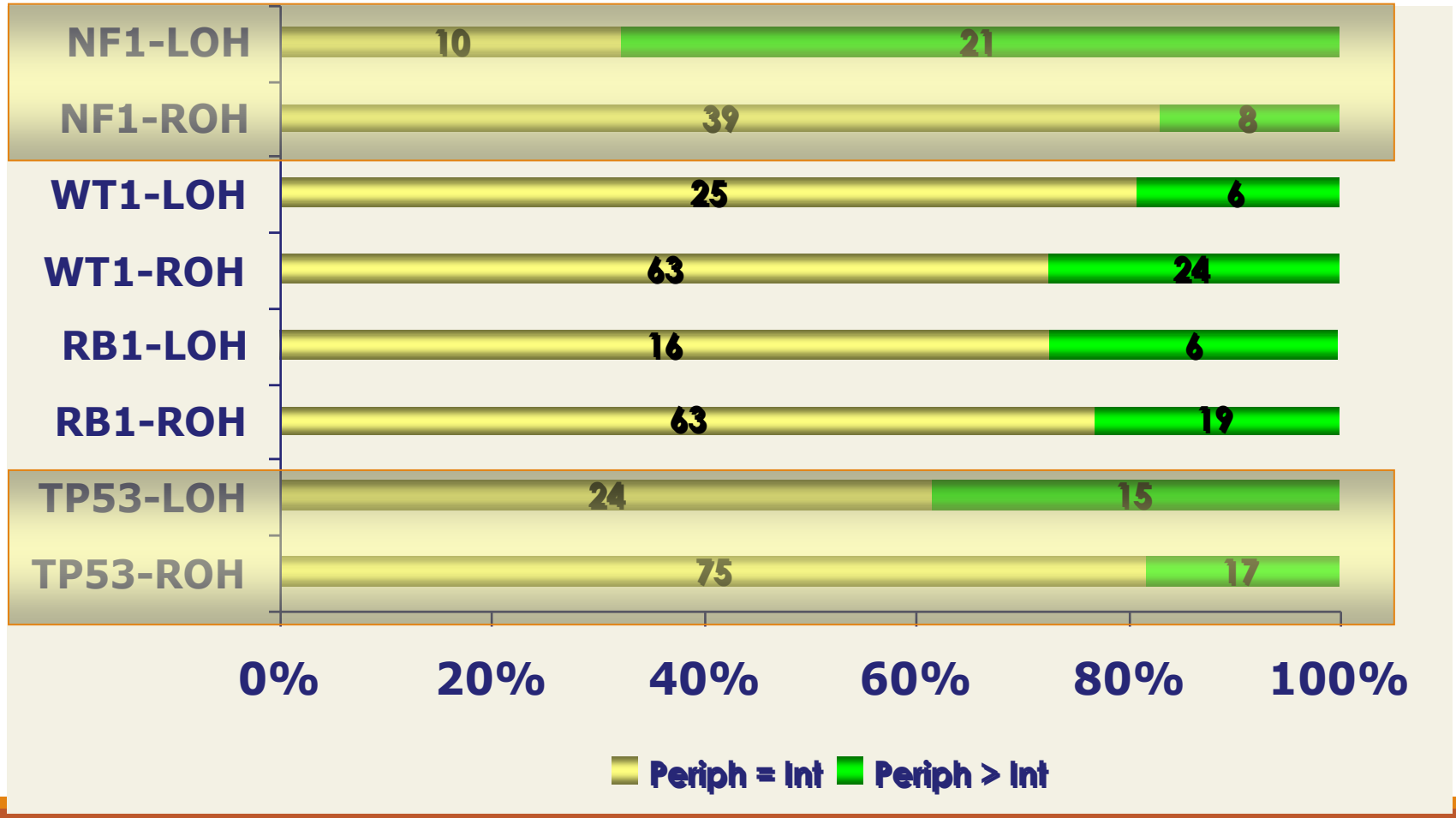

MSI and Defective DNA mismatch repair

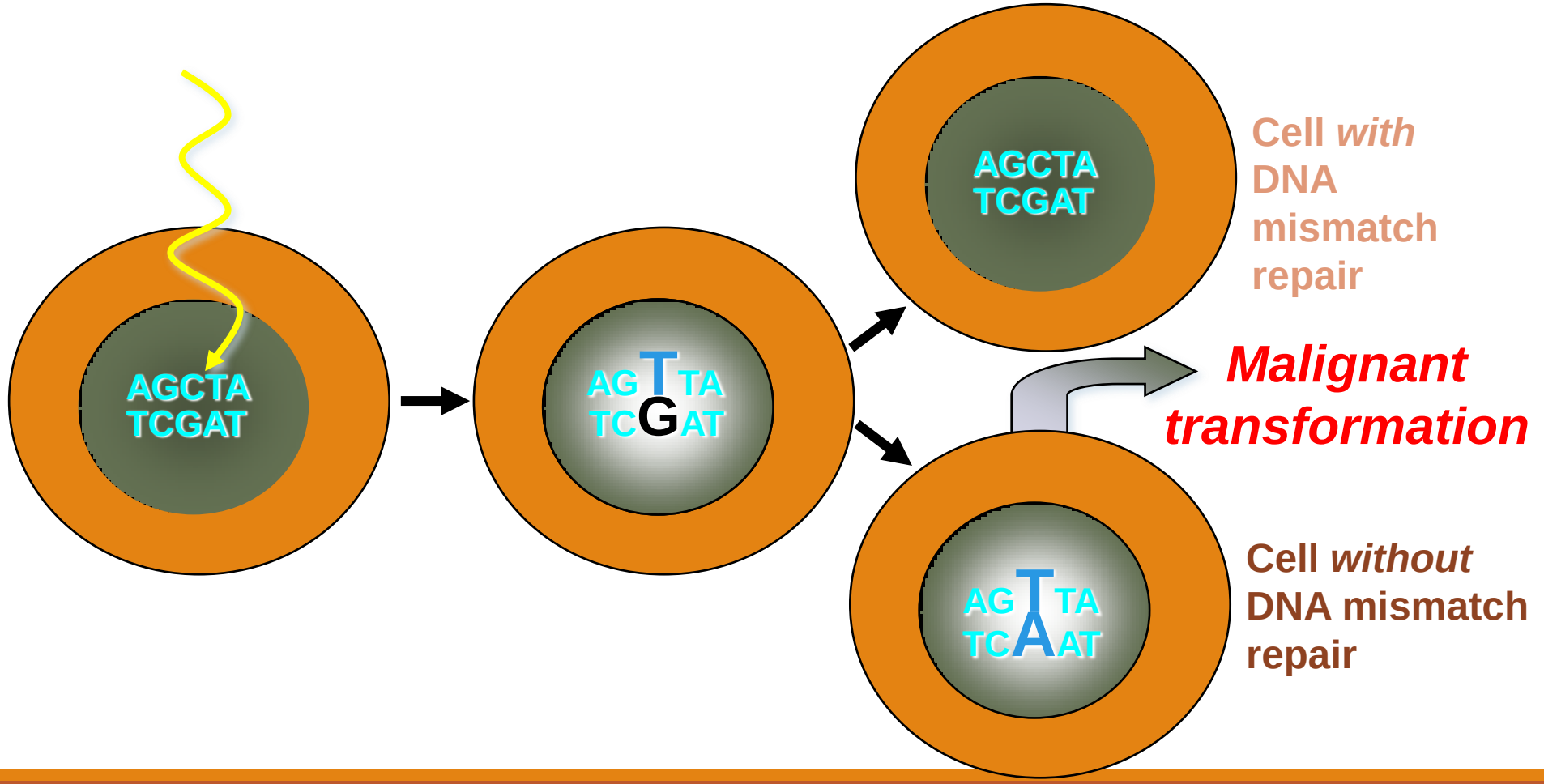

benign (97)
locally-invasive (30)

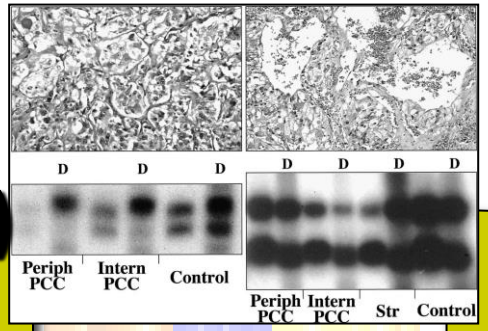

metastatic (node/liver/ bone, 16)

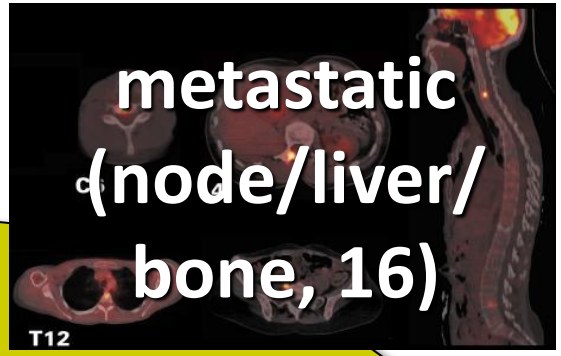

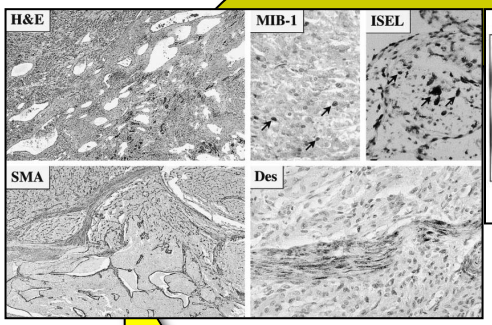

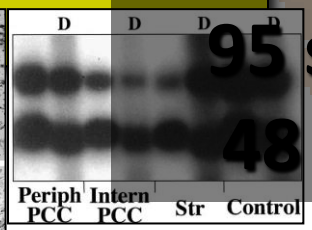

95 sporadic PCC,
48 MEN 2A PCC

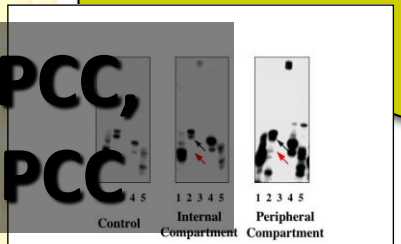

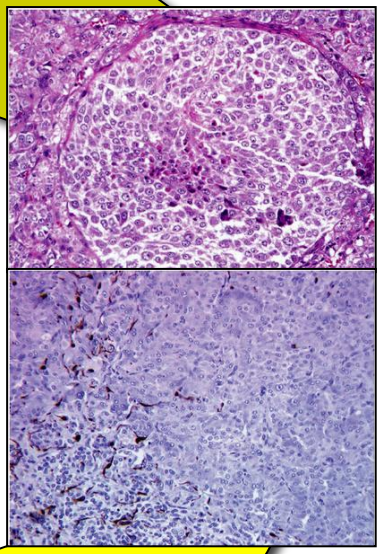

Malignant PCC
Loc-Invasive PCC
Benign PCC

? TP53, RB1, WT1, and *NF1* microsatellites (PCR/DGGE)

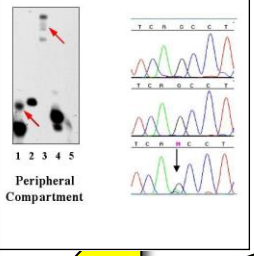

0.00% 0.20% 0.40% 0.60% 0.80% 1.00%
≤1 Locus ≥2 Loci

? MLH1/MSH2 immunoexpression

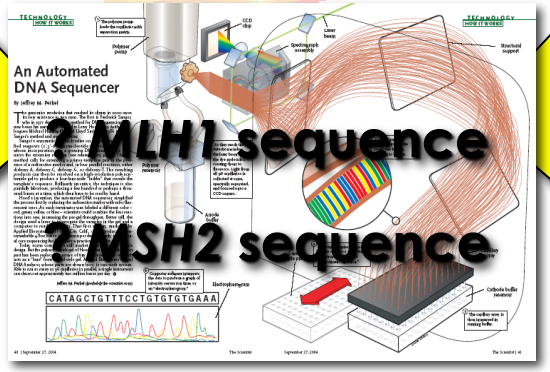

? MLH1 sequence
? MSH2 sequence

? MLH1/MSH2 immunoexpression

Microsatellite Profile of Sporadic and MEN 2A PCC

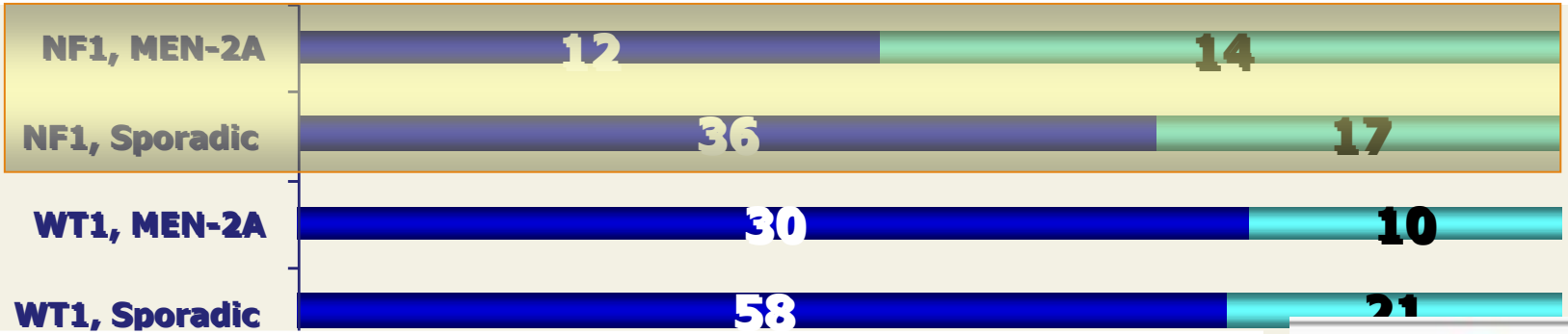

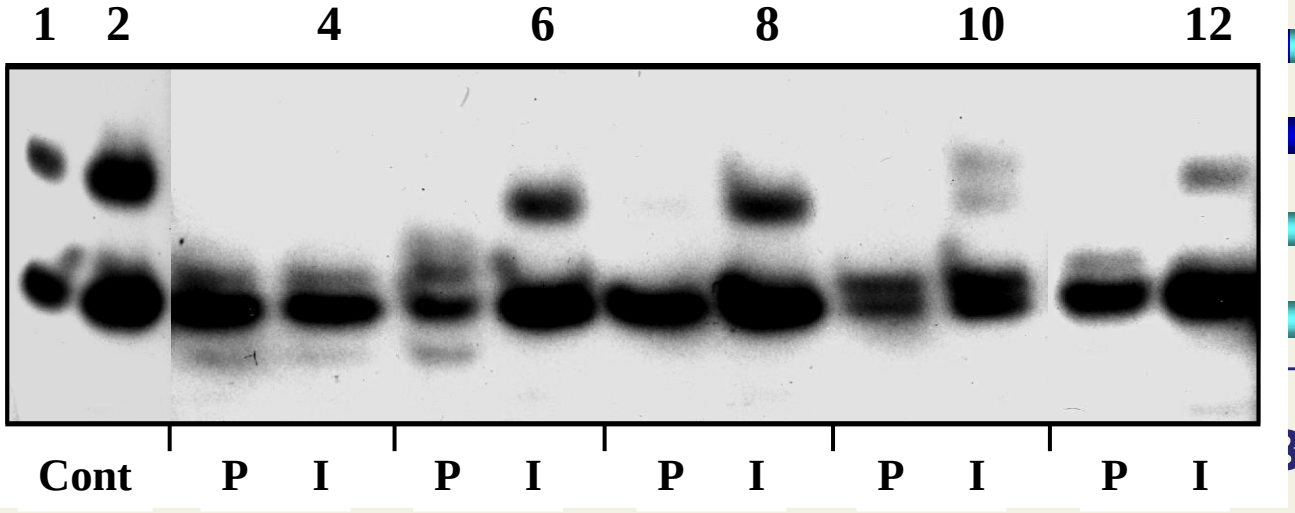

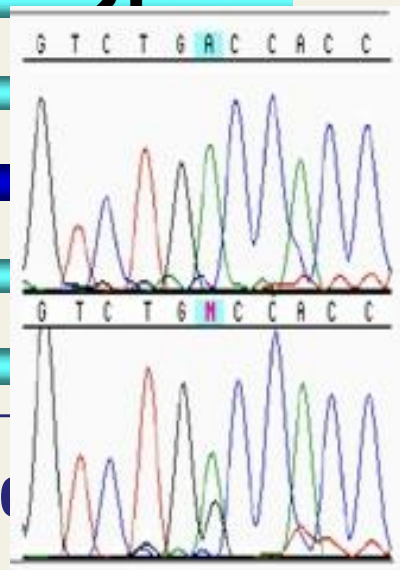

ROH LOH-SNP

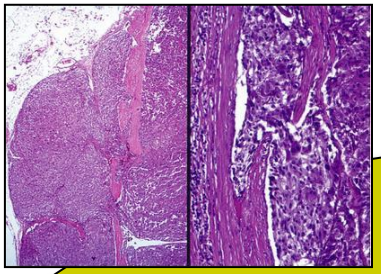

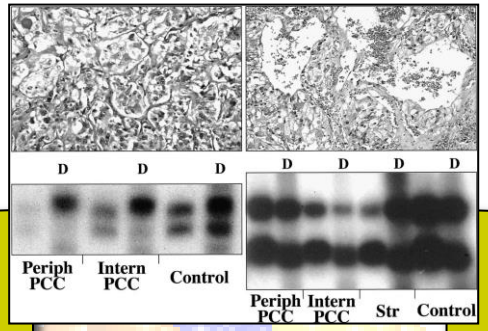

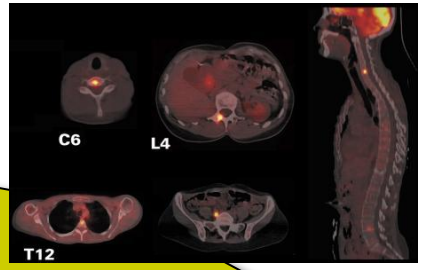

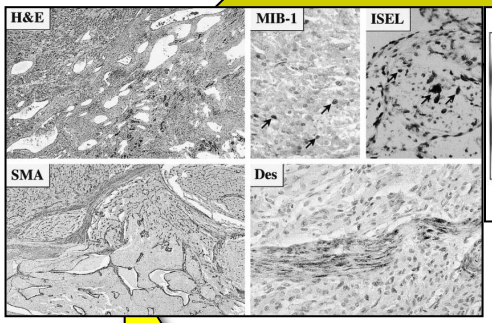

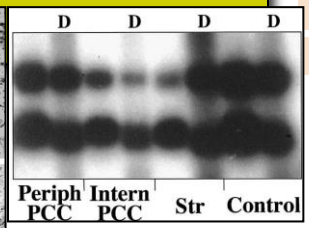

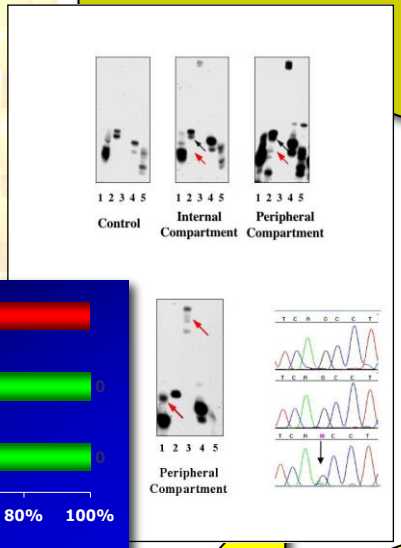

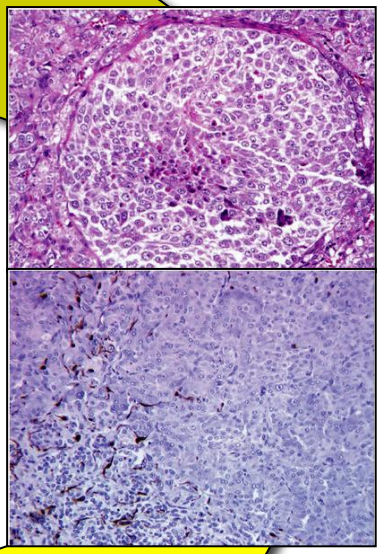

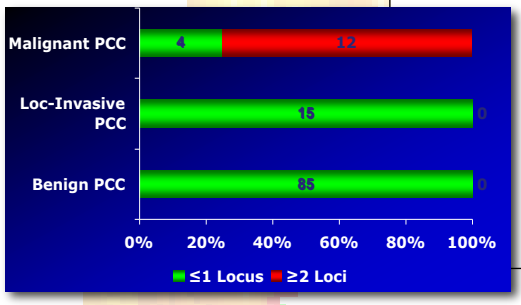

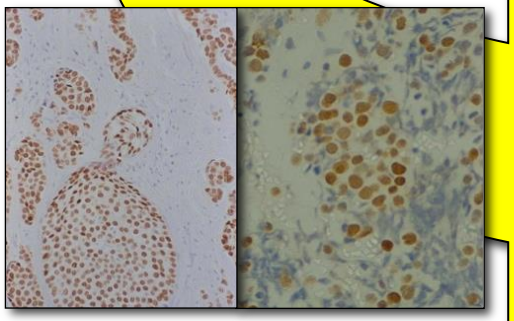

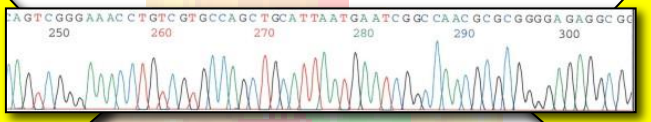

Normal *MLH1* sequence

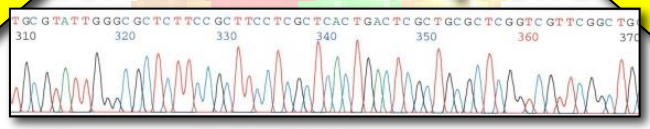

Normal *MSH2* sequence

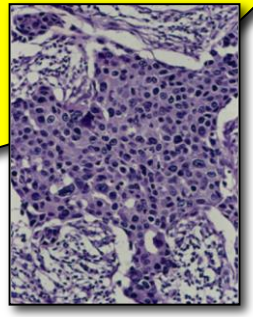

Topographic Heterogeneity and Behaviour in PCC

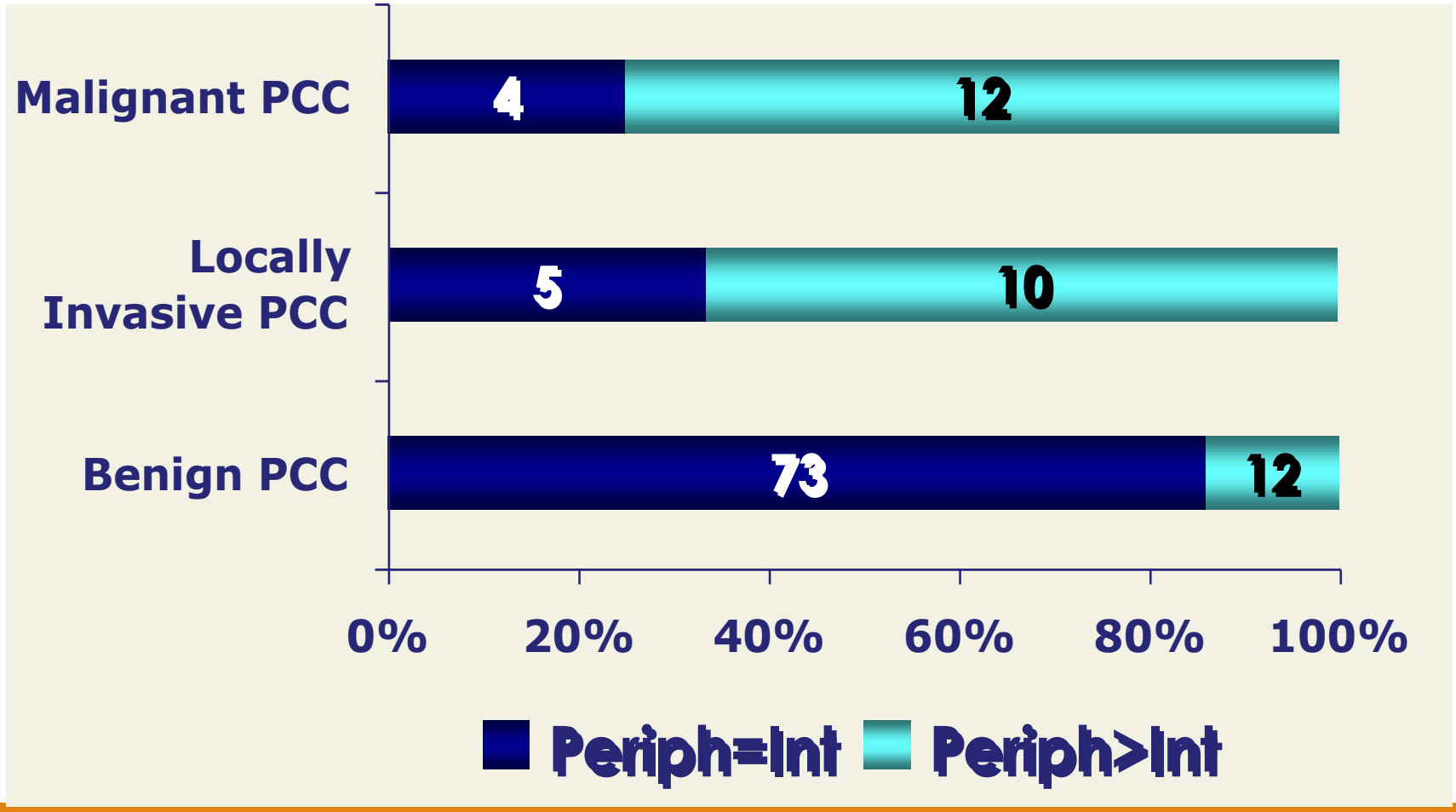

TSG Microsatellite Profile in PCC

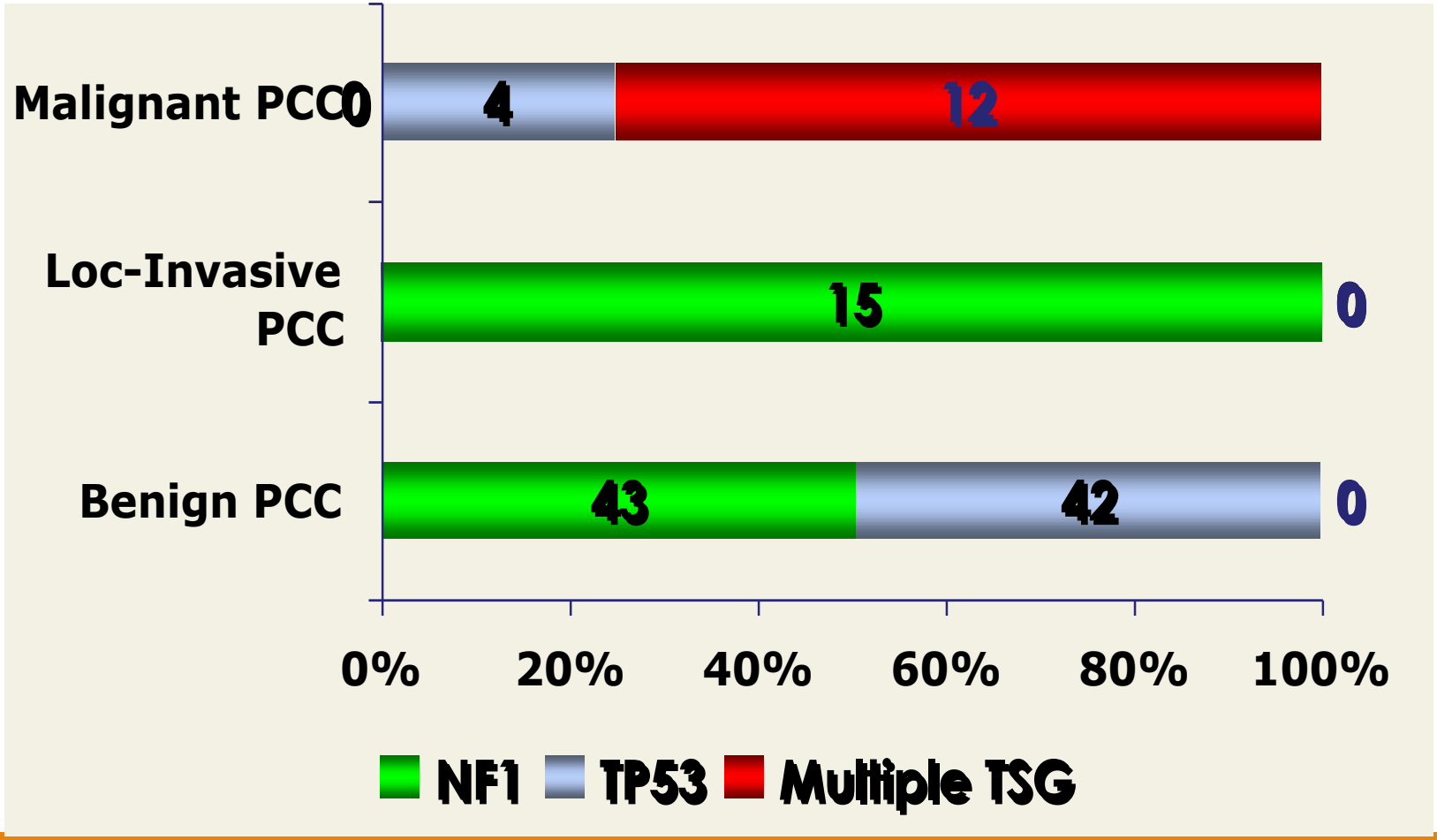

MMR Proteins in PCC Conclusions

Somatic topographic down-regulation of mismatch repair proteins contributes to the key features of malignant PCC

- **accumulation of microsatellite lesions in the peripheral compartment and**
- **intratumor heterogeneity.**

Locally invasive PCC frequently reveals single locus alterations, especially involving *NF1*.

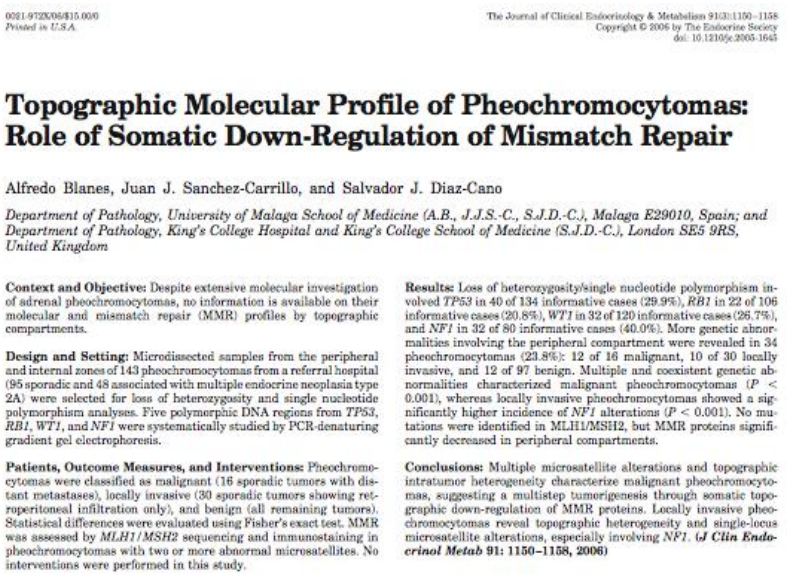

0021-972X/06/$15.00/0
Printed in U.S.A.

The Journal of Clinical Endocrinology & Metabolism 91(3):1150–1158
Copyright © 2006 by The Endocrine Society
doi: 10.1210/jc.2005-1645

Topographic Molecular Profile of Pheochromocytomas: Role of Somatic Down-Regulation of Mismatch Repair

Alfredo Blanes, Juan J. Sanchez-Carrillo, and Salvador J. Diaz-Cano

Department of Pathology, University of Malaga School of Medicine (A.B., J.J.S.-C., S.J.D.-C.), Malaga E29010, Spain; and Department of Pathology, King's College Hospital and King's College School of Medicine (S.J.D.-C.), London SE5 9RS, United Kingdom

Context and Objective: Despite extensive molecular investigation of adrenal pheochromocytomas, no information is available on their molecular and mismatch repair (MMR) profiles by topographic compartments.

Design and Setting: Microdissected samples from the peripheral and internal zones of 143 pheochromocytomas from a referral hospital (95 sporadic and 48 associated with multiple endocrine neoplasia type 2A) were selected for loss of heterozygosity and single nucleotide polymorphism analyses. Five polymorphic DNA regions from *TP53*, *RB1*, *WT1*, and *NF1* were systematically studied by PCR-denaturing gradient gel electrophoresis.

Patients, Outcome Measures, and Interventions: Pheochromocytomas were classified as malignant (16 sporadic tumors with distant metastases), locally invasive (30 sporadic tumors showing retroperitoneal infiltration only), and benign (all remaining tumors). Statistical differences were evaluated using Fisher's exact test. MMR was assessed by *MLH1*/*MSH2* sequencing and immunostaining in pheochromocytomas with two or more abnormal microsatellites. No interventions were performed in this study.

Results: Loss of heterozygosity/single nucleotide polymorphism involved *TP53* in 40 of 134 informative cases (29.9%), *RB1* in 22 of 106 informative cases (20.8%), *WT1* in 32 of 120 informative cases (26.7%), and *NF1* in 32 of 80 informative cases (40.0%). More genetic abnormalities involving the peripheral compartment were revealed in 34 pheochromocytomas (23.8%): 12 of 16 malignant, 10 of 30 locally invasive, and 12 of 97 benign. Multiple and coexistent genetic abnormalities characterized malignant pheochromocytomas ($P < 0.001$), whereas locally invasive pheochromocytomas showed a significantly higher incidence of *NF1* alterations ($P < 0.001$). No mutations were identified in MLH1/MSH2, but MMR proteins significantly decreased in peripheral compartments.

Conclusions: Multiple microsatellite alterations and topographic intratumor heterogeneity characterize malignant pheochromocytomas, suggesting a multistep tumorigenesis through somatic topographic down-regulation of MMR proteins. Locally invasive pheochromocytomas reveal topographic heterogeneity and single-locus microsatellite alterations, especially involving *NF1*. (*J Clin Endocrinol Metab* **91: 1150–1158, 2006**)